

**AN EFFICIENT ESTIMATION OF CHANNEL FOR  
5G WIRELESS COMMUNICATION SYSTEMS**

Thesis Submitted for the Award of the Degree of

**DOCTOR OF PHILOSOPHY**

in

**Electronics & Communication Engineering**

By

**NILOFER S K**

**Registration Number: 41900152**

**Supervised By**

**Dr. Praveen Kumar Malik (23314)**

**School of Electronics & Electrical Engineering (Professor)**

**Lovely Professional University**



**LOVELY PROFESSIONAL UNIVERSITY, PUNJAB**

**2023**

## DECLARATION

I hereby declare that this research work “An Efficient Estimation of Channel for 5G Wireless Communication Systems” has been composed solely by myself and has not been submitted anywhere. It was carried out by me for the degree of Doctor of Philosophy in Electronics and Communication Engineering under the guidance and supervision of Prof. Dr. Praveen Kumar Malik, Lovely Professional University, Phagwara Punjab, India.

The interpretations put forth are based on my reading and understanding of the original texts and they are not published anywhere in the form of books, monographs or articles. The other books, articles and websites, which I have made use of are acknowledged at the respective place in the text.

I certify that

- The work contained in this thesis is original and has been done by me under the guidance of my supervisor (s).
- The work has not been submitted to any other Institute for the reward of any other degree or diploma.
- I have followed the guidelines provided by the Institute in preparing the thesis.
- Whenever I used materials (data, theoretical analysis, figures and text) from other sources, I have given due credit to them by citing them in the text of the thesis and giving their details in the references.

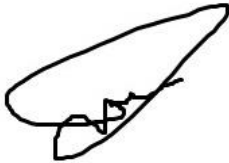
Date: 12/09/2023



Nilofer S K  
(41900152)

## CERTIFICATE

This is to certify that the thesis entitled “**An Efficient Estimation of Channel for 5G Wireless Communication Systems**” being submitted by **Nilofer S K** for the degree of Doctor of Philosophy in Engineering from Lovely Professional University, Jalandhar is a record of bonafide research work carried out by her under my supervision at the School of Electrical and Electronics Engineering. In our opinion, this is an authentic piece of work for submission for the degree of Doctor of Philosophy. To the best of our knowledge, the work has not been submitted to any other University or Institute for the award of any degree or diploma.



Supervisor

**Dr. Praveen Kumar Malik**, Professor  
School of Electrical and Electronics Engineering  
Lovely Professional University, Phagwara, Punjab-144011  
E-mail id: praveen.23314@lpu.co.in  
Phone No: +91-9719437711

## ABSTRACT

It should come as no surprise that every major wireless system in the globe is attempting to make it even quicker because everyone loves speed and, more specifically, fast internet. Stable internet connections are becoming more and more important for automobiles, homes, watches, and smartphones. The fifth generation of technology has arrived in order to live in a world where speed is changing every second and where we are constantly clamouring for new technology beyond fourth generation. A large amount of wireless connections and mobile data traffic are predicted to be made possible by the fifth-generation network. A demand for several wireless communication is to attain greater SE, EE, as well as quality of service in terms of delay, dependability, and security. To connect several numbers of user MIMO is utilized. MMIMO is a developing technique for the next-generation of wireless communication systems. The remedy for this rise in demand is mMIMO remote access systems. High spectrum and energy efficacy is achieved via massive multiple input and multiple technology, which combines transmitter and receiver antenna. These days mMIMO systems have become popular because of their enhanced data transmission rates, robustness against multipath fading, enhanced spectral efficacy, and ability to convey to a more significant number of users with extensive coverage. The critical challenge of the massive multiple input multiple output systems is precisely replenishing the information on the channel state and synchronizing the receiver and transmitter. The channel state information is recovered with the help of various channel estimation techniques of channel. So, this thesis also reviews on some of the existing channel estimation techniques for the massive multiple input and multiple output systems. The other main criteria of using fifth generation systems are because of its higher data rates. The mMIMO systems provide higher data rates with the help of multi carrier modulation techniques. The idea behind multi-carrier modulation is to use these sub carriers to modulate various carriers while breaking the stream into numerous bit streams, each of which has a considerably lower bit rate. In recent years orthogonal frequency division multiplexing multi carrier modulation technique has been an efficient choice for the transmission of the information. The decision on multi-carrier modulation still is the greatest difficulty for

the fifth-generation air interface, nevertheless. For the physical layer's design, a potential multi-carrier modulation is needed. So, a choice of an efficient multi carrier modulation technique for obtaining higher data rates without the loss of information is necessary. To accurately detect the channel an efficient channel estimation algorithm that is best suitable for multicarrier modulation technique is to be defined. Therefore, this thesis presents a modified entropy-based least square channel estimation technique for fifth generation massive multiple input multiple output for universal filtered multi carrier systems. The proposed channel estimation technique performance is novel and better in analogized with the least square and minimum mean square error channel estimation techniques. The evaluation of the suggested channel technique is implemented using MATLAB, and its performance results are shown in the simulation. The performance results of the proposed channel estimation are evaluated based on the mean square error and bit error rate of the obtained signal. The executed results prove that the suggested channel estimation efficacy is analogized to conventional channel estimation methods. The performance of the multi carrier modulation techniques concerning to the proposed channel estimation is also presented in this thesis. This thesis also explains the analytical assessment of the least square, minimum mean square error and modified entropy-based channel estimation techniques. The results show that at high values of signal to noise ratio, the proposed modified entropy-based channel estimation algorithm outperforms the conventional least square, minimum mean square error and alamouti for bit error rate. The results also prove that the proposed channel estimation method outperforms better compared to conventional channel estimation methods in terms of mean square error. The spectral efficiency value over the number of subcarriers is high for the proposed channel estimation method compared to conventional channel estimation methods.

## **ACKNOWLEDGEMENT**

Throughout the writing of this dissertation, I have received a great deal of support and assistance.

First and foremost, I would like to express my deep and sincere regards for my supervisor, Prof. Dr. Praveen Kumar Malik for providing me the opportunity, support and freedom to carry on this research work. His passion, guidance, and discipline have been indispensable to my growth as a scientist and as a person over these past four years. I am especially grateful for his devotion to his students' education and success.

I wish to acknowledge the infrastructure and facilities provided by School of Electronics and Electrical Engineering, Lovely Professional University and Research department to guide me on timely basis regarding norms and guidelines.

I would like to pay my special regards to faculty of BVRIT HYDERABAD College of Engineering for Women for their support in successful completion of the work.

Last, but not the least I would express my sincere gratitude to my family for their love, sacrifice and moral support for without their continued support this work would never have been possible.

# CONTENTS

<b>Declaration</b>	<b>II</b>
<b>Certificate</b>	<b>III</b>
<b>Abstract</b>	<b>IV</b>
<b>Acknowledgements</b>	<b>VI</b>
<b>Contents</b>	<b>VII</b>
<b>List of Figures</b>	<b>X</b>
<b>List of Tables</b>	<b>XIII</b>
<b>Acronyms and Abbreviations</b>	<b>XIV</b>
<b>List of Symbols</b>	<b>XX</b>
<b>Table of Contents</b>	
<b>CHAPTER-1</b> .....	<b>1</b>
<b>INTRODUCTION</b> .....	<b>1</b>
<b>1.1 INTRODUCTION</b> .....	<b>1</b>
<b>1.2. 5G VISION</b> .....	<b>4</b>
<b>1.3. 5G ARCHITECTURE</b> .....	<b>6</b>
<b>1.4. MASSIVE MIMO</b> .....	<b>11</b>
<b>1.5. 5G OPEN ISSUES AND CHALLENGES</b> .....	<b>15</b>
<b>1.6. 5G APPLICATIONS</b> .....	<b>18</b>
<b>1.7. MOTIVATION</b> .....	<b>23</b>
<b>1.8. THESIS OUTLINE</b> .....	<b>24</b>
<b>1.9. SUMMARY</b> .....	<b>25</b>
<b>CHAPTER-2</b> .....	<b>26</b>
<b>STATE OF ART</b> .....	<b>26</b>
<b>2.1. LITERATURE REVIEW</b> .....	<b>26</b>
<b>2.2. RESEARCH GAP</b> .....	<b>42</b>
<b>2.3. PROBLEM STATEMENT</b> .....	<b>42</b>
<b>2.4. RESEARCH OBJECTIVES</b> .....	<b>43</b>
<b>2.5. RESEARCH METHODOLOGY</b> .....	<b>43</b>
<b>2.6. CONTRIBUTION</b> .....	<b>44</b>
<b>2.7. SUMMARY</b> .....	<b>44</b>
<b>CHAPTER-3</b> .....	<b>45</b>

<b>MULTI-CARRIER MODULATION .....</b>	<b>45</b>
<b>3.1. INTRODUCTION .....</b>	<b>45</b>
<b>3.2. CP-OFDM SYSTEM MODEL .....</b>	<b>48</b>
<b>3.3. F-OFDM SYSTEM MODEL .....</b>	<b>49</b>
<b>3.4. FBMC SYSTEM MODEL .....</b>	<b>50</b>
<b>3.5. UFMC SYSTEM MODEL.....</b>	<b>53</b>
<b>3.6. GFDM SYSTEM MODEL .....</b>	<b>55</b>
<b>3.7. SIMULATION RESULTS &amp; DISCUSSION .....</b>	<b>56</b>
<b>3.8. SUMMARY .....</b>	<b>62</b>
<b>CHAPTER-4 .....</b>	<b>63</b>
<b>CHANNEL ESTIMATION.....</b>	<b>63</b>
<b>4.1 WIRELESS CHANNEL MODELLING.....</b>	<b>63</b>
4.1.1 FADING CHANNEL.....	63
<b>4.2 CHANNEL ESTIMATION .....</b>	<b>65</b>
4.2.1 NON-BLIND CHANNEL ESTIMATION SCHEME .....	66
4.2.2 SEMI BLIND CHANNEL ESTIMATION SCHEME .....	70
4.2.3 BLIND CHANNEL ESTIMATION SCHEME.....	70
<b>4.3 CHANNEL ESTIMATION ALGORITHMS.....</b>	<b>71</b>
4.3.1 LS CE TECHNIQUE .....	72
4.3.2 MMSE CE TECHNIQUE.....	74
4.3.3 DFT CE TECHNIQUE.....	77
4.3.4 SPARSE CE TECHNIQUE .....	78
4.3.5 ALAMOUTI CE TECHNIQUE.....	79
4.3.6 DOUBLE SELECTIVE CE TECHNIQUE .....	80
4.3.7 DNN CE TECHNIQUE .....	81
<b>4.4 SIMULATION RESULTS &amp; DISCUSSION .....</b>	<b>82</b>
<b>4.5 SUMMARY .....</b>	<b>85</b>
<b>CHAPTER-5 .....</b>	<b>87</b>
<b>MODIFIED ENTROPY BASED LEAST SQAURE CHANNEL ESTIMATION TECHNIQUE .....</b>	<b>87</b>
<b>5.1 UFMC SYSTEM MODEL.....</b>	<b>87</b>
<b>5.2 LSCE FOR UFMC SYSTEM.....</b>	<b>89</b>
<b>5.3 MMSE CE FOR UFMC SYSTEM .....</b>	<b>90</b>



<b>5.4 MELS CE FOR UFMC SYSTEM.....</b>	<b>92</b>
<b>5.5 SIMULATION RESULTS &amp; DISCUSSION .....</b>	<b>96</b>
<b>5.6 SUMMARY .....</b>	<b>103</b>
<b>CHAPTER-6 .....</b>	<b>104</b>
<b>CONCLUSION AND FUTURE SCOPE .....</b>	<b>104</b>
<b>6.1 CONCLUSION .....</b>	<b>104</b>
<b>6.2 FUTURE SCOPE.....</b>	<b>108</b>
<b>Research Publications .....</b>	<b>110</b>
<b>Bibliography .....</b>	<b>113</b>

## List of Figures

Figure 1.1 5G wireless communication applications .....	3
Figure 1.2 mm spectrum availability ranges from 3GHz to 300GHz .....	4
Figure 1.3 Primary 5G needs .....	5
Figure 1.4 Network centred architecture on base stations .....	6
Figure 1.5 Tiny cell network for 5G wireless communication systems .....	7
Figure 1.6 User centric network architecture for 5G.....	7
Figure 1.7 From omnidirectional to sophisticated beamforming directional antennas	8
Figure 1.8 Architecture of C-RAN .....	9
Figure 1.9 Architecture of a heterogeneous network .....	10
Figure 1.10 Separation of the client and the control plane .....	11
Figure 1.11 Fundamental structure of mMIMO .....	12
Figure 1.12 Different types of massive MIMO systems .....	13
Figure 1.13 Model of mMIMO transmission .....	13
Figure 1.14 A hybrid beamforming design with a large MIMO antenna array .....	15
Figure 1.15 Applications of 5G wireless communication systems .....	18
Figure 1.16 Device to device communication .....	19
Figure 1.17 Machine to machine communication .....	20
Figure 1.18 Internet of things and applications.....	20
Figure 1.19 Internet of vehicles and its applications.....	21
Figure 1.20 Classification of wearable devices .....	22
Figure 2.1 Structured turbo compressed sensing block.....	30
Figure 2.2 Optimal pilot symbol placement .....	31
Figure 2.3 A cell for time domain channel model.....	32
Figure 2.4 Architecture of artificial intelligence channel net .....	37
Figure 3.1 Multicarrier modulation basic block diagram .....	46
Figure 3.2 Block schematic of a waveform modulator .....	46
Figure 3.3 Block schematic of a CP-OFDM transceiver .....	48
Figure 3.4 F-OFDM transceiver.....	49
Figure 3.5 FBMC transceiver.....	51

Figure 3.6a FBMC prototype filter time domain spacing.....	52
Figure 3.6b FBMC prototype filter frequency domain spacing.....	52
Figure 3.7a SE of PHYDYAS and Hermite filter when $K=\min$ .....	53
Figure 3.7b SE of PHYDYAS and Hermite filter when $K= \infty$ .....	53
Figure 3.8 UFMC transceiver .....	54
Figure 3.9 GFDM transceiver .....	55
Figure 3.10 F-OFDM PSD.....	57
Figure 3.11 PSD of FBMC .....	57
Figure 3.12 PSD of UFMC .....	58
Figure 3.13 PSD of GFDM.....	58
Figure 3.14 PSD of OFDM.....	59
Figure 3.15 Signal power of the CW.....	60
Figure 3.16 BER of the CW.....	60
Figure 3.17 BER of GFDM and OFDM.....	61
Figure 4.1 Basic block diagram of communication system.....	63
Figure 4.2 Tier of wireless channel .....	64
Figure 4.3 Basic block diagram of channel estimation .....	65
Figure 4.4 Tier of CE schemes.....	66
Figure 4.5 Classification of pilot-based CE scheme .....	67
Figure 4.6 Pilot arrangement of block type .....	68
Figure 4.7 Pilot arrangement of comb type .....	69
Figure 4.8 Pilot arrangement of lattice type.....	70
Figure 4.9 Classification of blind CE scheme.....	71
Figure 4.10 LS CE block diagram.....	73
Figure 4.11 MMSE CE block diagram.....	75
Figure 4.12 The DFT based CE block diagram .....	77
Figure 4.13 Alamouti CE block diagram.....	79
Figure 4.14 BER vs SNR analogy of LS, MMSE and DFT CE .....	82
Figure 4.15 BER vs SNR analogy of LS and OMP CE .....	82

Figure 4.16 BER vs SNR analogy of alamouti and LS CE .....	83
Figure 4.17 BER vs SNR analogy of doubly selective CE with and without cancellation .....	83
Figure 4.18 BER vs SNR analogy of DNN, LS and MMSE CE .....	84
Figure 5.1 Pilot-aided UFMC system .....	88
Figure 5.2 Dolph Chebyshev filter window in time-frequency domain .....	89
Figure 5.3 MIMO-UFMC system with LS .....	90
Figure 5.4 Multiplying weight vector with LS estimate to obtain MMSE CE .....	91
Figure 5.5 MELS block diagram .....	92
Figure 5.6 MIMO-UFMC system with MELS .....	93
Figure 5.7 BER vs SNR analogy of MELS, LS and MMSE .....	97
Figure 5.8 MSE vs SNR analogy of MELS, LS and MMSE.....	98
Figure 5.9 BER vs SNR analogy of MELS and Alamouti .....	99
Figure 5.10 BER vs SNR analogy of MCM's utilizing MELS .....	100
Figure 5.11 MSE vs SNR analogy of MCM's utilizing MELS .....	101
Figure 5.12 Spectral efficiency of proposed CE, MMSE & LS CE methods.....	102

## List of Tables

Table 1.1 Wireless communication from 1G to 5G is compared.....	1
Table 1.2 Vision 5G by global vendors and operators .....	5
Table 1.3 5G WCS open issues and challenges towards research .....	17
Table 2.1 Highlights of existing CE for OFDM system.....	37
Table 3.1 Analogy of MCM technique(High- $\uparrow$ , Medium- $\leftrightarrow$ , Low- $\downarrow$ ).....	62
Table 4.1 Simulation parameters utilized for executing the specified CE's.....	85
Table 5.1 Simulation parameters of MELS CE .....	96
Table 5.2 BER vs SNR analogy of MELS, LS and MMSE .....	98
Table 5.3 MSE vs SNR analogy of MELS, LS and MMSE .....	99
Table 5.4 BER vs SNR analogy of MELS and Alamouti.....	100
Table 5.5 BER vs SNR for MCM techniques using MELS .....	101
Table 5.6 MSE vs SNR for MCM techniques using MELS .....	102

## Acronyms and Abbreviations

<b>Acronyms</b>	<b>Description</b>
<b>1G</b>	First Generation
<b>2G</b>	Second Generation
<b>3G</b>	Third Generation
<b>3GPP</b>	3 <sup>rd</sup> Generation Partnership Project
<b>4G</b>	Fourth Generation
<b>5G</b>	Fifth Generation
<b>AMPS</b>	Advanced Mobile phone systems
<b>AoA</b>	Angle of Arrival
<b>AoD</b>	Angle of Departure
<b>ABSP</b>	Auxiliary Information Based Block Subspace Pursuit
<b>AR</b>	Augmented Reality
<b>AWGN</b>	Additive White Gaussian Noise
<b>BAN</b>	Body Area Network
<b>PSK</b>	Phase Shift Keying
<b>BPSK</b>	Binary Phase Shift Keying
<b>BS</b>	Base Station
<b>BER</b>	Bit Error Rate
<b>BLER</b>	Block Error Rate
<b>BEM</b>	Basis Expansion Model
<b>BW</b>	Bandwidth

<b>BP-PC-SBL</b>	Belief Propagation-Based Pattern Coupled Sparse Bayesian Learning
<b>BMP</b>	Basic Matching Pursuit
<b>CDMA</b>	Code Division Multiple Access
<b>CIR</b>	Channel Impulse Response
<b>CFO</b>	Carrier Frequency Offset
<b>CE</b>	Channel Estimation
<b>CS</b>	Compressed Sensing
<b>CP</b>	Cyclic Prefix
<b>CW</b>	Candidate Waveforms
<b>C-RAN</b>	Cloud Radio Access Network
<b>CSI</b>	Channel State Information
<b>CRLB</b>	Cramer Rao Lower Bound
<b>D2D</b>	Device to Device
<b>DCS</b>	Distributed CS
<b>DCS-sdmp</b>	DCS Stage Determined Matching Pursuit
<b>DBPSK</b>	Differential Binary Phase Shift Keying
<b>DQPSK</b>	Differential Binary Phase Shift Keying
<b>DTC</b>	Device Type Communication
<b>DFT</b>	Discrete Fourier Transform
<b>DIP</b>	Deep Image Prior
<b>DNN</b>	Deep Neural Network
<b>EKF</b>	Extended Kalman Filter
<b>EM</b>	Expectation Maximization
<b>EE</b>	Energy Efficiency

<b>FDD</b>	Frequency Division Duplexing
<b>FDMA</b>	Frequency Division Multiple Access
<b>F-OFDM</b>	Filtered OFDM
<b>FBMC</b>	Filter Bank Multiple Access
<b>FFT</b>	Fast Fourier Transform
<b>GA</b>	Genetic Algorithm
<b>GMM</b>	Gaussian Mixed Model
<b>GSM</b>	Global System for Mobile
<b>GHz</b>	Giga Hertz
<b>GFDM</b>	Generalized Frequency Division Multiple Access
<b>HetNets</b>	Heterogeneous Networks
<b>IP</b>	Internet Protocol
<b>IoT</b>	Internet of Things
<b>IoV</b>	Internet of Vehicles
<b>ISI</b>	Inter Symbol Interference
<b>ICI</b>	Inter Carrier Interference
<b>IAM</b>	Interference Approximation Approach
<b>ISAGE</b>	Iterative SAGE
<b>IFFT</b>	Inverse Fast Fourier Transform
<b>IDFT</b>	Inverse Discrete Fourier Transform
<b>LTE</b>	Long Term Evolution
<b>LTE-A</b>	Long Term Evolution-Advanced
<b>LS</b>	Least Square
<b>LMS</b>	Least Mean Square



<b>LOS</b>	Line of Sight
<b>LMMSE</b>	Least MMSE
<b>LL</b>	Low Latency
<b>LLR</b>	Log Likelihood Ratio
<b>MSE</b>	Mean Square Error
<b>MMSE</b>	Minimum MSE
<b>MLD</b>	Maximum Likelihood Detection
<b>MELS</b>	Modified Entropy Based LS
<b>M2M</b>	Machine to Machine
<b>MAC</b>	Multiple Access Control
<b>MCM</b>	Multi-Carrier Modulation
<b>MIMO</b>	Multiple Input Multiple Output
<b>mMIMO</b>	Massive MIMO
<b>MU-MIMO</b>	Multi User-MIMO
<b>ML</b>	Maximum Likelihood
<b>MTC</b>	Machine Type Communication
<b>mm</b>	Millimeter
<b>MP</b>	Matching Pursuit
<b>NAMP</b>	New Adaptive Matching Pursuit
<b>NLOS</b>	Non-Line of Sight
<b>OQAM</b>	Orthogonal QAM
<b>OMP</b>	Orthogonal Matching Pursuit
<b>OFDM</b>	Orthogonal Frequency Division Multiplexing
<b>OOBE</b>	Out of Band Emission

<b>PF-OMP</b>	Polynomial Fitting OMP
<b>PAPR</b>	Peak to Average Power Ratio
<b>PF</b>	Prototype Filter
<b>PSD</b>	Power Spectral Density
<b>PSO</b>	Particle Swarm Optimization
<b>QBSO</b>	Quasi Block Simultaneous OMP
<b>QPSK</b>	Quadrature Phase Shift Keying
<b>QAM</b>	Quadrature Amplitude Modulation
<b>QoE</b>	Quality of Experience
<b>RF</b>	Radio Frequency
<b>stFBP</b>	Stage Wise Forward Backward Pursuit
<b>SA</b>	Smart Antennas
<b>SER</b>	Symbol Error Rate
<b>SAMP</b>	Sparsity Adaptive Matching Pursuit
<b>SDGS</b>	Steepest Descent Gauss-Seidel
<b>SDMA</b>	Spatial Division Multiple Access
<b>SDN</b>	Software Design Network
<b>SNR</b>	Signal to Noise Ratio
<b>SINR</b>	Signal to Interference Plus Noise Ratio
<b>SAGE</b>	Space Alternating Generalized Expectation
<b>StOMP</b>	Stagewise Orthogonal Matching Pursuit
<b>SE</b>	Spectral Efficiency
<b>SBL</b>	Sparse Bayesian Learning
<b>TB</b>	Tera Byte

<b>TDD</b>	Time Division Duplexing
<b>TDMA</b>	Time Division Multiple Access
<b>TOMP</b>	Tensor OMP
<b>TI</b>	Tactile Internet
<b>UHF</b>	Ultra-High Frequency
<b>UWB</b>	Ultra-Wide Band
<b>UMTS</b>	Universal Mobile Telecommunications System
<b>UE</b>	User Equipment
<b>UKF</b>	Unscented Kalman Filter
<b>UFMC</b>	Universal Filtered Multiple Access
<b>VC</b>	Vehicular Communication
<b>WAVE</b>	Wireless Access in Vehicle Environment
<b>WCS</b>	Wireless Communication System
<b>WER</b>	Word Error Rate
<b>Wi-Fi</b>	Wireless Fidelity
<b>WiMAX</b>	Worldwide Interoperability for Microwave Access
<b>WLAN</b>	Wireless Local Area Network
<b>WLS</b>	Weighted LS
<b>ZF</b>	Zero Forcing

## List of Symbols

Symbol	Description
$X[n]$	Transmitted Vector
$Y[n]$	Received Vector
$h[n]$	Channel Coefficient
$w[n]$	Noise Vector
$\hat{h}$	Channel Estimate
$\sigma$	Noise Variance

# CHAPTER-1

## INTRODUCTION

### 1.1 INTRODUCTION

Wireless communication system (WCS) has been around for over a decade, beginning with 1G communication systems. Over time, newer evolutions toward 2G, 3G, and 4G wireless communication systems have occurred. All of this resulted in the introduction of digital modulation procedures, reuse of frequency, internet on packet-based, and upgrades of the physical layer. All of this has significantly accelerated the evolution of intelligent devices in everyday life. The first 1G systems were analogue voice-only systems, but after that, WCS was a digital data and voice system. For WCS, IP-based 4G LTE is currently used. Data rates, bandwidth allocation, and other parameters have risen from 1G to 4G WCS. At the moment, an average user is expected to download 1 TB of data per year [1]. LTE networks are being investigated for new research using MIMO, small cells, Hetnets, and multiple antennas to strengthen data rates and capacity [1]. This traffic explosion is unlikely to be sustained in the long run by 4G LTE. As data traffic grows, so does the demand for the next generation WCS, or 5G WCS. Table 1 illustrates the similitude from 1G to 5G.

**Table 1.1:** Wireless communication from 1G to 5G is compared.

<b>Parameter</b>	<b>1G</b>	<b>2G</b>	<b>3G</b>	<b>4G</b>	<b>5G</b>
Year of deployment	1970	1993	2001	2009	2018
Technology	AMPS	GSM	WCDM A	WIMAX, LTE	mm- waves, MIMO

System accessed	FDMA	CDMA, TDMA	CDMA	OFDM	OFDM
Type of switching	Circuit switching	Circuit switching	Packet switching	Packet switching	Packet switching
Internet service	No	Narrowband	Broadband	Ultra-broadband	Wireless WWW
BW	2.4KHz	25MHz	25MHz	100MHz	30 GHz – 300GHz
Data rates	2kbps	64kbps	2Mbps	1Gbps	>1Gbps
Advantages	Voice calls	Emphasizes multimedia	International roaming, High security	Speed, high speed handoffs, global mobility	Low latency & Extremely high speeds

LTE is employed in 4G WCS. However, innovation for new applications is not optimal in 4G. IoT, MTC, VC, DTC, e-health care, wearables, and several other operations has benefited from the 5G promotion [2]. Figure 1.1 depicts the applications of 5G WCS.

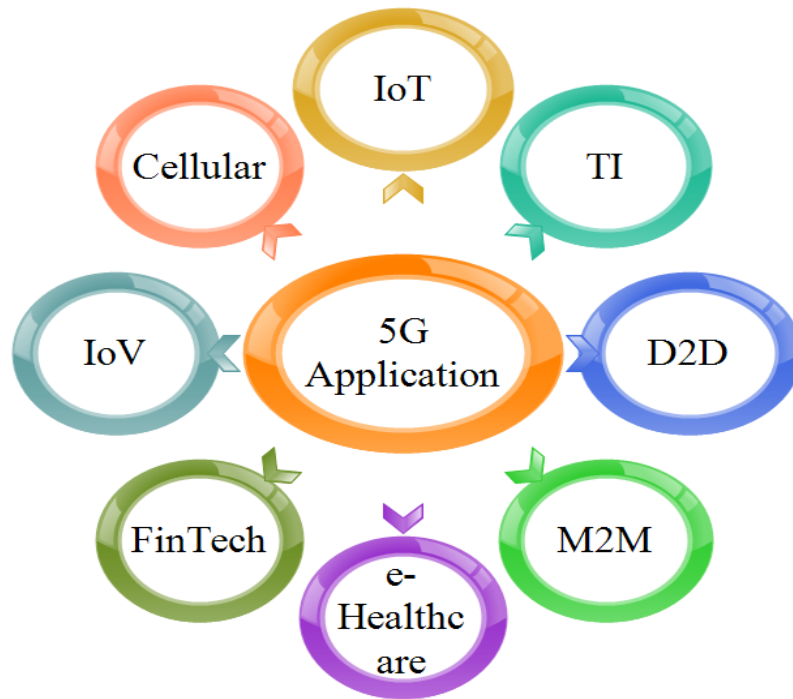


**Figure 1.1:** 5G wireless communication applications.

As a result, 5G systems deal with the hassles of 4G WCS, such as higher data rate, improved SE, and lesser latency. In 2023, 5G wireless technology for mobile communication mobile networks will be deployed. Currently, all wireless communications use a 300MHz to 3GHz frequency known as the beachside spectrum or sweet pot [3]. However, the current realm is overburdened with traffic, making it difficult to conquer. The new problem of bandwidth for high frequency is a critical component of 5G WCS, which investigates underutilized spectrum. The 5G frequency realm is split into three bands: mm waves, mid-band, and low band. 5G mm is the fastest wave, with speeds ranging from 1 to 2 Gb/s and frequency bands ranging from 24GHz to 72GHz. 5G mid band operates at frequencies ranging from 2.4GHz to 4.2GHz [4-5]. This band is now widely used in over 20 networks, with speeds ranging from 100 to 400Mbs over 100MHz. Other countries use the 3.3GHz and 4.2GHz bands, while China uses 3.5GHz. The low band operates similarly to 4G and employs a similar frequency range.

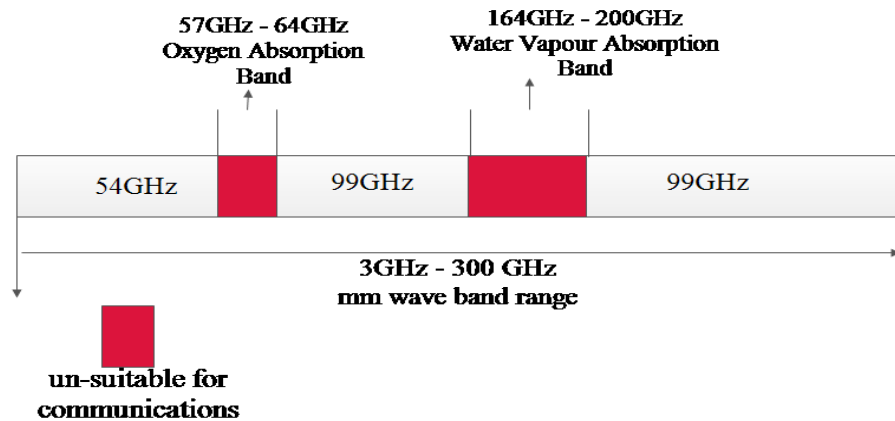


**Figure 1.2:** mm spectrum availability ranges from 3GHz to 300GHz.

Some WCS, such as radar, military, radio astronomy, radio, and others, are now utilizing the mm band to increase competency and throughput of data over the present spread. The 57GHz-64GHz and 164GHz-200GHz frequency bands are not competent for telecommunication. A large spectrum of the mm-wave band is also accessible for 5G WCS [6-7].

## 1.2 5G VISION

New applications and particular needs are driving the significant uprising in 5G WCS [8-9]. As a result, 5G systems overcome obstacles in 4G technologies like high data throughput, large spectrum efficacy, and lesser latency. The following are eight great significant 5G criteria [9] and is depicted in figure 1.3:

- 1-10Gbps speed of data for networks in the real world
- A round-trip delay of 1ms.
- Large bandwidth per unit area.
- A massive number of linked gadgets.
- 99.99 percent perceived availability.
- Full coverage for anywhere, at all-time connectivity.
- Energy utilization reduction.



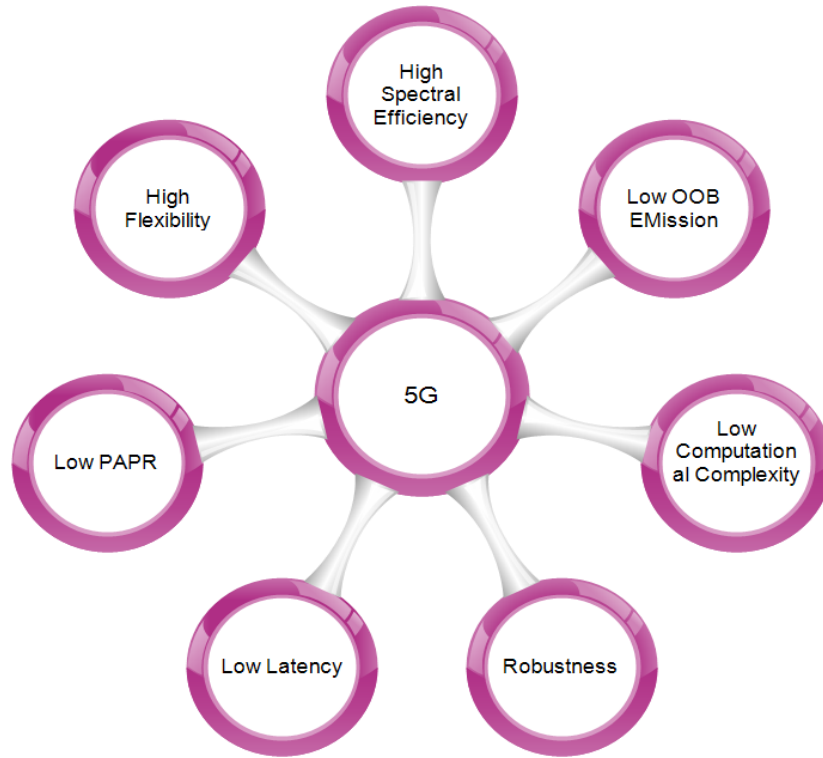


**Figure 1.3:** Primary 5G needs.

With these eight signified 5G requisites, academia, wireless industries and research organizations has started collaborating in different facets. The vision of 5G WCS from distinct globally, prominent vendors and operators are depicted in table 1.2.

**Table 1.2:** Vision 5G by global vendors and operators.

S.No	Industry	Vision
1.	5GPP, METS [10]	Software driven by 5G
		Scalability
		sustainability
		Multi-tenancy
2	5G Forum [11]	Intertwining hetnets
		Commercialization by 2020
3	Qualcomm [12]	Devices connected with industry
		Enhancement in user experience

		Enable novel services
4	Huawei [13]	Massive capacity
		Massive connectivity
		Deployment of network
		Diverse services and applications
5	Nokia solution networks [14]	Deployment of Hetnets
		AR
		TI
		Accurate channel models
6	Samsung electronics [15]	Enhanced multimedia experience
		Cloud computing
		IoT
7	Docomo [16]	Extensive and enriched content
		Connecting wirelessly

### 1.3 5G ARCHITECTURE

5G technology will support several numbers of subscribers, a broad ranch of gadgets, and a wide range of services. As a result, the LL and capacity limitations of traditional WCS necessitate breaking the ground station-centric networking paradigm depicted in figure 1.4.

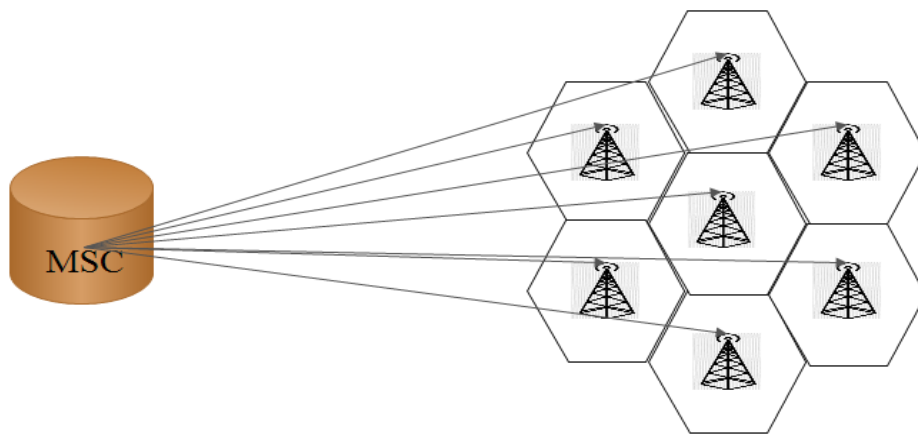


**Figure 1.4:** Network centred architecture on base stations.

The increased need for bandwidth availability prompted the wireless industry to shift from BS centric networks to small cell networks. However, from initial macro hexagonal coverage, other networks are projected to link different nodes utilizing tiny, pico, and femtocell networks. Figure 1.5 depicts the tiny cell network.

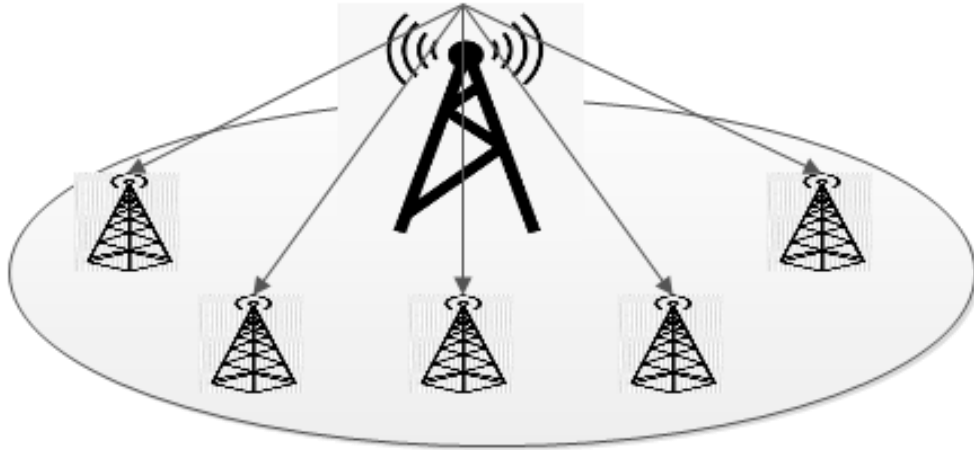


**Figure 1.5:** Tiny cell network for 5G wireless communication systems.

Researchers are now focused on innovative approaches to designing client-centric networks for 5G WCS. The client-centric network will replace the BS-centric network [17], allowing more users to be assigned; however, dense 5G networks will suffer from excessive co-channel interference. Figure 1.6 depicts the user-centric network.

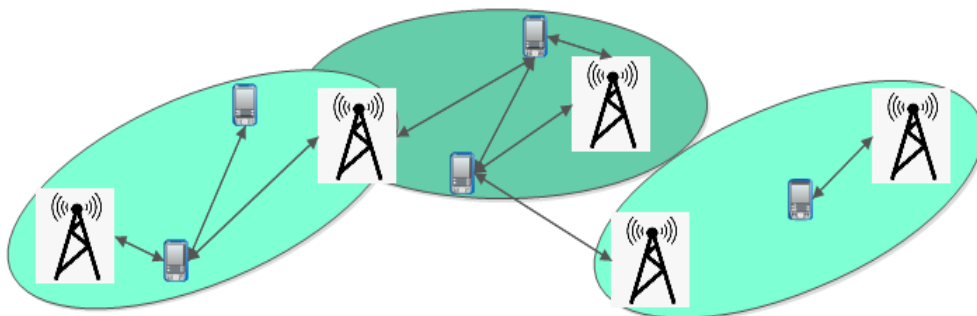


**Figure 1.6:** User centric network architecture for 5G.

The new idea of client-centric networks and tiny cell networks installed boosts the 5G network topology. However, there is still a challenge with interference because of co-channel, which can be mitigated by SA. SA is designed to replace traditional omnidirectional antennas with smart beamforming directional antennas, which cover a larger area and minimize transmission power across both ends of the user and BS [18]. In general, beamforming is a signal processing method that allows signals for directed transmission or reception. 5G beamforming is mainly utilized to direct 5G communications more precisely to receiving device. A typical 5G small cell that does not use beamforming during MIMO transmission will be unable to narrowly concentrate or focus its transmit beams to a specific location. Beamforming allows the tiny cell to guide transmission towards a mobile device such as a cell phone, laptop, self-driving car, or IoT node. This increases network efficiency and saves electricity. Figure 1.7 depicts common omnidirectional antennas and smart beamforming directional antennas. As a result of adaptive beamforming, SDMA is introduced [19]. SDMA boosts the frequency of beamforming antennas at either the transceiver ends [20].

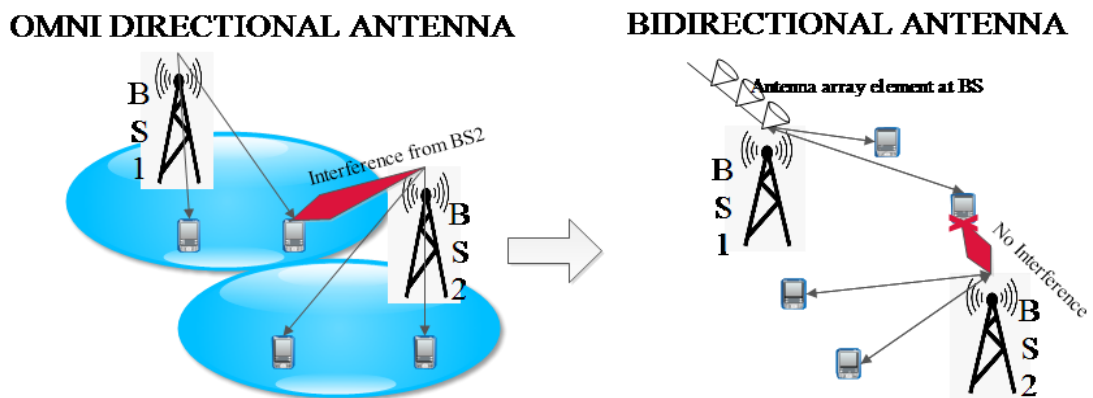


**Figure 1.7:** From omnidirectional to sophisticated beamforming directional antennas.

Another significant difficulty is the growing need for high data speeds. The C-RAN addresses some challenges associated with rising data-rate demands [21]. C-RAN provides mobility, EE, system design, and coverage efficacy while lowering network deployment and operating costs [22]. It is built on centralization and virtualization

concepts. Baseband resource pool at the remote central office's baseband unit [23]. Figure 1.8 depicts the C-RAN architecture. The shown reduced architecture paves the door for dense 5G deployment, making it adaptable, efficient, and cost-effective [24]. Powerful cloud computing handles the complicated control procedure with ease.

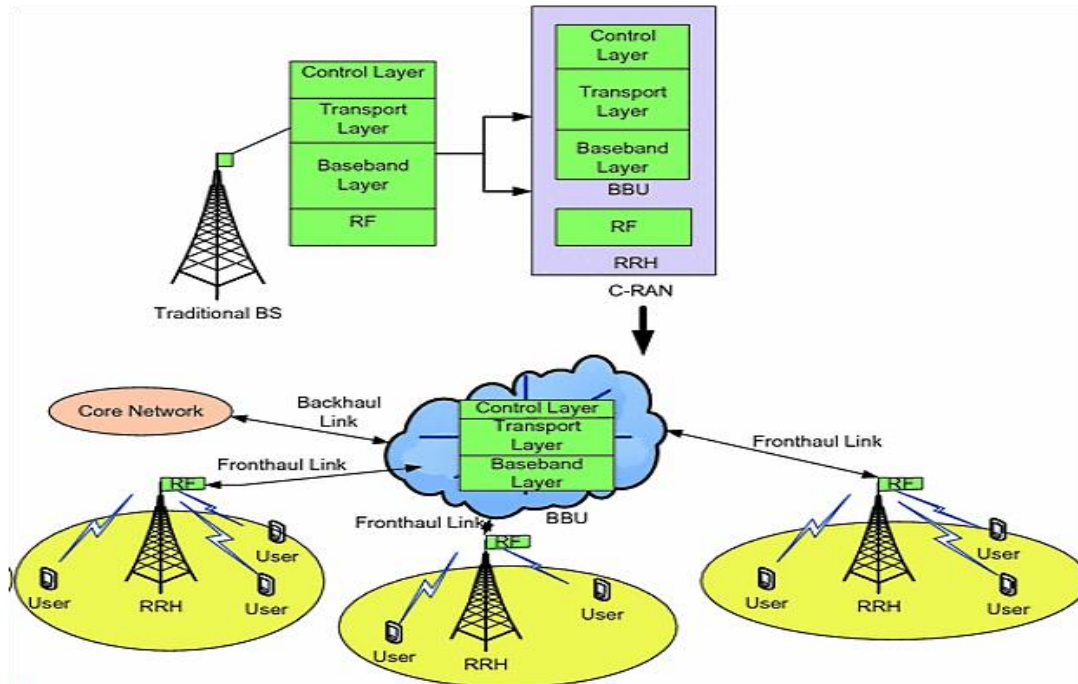


**Figure 1.8:** Architecture of C-RAN [25].

A huge number of tiny cells are installed in 5G wireless communication systems to accommodate traffic growth, resulting in HetNets. Aside from the heritage of macro cells, HetNets are made up of very tiny cells with little transmitted power. The deployment of reduced power base stations increases network capacity and extends coverage to coverage gaps [25-26]. The overlaying of tiny, pico, as well as femto cells with pre-existing macro cells results in better frequency reuse and effectiveness. Figure 1.9 depicts the HetNets architecture in relation to the 5G architecture. Smart handoff and location monitoring are employed in HetNets to provide smooth connectivity [27]. Small cells with diverse connection are a key component of 5G infrastructure. Directivity and design of tiny cell, together with

breakthroughs in resource allotment, hold promise for increased coverage and speeds of data in 5G WCS.

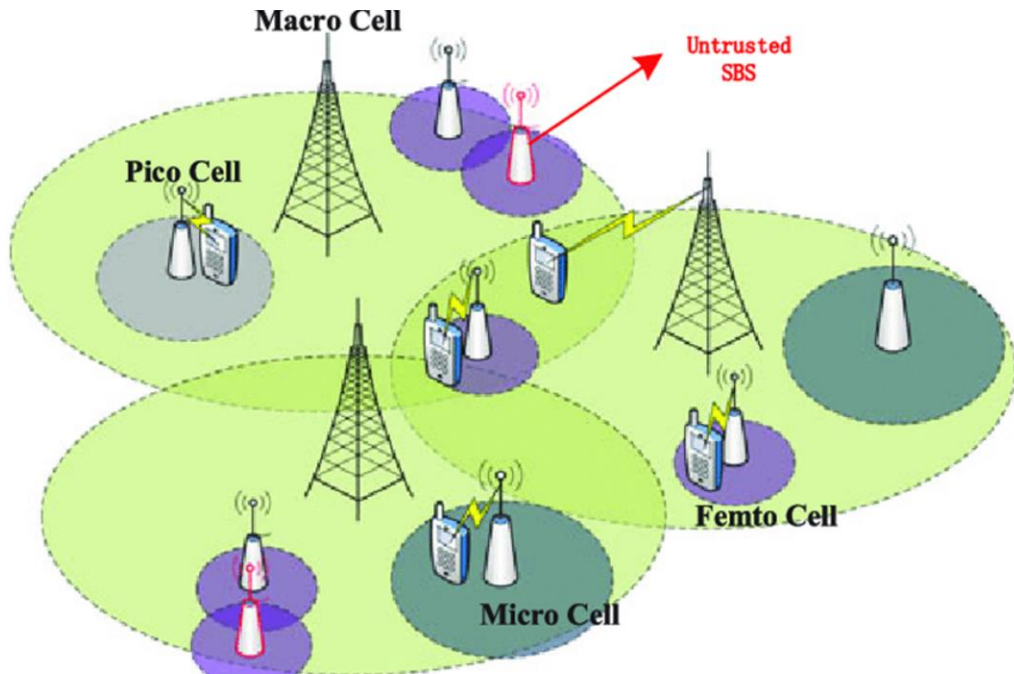


**Figure 1.9:** Architecture of a heterogeneous network [28].

The upgrades in 5G design increase the system's complexity. 5G must support many tiny cells with a raise in the number of antennas. It must configure and manage many servers and routers to keep the system running smoothly. As a result, a streamlined solution is necessary to reduce the system's complexity. The SDN provides a technique for minimizing system complexity. It will divide the control plane from the data, bringing flexibility to 5G WCS [28]. Figure 1.10 depicts the separation of client and control signals. Increase data rates at needed places without incurring the control plane overhead by separating the client plane from the control plane. Software components manage the control plane, which lowers hardware restrictions [29-30]. Open interfaces, similar to open flows, are used to interact with two planes, allowing for the switching of alternative configurations [31].

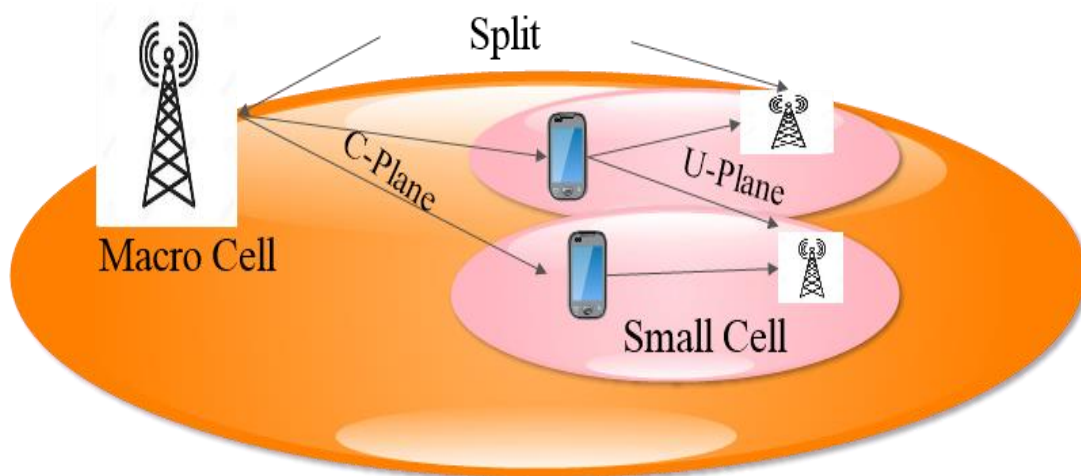


**Figure 1.10:** Separation of the client and the control plane.

#### 1.4 MASSIVE MIMO

In 5G wireless communication systems, the need for dependability, throughput, and user connectivity is growing. The need for multimedia applications necessitates high data transmission rates and reliance on communication networks. To circumvent this constraint, huge antennas are used to broadcast and obtain information at the same time. The technology of mMIMO is becoming increasingly prevalent in 5G WCS to increase both SE and EE. It is a sort of WCS in which the BS contains a huge number of antennas. In the current context, mMIMO technology is becoming increasingly important in the construction of 5G WCS architecture. It has mostly achieved success in the 5G WCS domains of LTE-A and LTE. They have been tailored to provide wireless subscribers with high data rate services. Figure 1.11 depicts how mMIMO delivers a larger number of antennas at the BS.



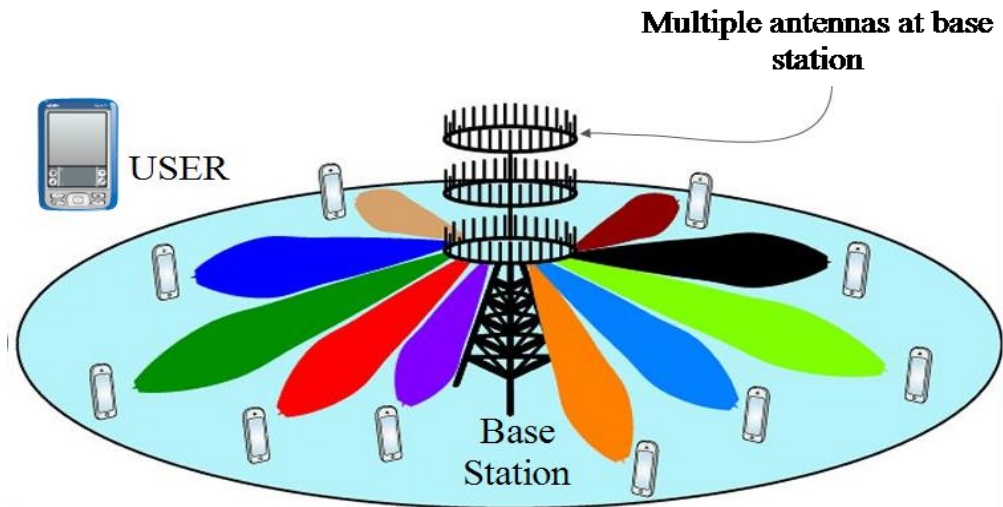


**Figure 1.11:** Fundamental structure of mMIMO.

mMIMO improves SE and EE [32]. Transmission directivity is obtained by placing each antenna at the base station [33]. The coherent superposition of wavefronts is the fundamental basis of mMIMO technology. The radiated wavefronts are constructively added at the required areas, reducing the intensity wherever it is unnecessary. In mMIMO technology, inserting wavefronts at the needed locations is known as spatial multiplexing, and it boosts bandwidth at the BS. As a result, advancements in modulation methods and the construction of appropriate algorithms are necessary for mMIMO.

It provides exceptionally high throughput while serving several customers at the same time. It also aids in solving the limitations of propagation losses through the use of beamforming processing methods. Small-scale fading is rejected depending on the orthogonality. mMIMO is an extension of MU-MIMO [34], in which the BS transmitter interlinks with many distant receivers at the destined time. It makes use of certain frequency-time domain resources, increasing spectrum effectiveness. Arrays of 100 or more antenna channels are used in mMIMO. Figure 1.12 depicts the many forms of MIMO systems. Large-scale antenna systems are another name for mMIMO.



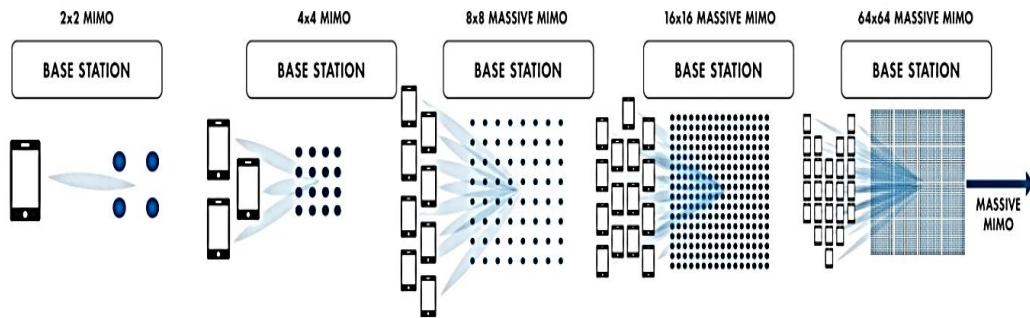


**Figure 1.12:** Different types of massive MIMO systems.

When compared with standards of LTE, mMIMO scales higher antennas in several numbers, whereas eight antennas are limited in LTE at the BS [35]. It also provides speed at the remote networks. It minimizes the chance of ergodic errors utilizing beamforming techniques, increasing network dependability. SNR variations are minimized when diversification approaches are used. To propagate through the multipath channel, the mMIMO network relies on spatial multiplexing and diversity. Spatial multiplexing is a form of multiplexing technique that employs several parallel data streams in the space between the transmitter and receiver. Figure 1.13 depicts the transmission and receiving system model for mMIMO.

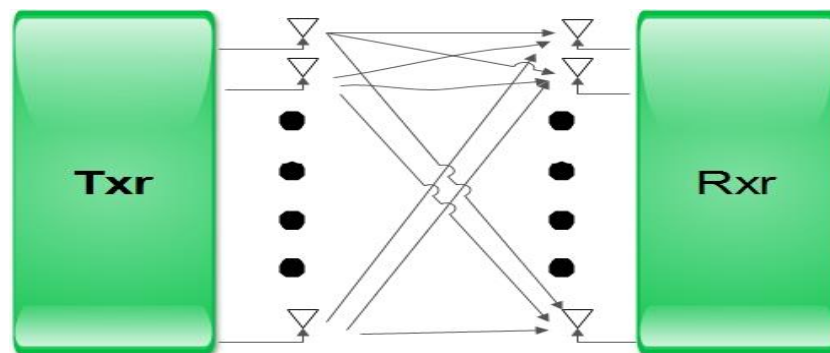


**Figure 1.13:** Model of mMIMO transmission.

The sophistication of the BS grows as the number of antennas rises since the channel vectors are not made orthogonal. TDD eliminates the sophistication involved with sharing of channel and CE in FDD. In mMIMO technology, dispersed antenna arrays and directional antenna arrays are also envisaged for future BS architecture.

mMIMO employs a lesser perishable power and low-cost components [36]. Because the circuit needed for such cells is tiny, the size of the antenna array is reduced. This is better suited to low-frequency mm-wave transmission [37]. As a result, the concerted impact of mMIMO technology with mm-wave is employed in 5G WCS, which advances toward future breakthroughs. Among the benefits of mMIMO systems are:

- Spectral Efficacy: Antenna arrays for UE primarily focus on narrow beams, allowing for excellent spectral efficacy. This spectral effectiveness is ten times that of current MIMO frameworks. It refers to the amount of information that may be delivered in a communication system across a certain bandwidth. It is a measure of how effectively the physical layer protocol and, the medium access control protocol uses a limited frequency spectrum. A digital communication system's link SE is measured in bps/Hz.
- Energy Efficiency: The antenna array is concentrated in a tiny specified location, reducing the radiated power.
- User Tracking: Because of the narrow signal beam directed at the user, the consumer tracking is precise and dependable.
- Less Fading: mMIMO is more effective over fading since it uses more antennas at the receiver end. [38].
- Lesser Latency: mMIMO devices minimize latency at the air interface [39].
- Stability: Interference and inner jamming are not a problem for mMIMO systems. It is also robust to one or two antenna failures. [40-41].
- Dependability: mMIMO systems have a large diversity gain, which boosts the reliability of system links [42].
- Increased Physical Security: Because of the orthogonality, it gives increased physical security [43].

Power consumption and channel reciprocity are the two key constraints of mMIMO devices.

- Energy consumption: mMIMO employs array design and spatial signal processing techniques to improve 5G standards and mm-wave range for distant equipment. As a result, power usage rises as the demand for this requirement rises.

Because BS quests for a specialized transmitter and reception module for each antenna element, consumes power and equipment costs rise. To address the issue of power consumption, hybrid beamforming is employed. The beamforming is divided into RF and digital domains. Multiple array antennas are combined to form the subarray modules. As a result, less send and receive are necessary to decrease power usage. Figure 1.14 depicts the hybrid beamforming design using the mMIMO antenna array.

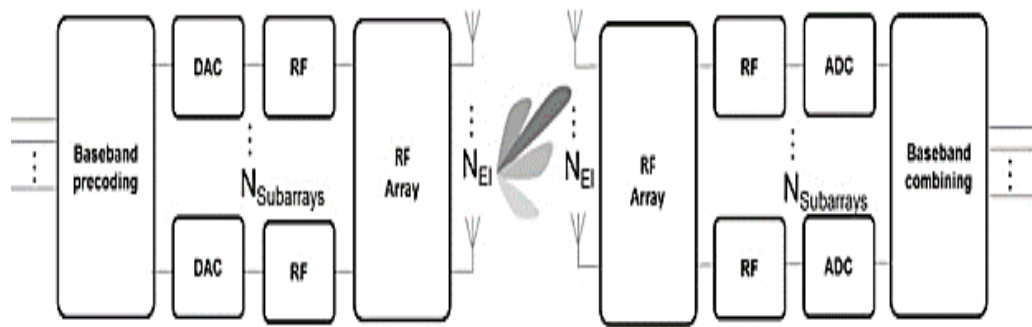


**Figure 1.14:** A hybrid beamforming design with a large MIMO antenna array.

- **Channel reciprocity:** In mMIMO systems, TDD and FDD versions are used. Because channel estimation depends on channel reciprocity, the mMIMO system performs well in TDD mode. Therefore, TDD mode is commonly assumed with mMIMO.

Contamination in the pilot, precoding, subscriber scheduling, CE, hardware limitations, and signal detection are the other significant problems of mMIMO systems.

## 1.5 5G OPEN ISSUES AND CHALLENGES

5G is a breakthrough technology that will alter the future of WCS. With new killer applications, current 3G/4G LTE networks will not be capable of sustaining greater data rates or enhancing spectrum efficiency. As 5G technology advances, researchers will be able to work on a broad range of design characteristics that will improve future WCS.

The following are the design parameters which compose a resource for 5G active research missions:

- Spectrum of mm-wave: The propagation properties of mm-wave are analogized to the existing beachfront. It allows investigators to investigate the spectrum range consisting of 3GHz - 300GHz for efficient utilization of BW capacity for transmission of data. Physics underlying the mm-spectrum includes scattering, doppler, propagation, atmospheric absorption, multipath, refraction, diffraction, and attenuation.
- Design of an anonymous channel: The development of an appropriate channel model is needed for accurate data transmission through the channel with no data loss. It needs a basic grasp of radio channels [44]. An in-depth study of channel models for outdoor, indoor and mm-wave communication is possible. The study raised the topic of the consequences of delay spread, angular spread, route loss, beamforming, NLOS propagation, and blocking [45].
- Reason for Array of antennas: Smaller wavelengths in mm-wave allow for a greater number of antenna components in an array on a smaller physical area. Larger arrays of antennas are required to capture beam energy coherently. For achieving directivity, research is being conducted in this direction for the development of both the BS and UE. The development of UWB antennas is a near-futurities research topic for 5G applications [46].
- Beamforming and training: Constructing a modem in real-time is an essential research requirement and an open problem for beamforming technologies that manage beamforming weights. This regulated weight of beamforming, which relies on beamforming architecture, results in the formation of a directing beam.
- Multiple access strategies: Another primary research goal is to develop unique multiplexing schemes to decrease the rate of interference and multipath interference. This is critical for NLOS and small cell deployment. This method is used in 5G WCS to achieve outstanding performance and low latency.
- Tiny cell deployment: Due to the apparent small cell installation, the BS density was predicted to be relatively high. Therefore, small cell architecture, often known as heterogeneous networks, is a crucial aspect of 5G research.

- C-RAN and H-CRAN: An essential prerequisite for 5G deployment is an EE and cost-effective solution. As a result, the C-RAN meets the criterion of the 5G as a research scope. Furthermore, the study involves a mix of C-RAN and heterogeneous networks known as H-CRAN, a more intricate design characteristic in 5G WCS.
- Low latency: A 1ms delay is required in a 5G WCS. It is accomplished by the investigator's efforts in the domains of non-orthogonality and asynchronism. Low latency research is also crucial in producing high QoE.
- Massive MIMO: An essential requirement in mMIMO is the number of tiny antennas at the BS. It presents a research challenge for developing an entirely new base station construction using a variety of small antennas and impulsive fewer power of antennas.
- 5G applications: The novel applications in 5G WCS contribute significantly to research directions. It is critical in meeting the problems of user connectivity and configuration [47].

**Table 1.3:** 5G WCS open issues and challenges towards research.

Research Challenge	Research Direction	Citations
Mm-wave Spectrum	Analysis of physics behind mm-waves	[6][7]
Channel Model	In-depth investigation of outdoor and indoor environment	[43][44]
Antenna Array	Design of smart antenna to attain desired directivity	[45]
Beam Training and Beamforming	Architecture for beamforming with protocols for beam alignment	[46]
Multiple Access Schemes	It requires novel multiplexing mainly for NLOS propagation	[19]
Deployment of small model	Introduction of HetNets for 5G WCS	[23]

C-RAN and H-RAN	Cost effective and EE novel design	[26]
Low Latency	A round trip latency of 1ms is required and investigation is going on	[9]
Massive MIMO	A several number of antennas at base station	[31]
5G Applications	Newer killer applications under 5G umbrella	[48]

## 1.6 5G APPLICATIONS

With improvements in software services, 5G architecture is planned to deliver network findings for a wide variety of corporate and public sectors, such as energy, city management, manufacturing, agriculture, transportation, and health care [49]. 5G networks offer a large number of connections while also supporting a wide range of devices and their service requirements. Figure 1.15 depicts some of the killer applications described in this study.

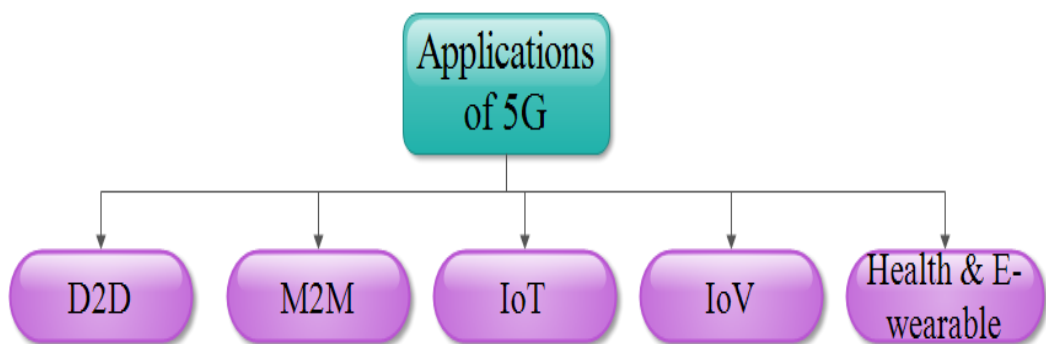


**Figure 1.15:** Applications of 5G wireless communication systems.

- i. D2D Communication: When enabled, the devices circumvent the cellular base station in order to exchange data with several other enabled devices [50]. It

enables 5G technologies to operate in a device-centric environment. Figure 1.16 depicts D2D communication.

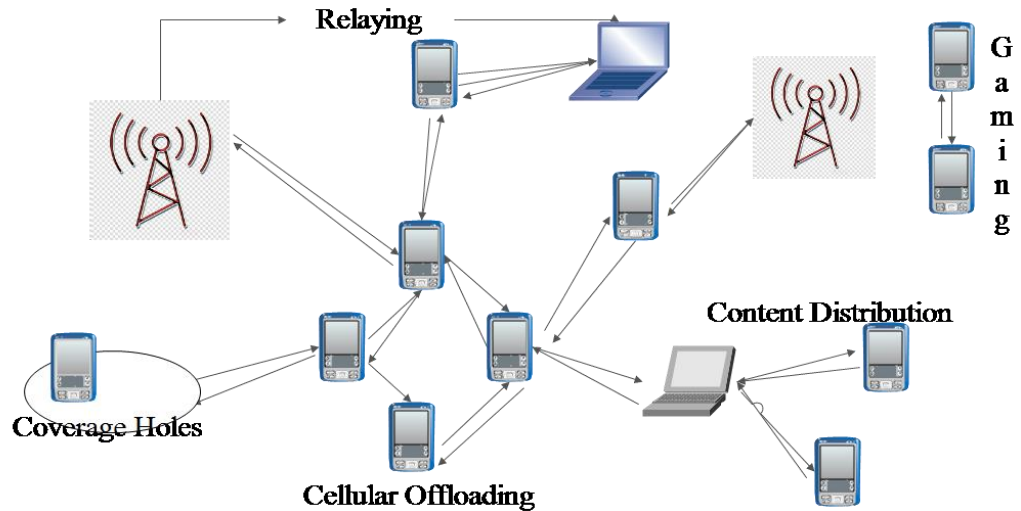


**Figure 1.16:** Device to device Communication.

It comprises prototypes for social networking, estimating the maximum permitted distance for commercial rollout, safety networks for the community, and pricing on game theory. In networks, D2D is used to limit operational signalling and end-to-end LL. It offers EE, scalability, and LL. It will also be aware of management for smart mobiles.

- ii. M2M communication: It is comparable to D2D type communication in many ways. These robots interact without using a cellular BS. The main characteristics are automated data production, processing, transport, and interchange between intelligent devices. It needs less human involvement [51]. Its objective is to integrate a large number of devices with tiny data transfer, high dependability, operation in real-time, and lesser latency. IoT also needs M2M. Figure 1.17 depicts M2M communication.

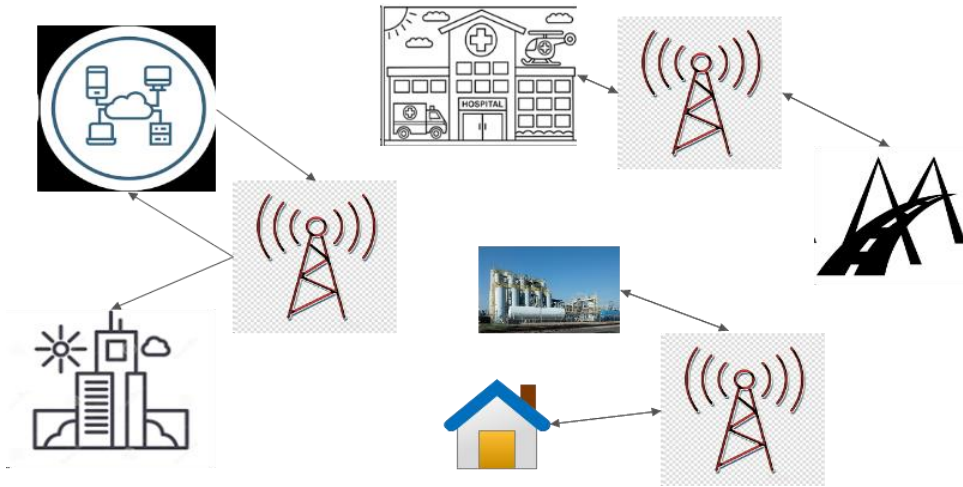


**Figure 1.17:** Machine to machine communication.

- iii. IOT: The IOT vision is to link a large number of devices at the same time, such as houses, smart grids, and intelligent transportation systems. Figure 1.18 depicts the IOT.

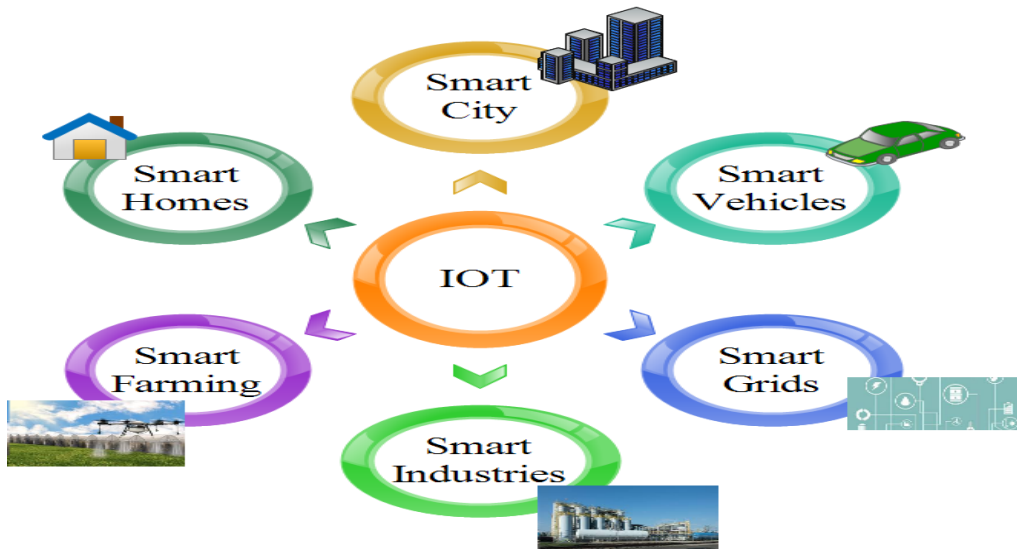


**Figure 1.18:** Internet of things and applications.

The IOT' slogan is to link everything, anybody, at any time, and everywhere. Linking these vast devices in several numbers needs more capacity for 5G WCS. The IoT



provides internet linking and data interoperability in a wide range of intelligent items and applications [52].

The 6 IOT difficulties are as follows:

- Configuration for automated sensor
- Discovery of context
- Acquisition, reasoning and modelling
- Service sensing
- Security, privacy, and
- Sharing of context

iv. IoV: The advancement of IoV is driven by the need for rugged traffic management and the deduction of collision risks [53]. With the involvement of IoT, which links automobiles, the vehicular communication system becomes intelligent. IoV necessitates hefty data that must be handled and transmitted in a secure and safe manner. IEEE 1609 standards for WAVE [54] have been created for IoV. Figure 1.19 depicts the IoV.

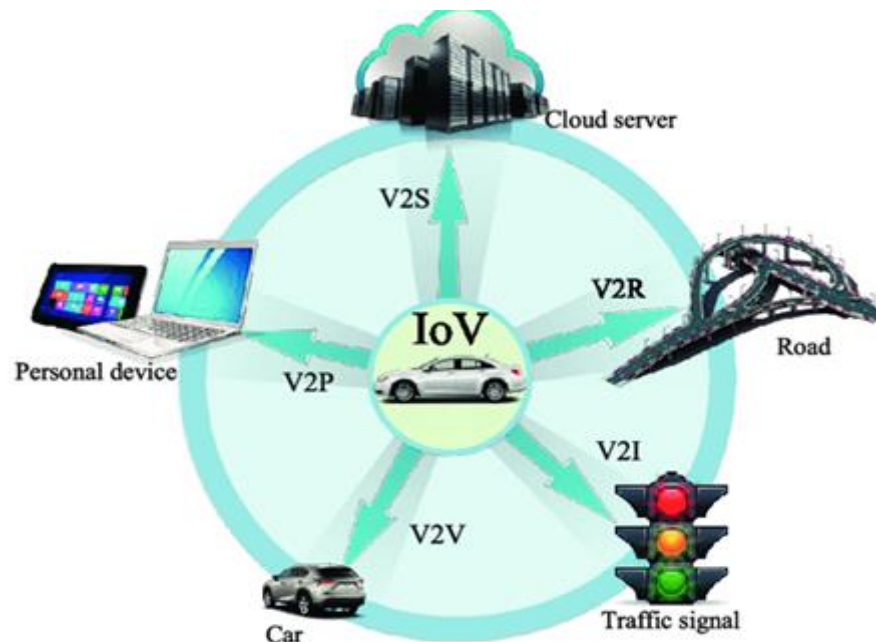


**Figure 1.19:** Internet of vehicles and its applications.

- v. E-Care and Wearable: Another possible use in the 5G WCS is wearable technology [55]. These gadgets can measure several physiological signs in an ambulance-like setting. It records many physiological signals over a lengthy period of time, which aids in illness understanding [56]. This, when paired with a BAN, permits a paradigm shift in remote patients' health monitoring in real-time. Figure 1.20 depicts the categories of wearable technologies.

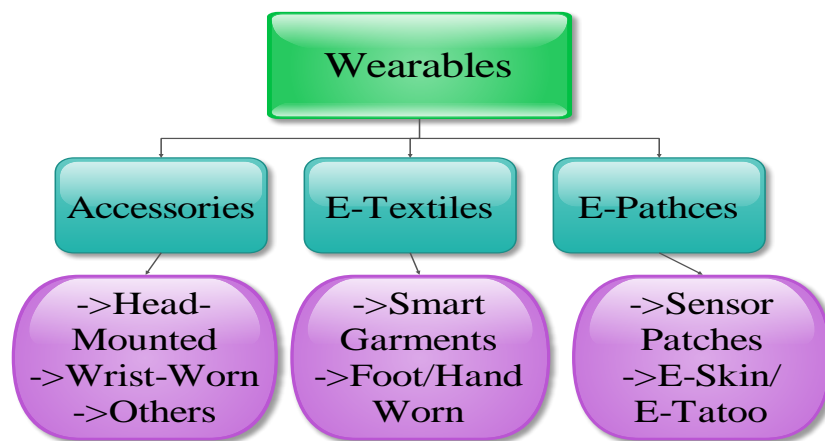


**Figure 1.20:** Classification of wearable devices.

Aside from this, there are also additional uses of 5G WCS, such as the financial industry, which has seen a surge in business and consumers that demand powerful computing and networking processing [57]. Future mobile networks based on 5G have greater potential for transitioning into various financial services [58], such as banking, payments, local commerce, and so on. It is also an essential mechanism for intelligent grids [59]. They provide large scale cyber-physical systems. 5G is also a foundation for automation in the home, providing security and reliability for all linked devices. All of these integrated solutions in 5G wireless networks pave the way for a new research path in killer applications for creating a smart world network. As a result, 5G systems overcome obstacles in 4G WCS, such as high data throughput, high SE, and LL. Symbols are often transmitted in wireless communication channels, and they encounter various detrimental consequences as they travel across the channel. This negative impact is caused by contact with surrounding objects like mountains and buildings, which causes multipath fading

and signal attenuation. In this regard, we must guarantee that sending signals are detected accurately. As a result, CE is extremely valuable in wireless communication systems. Precision CE is essential for the reliable detection of transmitted signals. CE allows the receiver to approximate the communication channel's CIR and predict/understand the impacts of the communication channel on the broadcast symbols. It is necessary for the accurate restoration of the information bits. Several CE approaches have been offered in the literature throughout the years to overcome the variable characteristics of the channel. The suggested solutions focus on improving system performance in terms of SER, BER, BLER, SNR, and WER. Some CE approaches even describe the decrease in computational sophistication.

## 1.7 MOTIVATION

mMIMO systems are critical in 4G wireless networks for delivering large data rates. It is quickly emerging as a potential technology for 5G WCS. To realize the enhancement in capacity provided by MIMO systems, the receiver or transmitter must have accessibility to CSI. Effective channel estimation methods are required to ensure communication performance. CE is a critical technique for eradicating ISI produced by multipath fading. As a result, efficient CE methods are required to ensure the functioning of mMIMO WCS.

The other main concern of the 5G WCS is the physical layer design for information transmission. Previously in 4G and the present, 5G uses the OFDM system to transmit information. However, the problem with OFDM is CP. CP is used in OFDM to reduce ISI but increases the symbol length by which OOB increases and the latency. So, the CE with an effective MCM technique is the primary work of this thesis.

This thesis major motivation is as follows:

- The available work on CE algorithms is focused chiefly on mMIMO OFDM systems. These current approaches may not apply to newer uses of 5G WCS. As a result, there is a need for a review of various MCM schemes suitable

for 5G WCS. Researchers will be motivated and understand the many forms of CE approaches and MCM as a result of this work.

- To study the existing CE techniques and based on the limitations, a channel estimation technique is proposed which is best suitable for MCM techniques other than the OFDM system. This study focuses on new CE and MCM approaches that perform better under more realistic channel situations.

## 1.8 THESIS OUTLINE

This thesis reports provides detailed explanation of 5G vision, mission, architecture and applications. It also explains about the MCM techniques and existing CE techniques. It mainly focuses about the proposed CE technique for different MCM technique. The complete process to achieve desired goal is divided into following chapters.

**Chapter-1:** It provides the explanation 5G WCS, vision, mission, architecture and applications.

**Chapter-2:** This chapter presents, the literature survey on the existing CE methods. It also explains the research gap, problem statement and contribution of this thesis. The research objectives and research methodology of thesis is also explained in this chapter.

**Chapter-3:** It provides a detailed explanation on the wireless channel models and CE techniques. It presents extensive literature review on existing CE methods along with the simulation results, advantages and disadvantages of these methods. The results are executed using the MATLAB software

**Chapter-4:** It explains the different types of MCM techniques that are better for 5G systems. It explains in detail about the system model of each MCM techniques. It compares the parameters such as PSD, signal power and BER to analyze the performance of each MCM technique.

**Chapter-5:** In this chapter, details explanation of proposed channel estimation using UPMC based 5G system is done. The proposed CE is compared with the existing conventional CE method such as LS and MMSE. The parameters such as BER and

MSE are used for comparison. It also compares the MELS UFMC with the other MCM techniques also. The results are executed using the MATLAB software.

**Chapter-6:** In this chapter, explanation is given about conclusions drawn from this research work and suggestion are given for future research work.

## 1.9 SUMMARY

This chapter starts with an overview of wireless communication technology and the many wireless technologies employed. It starts with the 5G vision and 5G architectures such HetNet, and C-RAN. Then, it mainly discusses mMIMO systems, which are majorly used in 5G wireless communication systems to achieve higher data rates and connect several numbers of users. It also discusses the advantages and limitations of the mMIMO systems. Based on the architecture and mMIMO system, it also discusses 5G applications. Later on, based on the advantages of 5G for newer applications, the motivation, research objectives, and research methodology of the research work are discussed. Finally, the outline of the complete thesis is specified.

## **CHAPTER-2**

### **STATE OF ART**

Many research groups have worked on a CE for OFDM systems and estimators' complexity. We discuss some of the methods which are related to existing CE techniques.

Some resources and resource scheduling are reserved at the BS and user equipment to predict a channel transmission design. These resources are used to send pilot or reference symbols. These symbols are recognized both at the BS and on the client equipment. The channel frequency response is calculated by correlating the obtained symbols with the pilot or reference symbols. First, the channel is used to send the reference pilot symbols. Next, these symbols are subjected to fading, attenuation, distortion, phase shifting, and other effects before being recognized at the receiver end and correlated with the broadcast signal.

#### **2.1 LITERATURE REVIEW**

Many research groups have worked on CE for for mMIMO 5G WCS.

Ye Li (2000) suggested a pilot-aided CE in WCS for OFDM. A non-rectangular channel correlation spectrum along both frequency and time directions is recommended for rugged CE, at least for finite-number observations. The pilot-aided estimator is unaware of the channel's statistical features. The MATLAB program carries out the simulation, and the results show an improvement in SNR compared to WER. As SNR grows, WER decreases, which improves system performance. A strong doppler frequency with noise impairment is evident for dispersive fading channels, notwithstanding some performance degradation for frameworks with modest Doppler frequencies [60].

K. Sathanathan et al. (2001) suggested investigating OFDM performance with phase noise and CFO. Orthogonality is lost in OFDM systems because they are susceptible to CFO and phase noise, resulting in ICI. As a result, the work

demonstrates system performance decrease. The statistical average of the ICI was one way, while the BER was another. Because ICI is considered to be Gaussian, BER may be estimated. A rigorous numerical approach calculates the influence of phase noise and CFO in an OFDM system on the BER/SER. For simulation, MATLAB software is utilized. The results demonstrate that the OFDM system's performance has deteriorated. So, a method that reduces ICI and improves estimation accuracy while conducting the CE technique must be suggested [61].

W. Song ping et al., (2004) and M. Jalloh et al., (2006) studied the impact of phase noise and errors of CE in Rayleigh fading that affects adaptation on OFDM systems. The work assumes little phase noise. Even at high SNRs, phase noise significantly degrades system adaptation. The inclusion of CE faults further harms the system. A phase noise degradation method enriches system adaptation for channel detection. MATLAB is the simulation software [62-63].

S. Mallick et al. (2008) provided a paradigm for performance analysis across Rayleigh fading channels in the presence of timing jitter, CFO, and phase noise in an OFDM system. Closed-form expressions are used to calculate the SINR. Synchronization issues are demonstrated using BER execution for a BPSK-OFDM architecture over a Rayleigh fading channel. MATLAB is the simulation software. SINR suffers penalty due to CFO and jitter in OFDM systems when phase noise becomes more prevalent. Jitter, CFO, and the effect of phase noise all degrade mMIMO system performance [64].

Lashkar et al. (2012) suggested a framework for CE based on the LMS approach. His study utilized the LS approach for the initial CE estimate. The LMS method was used to uprise the accuracy of CE. The receiver promises output feedback and increases the system's BER performance. The effectiveness of the LMS algorithm is primarily determined by a coefficient" that ranges from 0 to 1. If the coefficient value is meager, the method performs well in terms of SNR. The simulation is carried out using the MATLAB program, and the results show that the approach has poor BER performance [65].

Madhurendra Bengan et al. (2012) suggested a framework for monitoring OFDM systems that use the EKF to reduce phase noise. They have expanded their research on the Kalman filter to identify phase noise and suppress it in the OFDM

transmission. MATLAB is the simulation software, and the findings show that the EKF is effective for OFDM systems [66].

Peng Xu et al. (2015) provided analysis and design of multicell multiuser MIMO OFDM systems. For multipath and multicarrier channels, the strategy was developed to limit pilot contamination. A simple H-infinity CE technique was devised to reduce polluted pilot symbols and estimate a better channel. SAGE maximization employs an iterative technique to break down a multicell multiuser MIMO (MU-MIMO) system into a succession of single cell single, user SISO systems. The performance of the proposed CE algorithm is not impaired if the number of antennas at the BS is raised using the SAGE process. The approach was created primarily for use in uplink multicell MU-MIMO systems. To minimize the complexity of systems, the SAGE iterative approach is used. MATLAB is the simulation software, and a comparison graph is created for several CE strategies. The assumption is that each cell has three cells and ten users, with pilot sequences reused [67].

Dongjage Lee (2016) suggested a block StOMP CE framework for mMIMO. The StOMP method is presented to tackle measurement for multiple vector issues utilizing frequency selective channels. This solution is utilized to solve the problem in FDD mMIMO systems. MATLAB is the simulation software, and the results indicate the adaptation of the framework in relation to BLER. It improves the system's performance accuracy [68].

Qibo et al. (2018) suggested a sparse CE framework for mMIMO OFDM, which includes time-varying channels. The suggested approach is primarily intended to downlink OFDM across a time-varying channel. However, it isn't easy to compute many channel coefficients over time-varying channels. This issue was solved by the QBSO method, which was suggested using sparse channel estimation. The BEM is used in CE to minimize the number of channel coefficients. To increase recovery accuracy, the adaptive QBSO approach is also used. MATLAB is the simulation software, and the results reveal an uprise in the accuracy of the channels calculated by utilizing sparsity in the delay domain [69].

Chih et al. (2018) presented papers for MIMO-OFDM systems on Joint AoD, AoA, and CE. This approach was created with the reception antenna to properly estimate the channel. The CS approach is utilized for CE. This approach also makes use of



the sparsity aspect of wireless channels. After using the CS technique, AoA and AoD are merged to estimate each identified route. The training symbols are decreased in the approach, and just two pilot symbols are utilized for an estimate, reducing computing complexity. MATLAB is the simulation software, and the results display a reduction in MSE concerning the CE error power ratio [70].

To decrease computational complexity, Imran et al. (2018) suggested a channel estimation strategy for 5G WCS. The approach presented was for mMIMO systems. The approach suggested is a hybrid SDGS joint detection is mostly used to minimize computational complexity in CE. This approach was created to address the issue with the matrix inversion method used in MMSE CE algorithms. For signal identification in soft decoding, a channel, bit LLR is employed. MATLAB is the simulation software, and the CE technique results show improved performance with signal detecting capabilities by 31.68 percent and a 45.72 percent reduction in computational complexity. The comparison graph for BER concerning SNR for several CE techniques is generated. The approach is still used in typical MIMO systems with 4x4 or 8x8 scale systems. Although the suggested SDGS technique decreases computing complexity by orders of magnitude, there is still room for improvement in channel identification performance [71].

Elina Nayebi and Bhaskar D. Rao (2018) suggested a semi-blind CE in mMIMO frameworks that uses different priors on information symbols. Two double CE computations linked to EM are proposed. For the ambiguous information symbols, one depends on a Gaussian earlier and the other on a GMM. The analytical results show that semi-blind estimation strategies provide more significant CEs than an estimate based on training symbols alone. In a low SNR system, the EM calculation with a Gaussian prior produces better CEs than the EM calculation with a GMM prior. Regardless, the latter one beats the EM calculation with Gaussian earlier as the SNR or as the massive antennas at the BS increments. Furthermore, when the number of receiving antennas at the BS increases, the presentation of the semi-blind CE approaches that of the genie-supported ML estimator based on known information symbols. MATLAB programming is used for simulation [72].

Hayder AL-Salihi (2018) suggested channel estimation algorithms based on DFT for mMIMO frameworks. In mMIMO systems, productive and highly accurate CSI

at the BS is a critical prerequisite for dealing with the influence of pilot defilement and reaping the full benefits of the frameworks. The proposed solutions eliminate pilot contamination by modifying the DFT-based estimate through cycles and the essential tapping approaches. The simulation findings obtained through these techniques demonstrate the usefulness of DFT-based direct estimation strategies in removing pilot contamination compared to standard channel estimators as per CE accuracy for uplink rate [73].

Kuai and colleagues (2019) suggested a hierarchical turbo CS computation for mMIMO CE. To decrease pilot overhead, the CS approach is used. Structured turbo CS is a common generic framework for organized sparse signal restoration. Figure 2.1 depicts a structured turbo-CS architecture. For organised sparsity, probability models such as angle delay and frequency domain are utilised. The suggested framework has the advantages of decreased processing complexity, reduced storage needs, and speedier convergence, resilience, and error performance. For the recommended technique's performance calculation, simulation software is MATLAB [74].

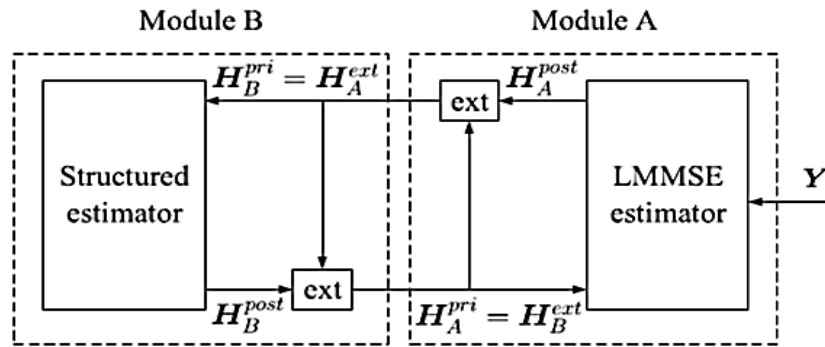


**Figure 2.1:** Structured turbo compressed sensing block [74].

Araujo et al. (2019) suggested a CE strategy for mMIMO systems based on tensors. The primary goal of CE for mMIMO frameworks is to attain the standard benefits in terms of SE and EE. By foregoing spectral effectiveness, a large number of pilots are scattered throughout countless time frequency resources to estimate massive

channel coefficients in space and frequency areas. To address this issue, a tensor compressive sensing approach with a formulation for TOMP was presented. This approach compressively samples the channel in frequency, time, and space. MATLAB is the simulation software, and analysis is performed to calculate the adaptation of the suggested method. In analogy to SNR performance, the performance calculation demonstrates an increase in SE and EE [75].

Anthony et al. (2019) developed extremely mobile SE mMIMO systems for doubly selective channels based on DCS CE. This DCS-sdmp method, which includes a novel pilot, is primarily intended to prevent ICI. Figure 2.2 depicts the use of a pilot cluster design in the frequency domain.

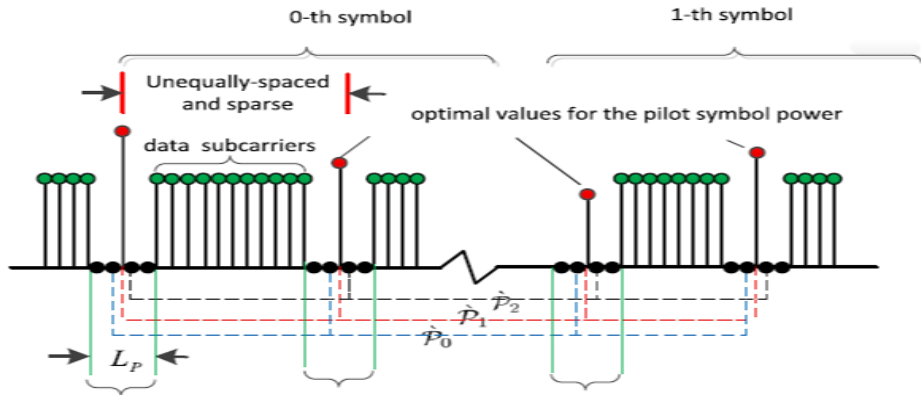


**Figure 2.2:** Optimal pilot symbol placement [76].

Jakes channels are employed with a wide range of doppler spreads and in the doppler delay domain (i.e., 2-D channel coefficients). MATLAB is the simulation software, and the performance calculation of the suggested approach shows a 25.56 percent gain in SE compared to the standard LS CE technique [76].

For selective mMIMO systems, Javad et al. (2019) offered a semi-blind time domain CE approach. At CE, the channel coefficients should be repeated in the frequency flat process for each frequency slot. The number of channel coefficients calculated in the frequency domain is more significant than the number of channel coefficients estimated in the time domain. As a result, a subspace-based strategy is used, with a

solution based on the discovered signal's eigenvectors and covariance matrix. Figure 2.3 depicts a time domain channel model between the client's cells.

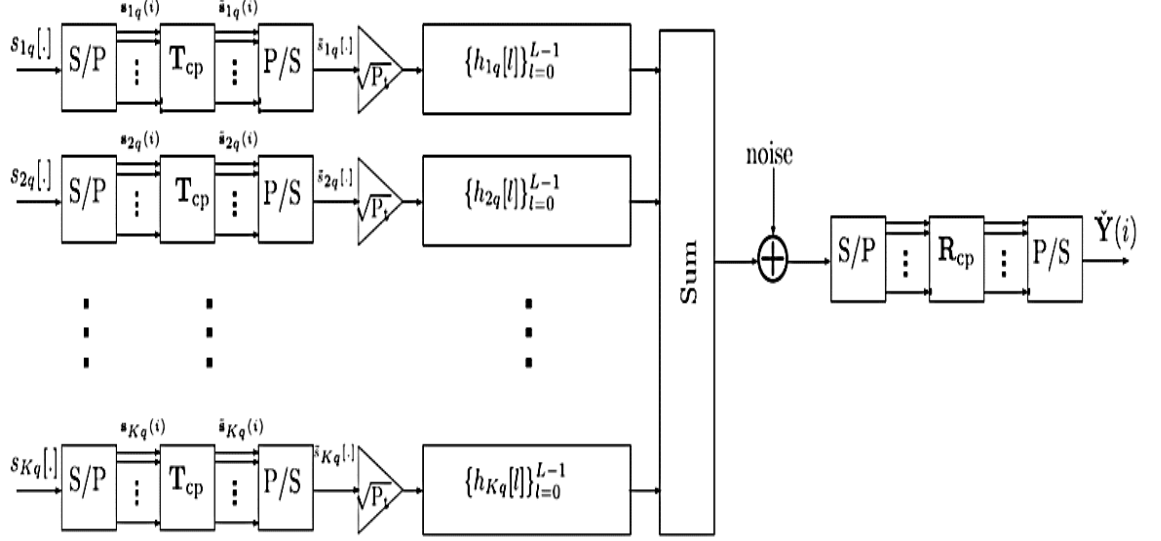


**Figure 2.3:** A cell for time domain channel model [77].

A collection of training symbols is employed as a linear combination of signal eigenvectors is evaluated. Because orthogonality between training symbols is not needed in all cells, contamination in the pilot is also decreased. MATLAB is the simulation software, and analysis is performed to calculate the performance of the suggested method. According to the simulation results, time-domain estimation beats traditional frequency-domain estimation [77].

DCS CE for mMIMO systems was proposed by Abbas et al. (2019). In mMIMO-OFDM frameworks, the stFBP computation approach is employed to calculate joint sparsity. It improves estimating accuracy and convergence. The technique is to construct a large number of large atoms in frequent advancement and to leverage basic sparsity in the framework individually. A retrograde step enhances precision by removing bad recently formed atoms. MATLAB is the simulation software, and analysis is performed to calculate the adaptation of the suggested method. The findings of the simulation are compared to those of the well-known ABSP CE approach. The accuracy of the estimate is demonstrated by simulation results [78].

Yuan et al. (2019) established a novel adaptive greedy CE approach in MIMO systems. It is also a CS method that employs a NAMP strategy. The strategy of this calculation is to handpick atoms with constant step size and expel the segments of low energy by singular entropy request assurance in the sparse solution for boosting effectiveness and providing reduced computational complexity. MATLAB is the simulation software, and analysis is performed to calculate the performance of the suggested method. The SAMP algorithm is used to simulate the outcomes of the NAMP method comparison. The simulation findings display that MIMO is a more enhanced system [79].

Imran Khan et al. (2019) proposed an aggressive CE for 5G mMIMO frameworks. Because of the large pilot overhead, CSI criticism in large MIMO frameworks is disproportionately large. Pilot overhead is caused by massive channel matrix measurement, which is relative to the quantity of BS antennas and utilizes the vast majority of valuable radio resources. To unravel this issue, an effective CSI acquisition strategy and a lowered pilot overhead plan are necessary. It is determined by the channel matrix's partition component. Spatial correlation is used to split channel matrices among MU channel matrices in terms of virtual angular. At that time, an equal fraction of the matrix is assessed using CS techniques. In this technique, the UE simply passes the acquired data from BS to the device, resulting in a combined recovery of CSI at the BS. In comparison to other ways, the suggested CE results congregate properly to predict the channel with less pilot overhead and better execution [80].

Prem Singh et al. (2019) suggested a time domain CE based on a preamble for the MIMO-FBMC framework that relies on OQAM. The time domain configuration doesn't require that the symbol time be more than the channel's delay spread. As a result, it is compared to the frequency domain CE model relay on the IAM. For the time domain, the WLS and MMSE CEs for MIMO-FBMC/OQAM frameworks are inquired. The CRLB is found for the IAM, MMSE, and WLS estimators. All of the CEs achieve their respective bounds, and the suggested MMSE and WLS estimators fundamentally outperform the present IAM CE. The work is also approved by the correlation of the BER execution of the earlier estimators mentioned [81].

Riadi and colleagues (2020) suggested an LS CE method for mMIMO-OFDM systems. In this mMIMO system, the transmission antennas are kept constant at 50, while the detector antennas are raised from 50 to 200, demonstrating the framework's efficiency. The system's efficiency is also increased by employing linear ZF and MMSE detectors. The mMIMO system demonstrates BER reduction in relation to SNR. This strategy is used to increase the system's performance. MATLAB is the simulation software. The simulation investigations also reveal that the BER for the MMSE linear detector is lower than that of the ZF linear detector [82].

Jianqiao Chen and Xi Zhang (2020) developed a SBL CE plot for recovering block-sparse uplink links in TDD mMIMO-based 5G mobile systems. A pattern combined with multiple levels of Gaussian preceding explains the reliance of a sparse channel among neighboring antennas, and a birth passing process is used to represent dependent coefficients. The hyper parameters are inferred and used to grasp the sparsity of the channel coefficients. Iteratively improving an EM plan provides a lower constraint on the back probability. In the M-step, a PSO algorithm is used to effectively increase the lower limit. Finally, a BP-PC-SBL computation is developed to recover block sparse uplink channels. As a result, while updating the data, they had to refresh their techniques and variances. The BP-PC-SBL calculation yields the same exact matrix approximation reversal as the standard SBL calculation, which boosts effectiveness in terms of computing complexity. The numerical assessments use MATLAB software to authorize and analyze the efficacy of proposed procedures and computations [83].

Khushboo et al. (2020) suggested a semi-blind CE based on SAGE for pilot polluted MU- mMIMO setups. It employs a few information symbols and a pilot for CSI estimation in 2 stages, namely initializing and ISAGE. In the introduction step, an underlying CE is obtained with the aid of a training-supported linear MMSE estimator. Early estimates are acquired and iteratively refreshed by SAGE computation with the combined usage of the pilot and a few information symbols collected from the previous stage in the ISAGE stage. The introduction of information data into the ISAGE phases' estimating technique aids in the simultaneous development of CSI accuracy and SE of a mMIMO framework, which

is unlikely for training-based CE. At an evident increase in complexity, the simulation indicates that the estimator achieves a considerable improvement over the present pilot-aided plans in terms of MSE, BER, SE, and EE. In general, it completes assembly in approximately two cycles. To validate the estimating skill, an altered CRLB is used. It also evaluates a CFE for a lower constraint on the UL possible speed of MU-mMIMO frameworks under both good and bad CSI conditions. It also discusses the compromise reached with both SE and EE. [84].

Yong Liao et al. (2020) presented a powerful CE based on a nonlinear Kalman filter (NKF) for high flexibility OFDM frameworks. For non-fixed time domain and high mobility situations, an NKF channel is proposed. This is intended for fading channels in the frequency selective domain. A BEM is received to rid of the ICI caused by the rapid time-shifting features. A channel interpolation computation is performed for non-fixed channel properties during high mobility. It is dependent on EKF, who is familiar with integrated CIR estimation and time correlation coefficients. To prevent error propagation, the EKF CE employs a feedback decision framework to construct the perception matrix. Through hypothetical induction, the paper dissects the age of mistake propagation. The computation of the UKF illustrates the error propagation in EKF to conduct a Gaussian estimate of the non-Gaussian observing framework. It reduces the impact of KF. Simulation outputs display that the CE exactness of BEM-UKF is also enhanced. When compared to previous approaches, it is discovered that the influence of pilot distance is minimal, which boosts the calculation's resilience [85].

Eren Balevi et al. (2020) suggested a DNN CE approach for interference in multi-cell limited mMIMO frameworks. BSs equipped with a large antenna service for many one-to-one antenna clients. The suggested CE employs an especially designed DNN based on the DIP system to initially de-noise the obtained signal, followed by a typical LS CE. It is proved diagnostically that LS-type deep CE may proceed toward MMSE CE implementation for high-dimensional signs while avoiding complicated channel reversals and channel covariance network information. This explanatory, albeit asymptotic, is evident in execution, where they are only operational for 64 subcarriers and 64 antennas for each OFDM signal. The proposed

method does not need learning and uses far fewer boundaries than typical DNNs. The suggested deep CE is also strong enough to control contamination and, in some instances, eliminate it [86].

Han Wang et al. (2020) proposed an FBMC with offset OQAM as physical layer advancements in future WCS. IoT requires good remote transmission innovation. However, one of the difficulties in recognizing profoundly accessible FBMC systems is the productive CE parameter. A BCS CE approach is being investigated for FBMC/OQAM frameworks. This approach, which is given in a MIMO scenario, is also broken down. For high CE, an iterative rapid Bayesian MAP computation is proposed. The initial computation introduced by studying previous statistical data of a sparse channel is known as Bayesian CE. It has been proved that the BCS CE plan can successfully evaluate the CIR. A modified FBMP computation is presented to streamline the iterative end conditions. The simulation results display that the suggested approach outperforms traditional CS techniques as per MSE and BER execution [87].

Chien et al., (2021) proposed a novel CE approach that uses deep learning to support LS estimation, a low-cost method with relatively significant CE errors. It is accomplished by employing a MIMO system with a multi-path channel profile for simulations in 5G networks under the severity of Doppler effects. In terms of MSEs, numerical findings show that the proposed deep learning-assisted CE approach outperforms other CE methods in prior research. The problem with this method is that the use of the OFDM and design complexity increases as the number of test vectors increases [88].

Zhang et al., (2022) proposed an artificial intelligence-based channel estimation technique for high-speed networks. In this method CNN and long short-term memory of a channel are used to extract temporal features. The architecture of channel net is depicted in figure 2.4. A reference-based algorithm is used for training and proposed algorithm is will enable artificial intelligence channel net is used to track the channel variation in high-speed networks. The proposed method outperforms better compared to conventional CE methods w.r.t BER and throughput. The proposed method also works good without the change in the radio



frame of 5G and also without the loss of transmission efficacy. The main limitation of this method is computational complexity [89].

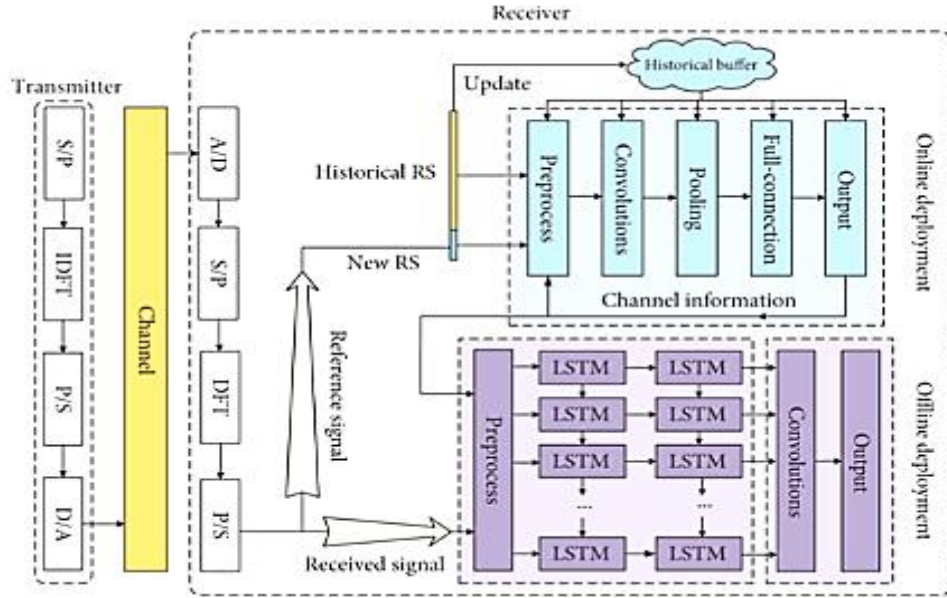


**Figure 2.4:** Architecture of artificial intelligence channel net [89].

**Table 2.1:** Highlights of existing CE for OFDM system.

Reference	Journal/ Conferences	Proposed Algorithm, Analysed parameter, Findings
Ye Li (2000) [60]	Institute of Electrical and Electronics Engineering	Pilot aided CE, WER, System performance enhancement
K. Sathananthan et al., (2001) [61]	Institute of Electrical and Electronics Engineering	Phase noise reduction using filters, WER, BER, Degradation of performance because of phase noise

M. Jalloh et al., W. Song ping et al., (2004- 2006) [62-63]	Institute of Electrical and Electronics Engineering	Filters, Weiner phase noise w.r.t SNR, Suppression of phase noise
S. Mallick et al., (2008) [64]	International Conference on Electrical and Computer Engineering	Filters, BER, System performance enhancement
Aboozar lashkari et al., (2012) [65]	International Journal of Computer Science Issues	LMS, BER, System performance enhancement
Madhurendra Bensan et al. (2012) [66]	International Conference on Computational Intelligence and Communicatio n Networks	EKF, SNR, Suppression of phase noise
Peng xu et al., (2015) [67]	Institute of Electrical and Electronics Engineering	SAGE, MSE, Lowered pilot contamination
Dongjage lee (2016) [68]	Institute of Electrical and Electronics Engineering	stomp, BER, System performance enhancement
Qibo et al., (2018) [69]	Institute of Electrical and	QBSO, BER, System performance enhancement

	Electronics Engineering	
Chih et al., (2018) [70]	Institute of Electrical and Electronics Engineering	CS, Joint AoA, AoD, MSE, Reduced computing complexity
Imran et al., (2018) [71]	Institute of Electrical and Electronics Engineering	SDGS, BER, Reduced computing complexity
Elina Nayebi and Bhaskar D. Rao, (2018) [72]	International Conference on Acoustics, Speech and Signal Processing	Semi-blind CE, BER, System performance enhancement
Hayder AL-Salihi., (2018) [73]	International Conference on Telecommunications	DFT based CE, BER, Performance improvement in system
Kuai et al. (2019) [74]	Institute of Electrical and Electronics Engineering	Structured CS, Reduced computing complexity, minimal storage needs, better convergence speed, resilience, and error performance
Araujo et al., (2019) [75]	Institute of Electrical and Electronics Engineering	TOMP, Improvement in SE and EE
Anthony et al., (2019) [76]	Institute of Electrical and	DCS-sdmp, To cobat ICI, Improvement in SE

	Electronics Engineering	
Javad et al., (2019) [77]	Institute of Electrical and Electronics Engineering	Semi-blind CE for frequency flat channels, BER, Performance refinement in system
Abbas et al., (2019) [78]	Institute of Electrical and Electronics Engineering	stFBP, BER, exactness of the system
Yuan et al., (2019) [79]	Institute of Electrical and Electronics Engineering	NAMP, BER, up rise in efficacy of system
Imran Khan et al., (2019) [80]	Institute of Electrical and Electronics Engineering	CS, BER, to reduce pilot contamination in the channel & to improve adaptation of the system
Prem Singh et al., (2019) [81]	Institute of Electrical and Electronics Engineering	Time domain CE based on preamble for FBMC, WLS & MMSE, BER, Improve performance of the system
Riadi et al., (2020) [82]	Institute of Electrical and Electronics Engineering	LS, BER, to reduce pilot contamination in the channel & to improve adaptation of the system
Jianqiao Chen et al., (2020) [83]	Institute of Electrical and Electronics Engineering	BP-PC-SBL, recovery of block-sparse uplink directs in TDD mMIMO, Reduction in computational complexity

Khushboo et al., (2020), [84]	Institute of Electrical and Electronics Engineering	SAGE based Semi-blind CE, Concurrent enhancement of CSI precision and spectral effectiveness
Yong Liao et al., (2020) [85]	Institute of Electrical and Electronics Engineering	UKF, Reduction of ICI & impact of pilot distance is low for non-Gaussian system
Eren et al., (2020) [86]	Institute of Electrical and Electronics Engineering	Untrained DNN, MSE, to reduce pilot contamination in the channel
Hang et al., (2020) [87]	Hindawi, Wiley	BCS, MSE & BER, Reduction in computational complexity
Chien et al., (2021) [88]	International Conference on Ubiquitous Information Management and Communication	LS using Deep learning, BER, MSE, Increase in performance of the system
Zhang et al., (2022) [89]	Hindawi	AI-based CE scheme for 5G WCS, BER, Throughput, Improve communication performance in high-speed networks

Table 2.1 summarises the authors' contributions to CE techniques for OFDM systems. However, there is still a need to develop CE algorithms for sophisticated MCM systems, which will boost the effectiveness of 5G WCS.

## 2.2 RESEARCH GAP

- Major of present channel estimation techniques is implemented for LTE, 3GPP, Massive MIMO 4G systems only.
- CE techniques are implemented majorly for mMIMO-OFDM systems only.
- One of the CE algorithms yields a computational complexity reduction of 45.72% with a signal detection of 31.68%.
- CE methods that are used to combat ICI and to reduce pilot contamination scales a signal detection of 25.56% only with SE of 14 bits/sec/Hz at a SNR of 50 dB.
- A channel estimation yields a bit error rate of  $7.43 \times 10^{-5}$  for SNR of 15dB & 100 antennas.
- For semi blind channel estimation BER is  $5 \times 10^{-5}$  for 250 antennas, 24 pilot symbols and transmitter power of 20dBm.
- In FDD mode having low feedback overhead with low training implementation is difficult.
- Implementing massive MIMO system in TDD mode leads to pilot contamination.
- An efficient CE for combined uplink and downlink scenario is still an issue.

## 2.3 PROBLEM STATEMENT

From the above research gap, it is evident that there is still a requirement in designing the effective CE for the 5G WCS. The first problem is the choice of MCM techniques other than OFDM in the design of a 5G system for the transfer of information. The second problem is the design of an effective CE technique that provides higher data rates, low bit error rates, low mean square error, low complexity, and high accuracy.

## **2.4 RESEARCH OBJECTIVES**

The research objectives are as follows

- i. To study and analyze existing massive multiple input multiple output-based channel estimation techniques.
- ii. To propose and design an effective channel estimation for multicarrier modulation based on Massive MIMO system.
- iii. To optimize channel estimation parameters such as BER, MSE with respect to SNR.
- iv. To verify and compare the results using analytical and Monte Carlo analysis.

## **2.5 RESEARCH METHODOLOGY**

To fulfil the aims of this research, a pragmatic methodology was used. The methodology employed may be summarised as follows:

- i. Examine the current CE methods for Massive MIMO systems.
- ii. To examine MCM methods that are most appropriate for mMIMO systems.
- iii. Using MATLAB software, create an effective CE approach for MCM mMIMO systems.
- iv. Analytical and Monte Carlo simulation is used to examine CE parameters such as BER and MSE in relation to SNR.
- v. Finally, the executed algorithm's performance is compared to the current CE methods.

## 2.6 CONTRIBUTION

The main contribution of this thesis is:

- Existing channel estimation techniques are analyzed based on the OFDM system.
- The choice of the best suitable multi-carrier modulation technique is analyzed based on BER and MSE.
- From the above analysis, the UFMC MCM method is chosen to transfer information in 5G systems.
- MELS CE technique is designed for the UFMC system and is compared with the existing conventional CE techniques such as LS and MMSE CE techniques.
- Finally, the designed MELS CE is used for other MCM techniques, and it is compared which it is shown that UFMC outperforms better compared to other MCM techniques.

## 2.7 SUMMARY

This chapter starts with a retrospection of the existing CE techniques. This chapter discusses mMIMO-OFDM system analysis with existing channel estimation methods. In addition, this study investigates pilot design, positions, and various channel estimate strategies. Then, based on a literature review, the research need is identified, and the primary findings of the present study are specified. This chapter also specifies the research objectives of the thesis along with the methodology to satisfy objectives.



## **CHAPTER-3**

### **MULTI-CARRIER MODULATION**

#### **3.1 INTRODUCTION**

Another new developing technology in 5G is multi-carrier modulation, which alters the MAC layer. The new CW or MCM is being deployed to support mMIMO BSs. CW forms are used to make the most of the restricted frequency spectrum. The availableness of frequency spectrum creates a significant need in WCS. Because of the rapid expansion of WCS, the frequency spectrum is becoming a limited resource [90] [91]. As a result, MCM techniques are employed in the 5G wireless communication system. CW's previous problems include complexity in designing, temporal localization, ruggedness, scalability, adaptability, OOB, and PAPR. As a result, new MCM methods are being developed to circumvent these wave patterns. The idea behind MCM is to divide high information rate transmissions into numerous lower information rate signals. Lesser information rate signals are again modulated onto orthogonal narrowband subcarriers. It facilitates synchronous data transfer across the wireless channel [92]. Splitting wideband signals into small band orthogonal signals provides excellent SE. This is because the orthogonal signals overlap during channel division. A novel MCM approach is devised [93] based on propagation channel parameters, hardware limitations, and spectrum confinement [94]. Figure 3.1 is a block diagram representing CW analysis and synthesis. Several wireless channel access methodologies have been introduced throughout the years to allow for better compatibility of the limited frequency spectrum at high data rates applications.

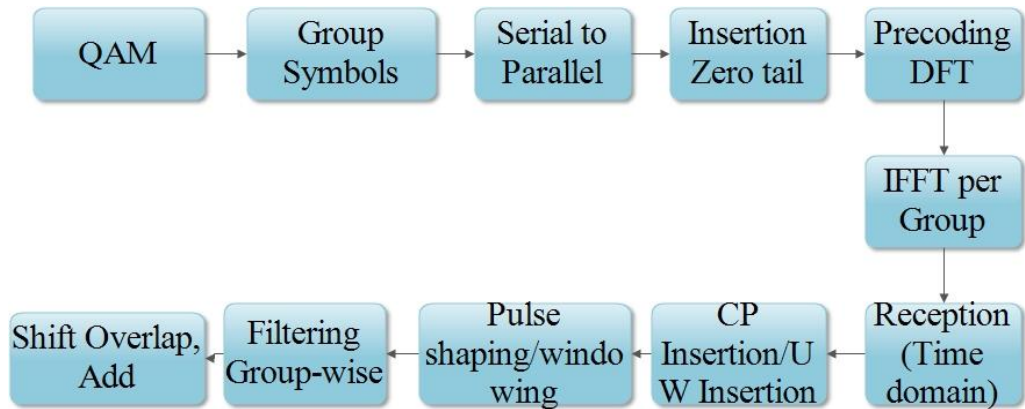


**Figure 3.1:** Multicarrier modulation basic block diagram.

CP-OFDM, F-OFDM, FBMC-OQAM, UFMC, and GFDM based transceivers are the new CWs for 5G WCS [95]. Figure 3.2 depicts the waveform modulator block diagram.

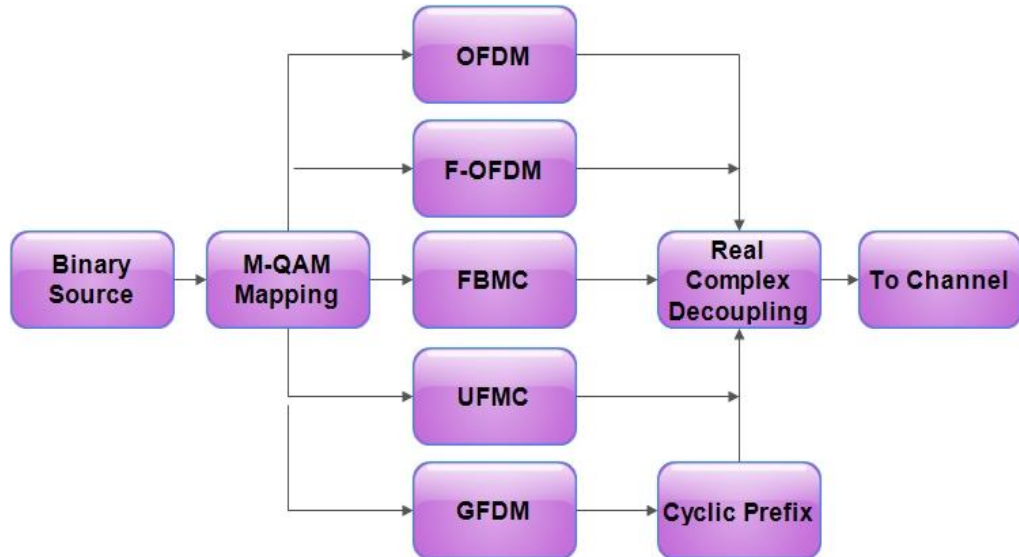


**Figure 3.2:** Block schematic of a waveform modulator.

A novel CW is being proposed for the physical layer development in 5G system design to achieve high information rates, high SE, low latency, and extending battery capacity by lowering PAPR and mMIMO connectivity.

Multi-carrier systems transmit information through pulses with frequency and temporal overlap. Because the pulses have a small bandwidth, this is a significant benefit. Broadband frequency selective channels are transformed into many frequencies flat subchannels with little or no interference. It improves on simple equalizers that employ a single tap and is linked to symbol recognition using ML for a Gaussian noise environment. It significantly streamlines the CE technique, the adaptive coding, and the modulation procedures used in mMIMO [96]. The mathematical equation of MCM transmitted signal in the time domain is provided as

$$s(t) = \sum_{k=0}^{K-1} \sum_{l=0}^{L-1} g_{l,k}(t) x_{l,k} \quad (3.1)$$

Where  $x_{l,k}$  symbolizes the transferred symbol at time position  $k$  and subcarrier position  $l$ . It is picked from the QAM symbol alphabet. The transferred basis pulse is represented by

$$g_{l,k}(t) = p(t - kT) e^{j2\pi lF(t - kT)} e^{j\theta_{l,k}} \quad (3.2)$$

Here  $p(t)$  is indeed the frequency -time-shifted PF.

$T$  = Time intervals

$F$  = Subcarrier spacing, also referred as frequency spacing.

$\theta_{l,k}$  = Phase shift

The generated symbols are decoded as the signal travels across a channel by projecting the received signal onto basis pulses, and the outcome is delivered as

$$y_{l,k} = \int_{-\infty}^{\infty} r(t) g_{l,k}^*(t) dt \quad (3.3)$$

In an AWGN channel SNR is maximized. The maximizing the SNR value is done using the matched filter. Depending on the application, the transceiver selects different basis pulses. Some of the important properties of a multi-carrier system are as follows:

- i. A symbol's density (Maximum)  $TF = 1$
- ii. Time-localization  $\sigma_t < \infty$  and Frequency-localization  $\sigma_f < \infty$
- iii. Orthogonality

Using the Balian-Low theorem, it was asserted that at least one of these needed properties must be sacrificed while constructing the candidate waveforms system.

### 3.2 CP-OFDM SYSTEM MODEL

CP-OFDM is a MCM method. This method is primarily intended for LTE networks based on 3GPP. M-QAM or M-PSK modulation schemes are employed. These modulations in digital methods are used to map the digital input. These modulation algorithms are used to create complicated symbols. The IFFT is used to map them into orthogonal sub-carriers. IFFT performs frequency to time domain translation. To avoid overlapping transmitted signals, CP or guard bands are utilized. The CP is used to offer further resilience to signal propagation. Inserted CP is used to solve the problem of ICI. Figure 3.3 depicts the CP-OFDM transceiver model. CP is chosen to be longer in time than the channel delay spread between the transceiver endpoints.

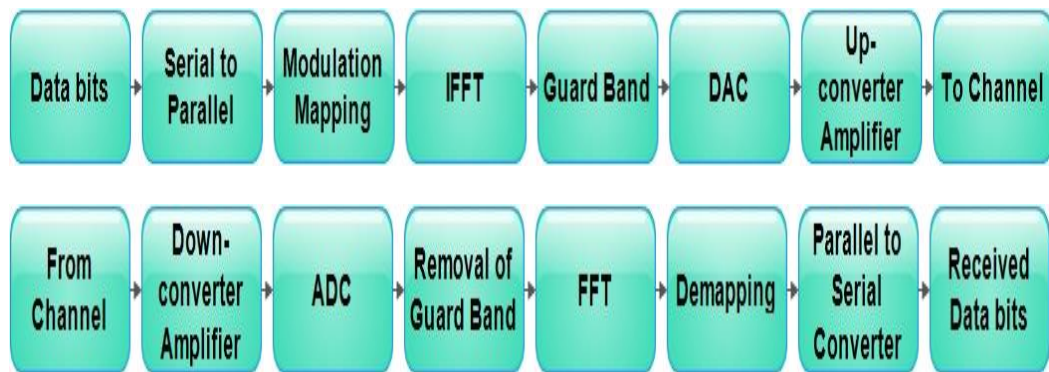


**Figure 3.3:** Block schematic of a CP-OFDM transceiver.

CP-OFDM employs rectangular transceiver pulses to decrease computing complexity. The transmission pulse is quite similar to the obtained pulse. It is utilized to sustain orthogonality in frequency-selected channels. The transmitter PF is specified.

$$P_{Tx}(t) = \begin{cases} \frac{1}{\sqrt{T_0}} & \text{if } -\left(\frac{T_0}{2} + T_{cp}\right) \leq t < \frac{T_0}{2} \\ 0 & \text{Otherwise} \end{cases} \quad (3.4)$$

The receiver PF is given as

$$P_{Rx}(t) = \begin{cases} \frac{1}{\sqrt{T_0}} & \text{if } -\frac{T_0}{2} \leq t < \frac{T_0}{2} \\ 0 & \text{Otherwise} \end{cases} \quad (3.5)$$

Where  $T_0$  is the time spacing &  $T_{cp}$  is the time spacing for the CP.

Because of the rectangular pulse, the fundamental drawback of CP-OFDM which has no control over OOB. Other CP-OFDM drawbacks include significant PAPR and transmitting overhead as a result of CP insertion.

### 3.3 F-OFDM SYSTEM MODEL

A bigger bandwidth must be provided to 5G systems to be able to improve data rate of network [97]. Among the most efficient possible CW for 5G networks is F-OFDM [98-99]. Figure 3.4 depicts the F-OFDM transceiver.

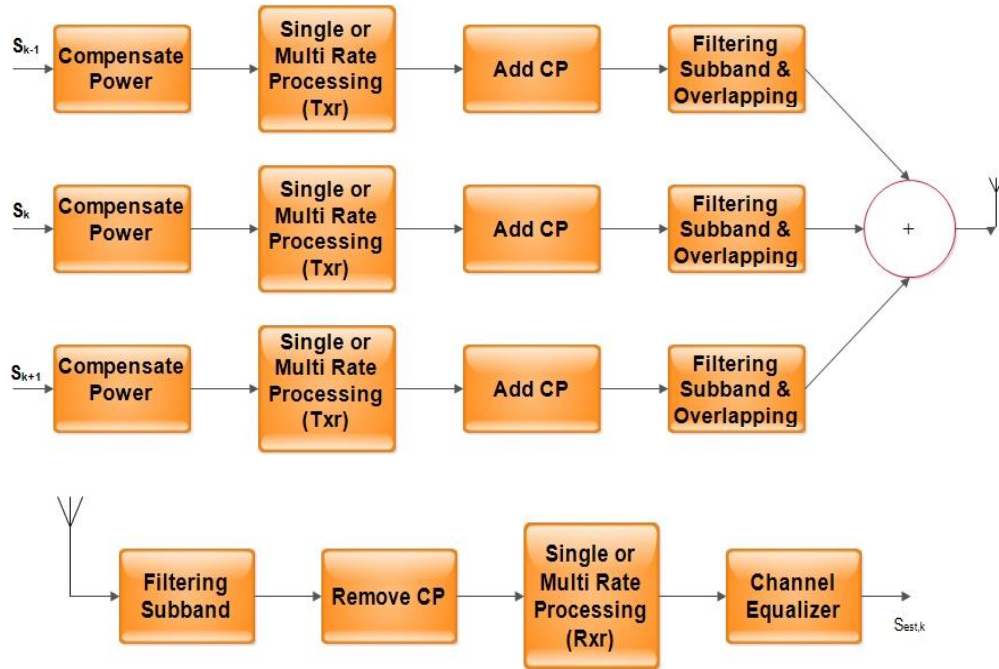


**Figure 3.4:** F-OFDM transceiver.

F-OFDM employs a full-size IDFT with a low dimension. An N-point DFT/IDFT is signal mapping to a sub-band utilizing the corresponding column. IDFT will get the same quantity of subcarriers as one subband. The entire baseband BW is distributed throughout the signal. The signal is divided into 1/K of its full BW by up-sampling. It uses the sampling theorem to execute (K-1) image signals. It also generates anti-image subband filters, which are used to eradicate image-containing signals. One of the disadvantages of the F-OFDM is that it utilizes non-ideal filters, which reduces system adaptation [100]. The usage of low-dimension DFT reduces complexity, and the filtering process helps reduce sophistication by employing the up-sample technique. Keeping the filter length as long as possible lowers OOB and interference. DFT spreading is used in the uplink transmission to decrease PAPR. The signal derived by sampling the  $k^{\text{th}}$  sub-band is denoted as

$$y_k = \sum_{l=1}^K \frac{1}{\rho_l} V^H U^H T C_k B_l A_l R U V E_l s_l + \widetilde{v}_k \quad (3.6)$$

Where V is the M-point matrix of IDFT (Normalized), U is the matrix with factor K (up sampling), and  $v$  is the noise matrix.

F-OFDM has a larger complexity than OFDM; however, it enables numerous users or services. In single-rate F-OFDM systems, the sampling rate is fixed and remains constant throughout all subbands. On the other hand, the sample rate in multi-rate F-OFDM systems is changeable, and it employs low complexity low dimension DFT. As a result, F-OFDM is suited for 5G systems.

### 3.4 FBMC SYSTEM MODEL

In comparison to the limits of OFDM, FBMC has achieved a potential benefit in 5G networks. The primary use characteristics are great spectrum efficiency and rigorous synchronization limitations. Figure 3.5 depicts the FBMC transceiver.

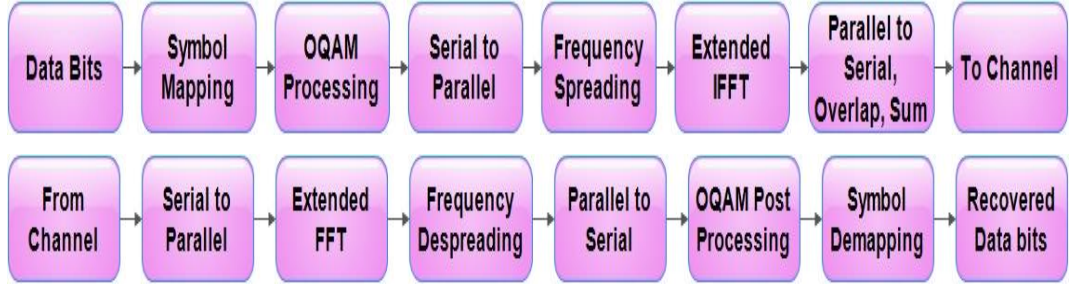


**Figure 3.5:** FBMC transceiver.

The FBMC system is created with little change to the basic OFDM system. Each subcarrier is filtered to remove side lobes, lowering interference and hence the OOB. There is no need to add CP to boost the attainment of high data rates. The symbol density of FBMC is the same as OFDM; however, CP is unemployed. It operates based on first creating a PF with  $p(t)=p(-t)$ . Frequency and time spacing are orthogonal in nature, with time spacing expressed as  $T=T_0$  and spacing in frequency provided as  $F=2/T_0$ . For FBMC, a PF Hermite is provided as

$$p(t) = \frac{1}{\sqrt{T_0}} e^{-2\pi(\frac{t}{T_0})^2} \sum_{t=\{0,4,8,12,16,20\}} \alpha_i H_i(2\sqrt{\pi} \frac{t}{T_0}) \quad (3.7)$$

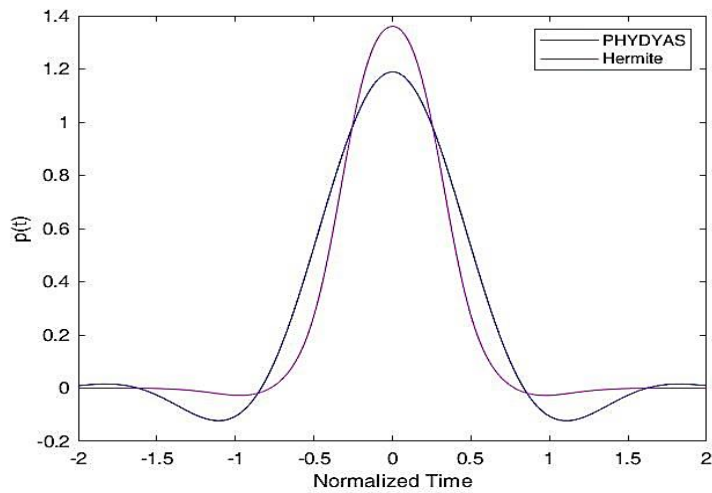
The PF is presented on the basis of  $H_n(\cdot)$  Hermite polynomials [101], and  $\alpha_i$  coefficients may found [102]. PHYDYAS PF [103] is another form of PF utilised for FBMC and is given as

$$p(t) = \begin{cases} \frac{1+2\sum_{i=1}^{O-1} b_i \cos(\frac{2\pi t}{OT_0})}{O\sqrt{T_0}} & \text{if } -\frac{OT_0}{2} < t < \frac{OT_0}{2} \\ 0 & \text{Otherwise} \end{cases} \quad (3.8)$$

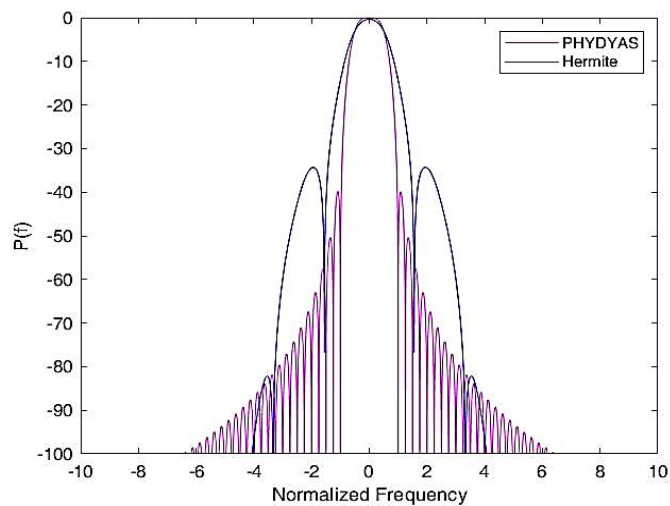
The  $b_i$  coefficients are taken from [104]. The second FBMC concept is to downgrade orthogonal by a factor of 2 for temporal spacing, which is  $T=T_0/2$  and  $F=1/T_0$ . Finally, the created interference is moved to the completely hypothetical domain, as well as the phase difference is given as

$$\theta_{l,k} = \frac{\pi}{2} (l + k) \quad (3.9)$$

The shortcoming of FBMC is the loss of complex orthogonality. Figure 3.6a and 3.6b depicts the Hermite and PHYDYAS PF filters, together with their time-frequency spacing representations.



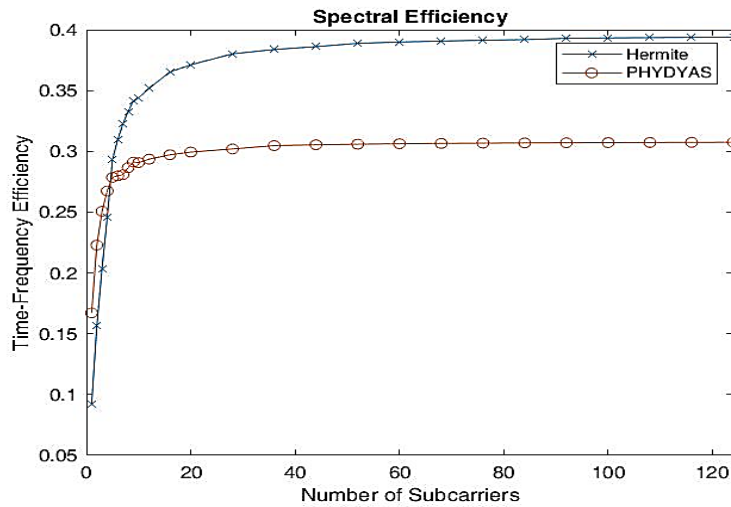
**Figure 3.6a:** FBMC prototype filter time domain spacing.



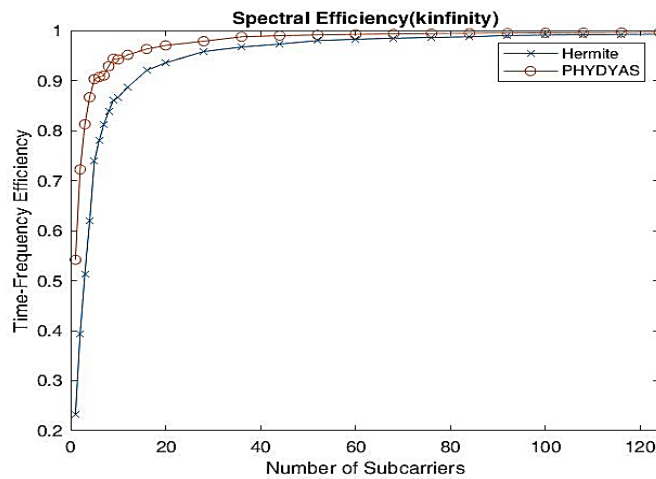
**Figure 3.6b:** FBMC prototype filter frequency domain spacing.

Figure 3.7a and 3.7b depicts the spectrum effectiveness of the Hermite and PHYDYAS filters. When subcarrier spacing is considered normal, the SE of the Hermite PF is worthy; when subcarrier spacing is regarded as infinite, the PHYDYAS filter's SE is worthy compared to the Hermite filter.





**Figure 3.7a:** SE of PHYDYAS and Hermite Filter when  $K = \min$ .



**Figure 3.7b:** SE of PHYDYAS and Hermite Filter when  $K = \infty$ .

### 3.5 UFMC SYSTEM MODEL

It is a CW with subcarrier filtering. Regarding BER and side lobe attenuation, UFMC performs well in contrast to OFDM [105]. The UFMC CW is the same as the F-OFDM and FBMC CW. A set of subcarrier modulation is performed in UFMC. The filter length and performance time are lowered due to subcarrier grouping. Figure 3.8 depicts the UFMC transceiver.

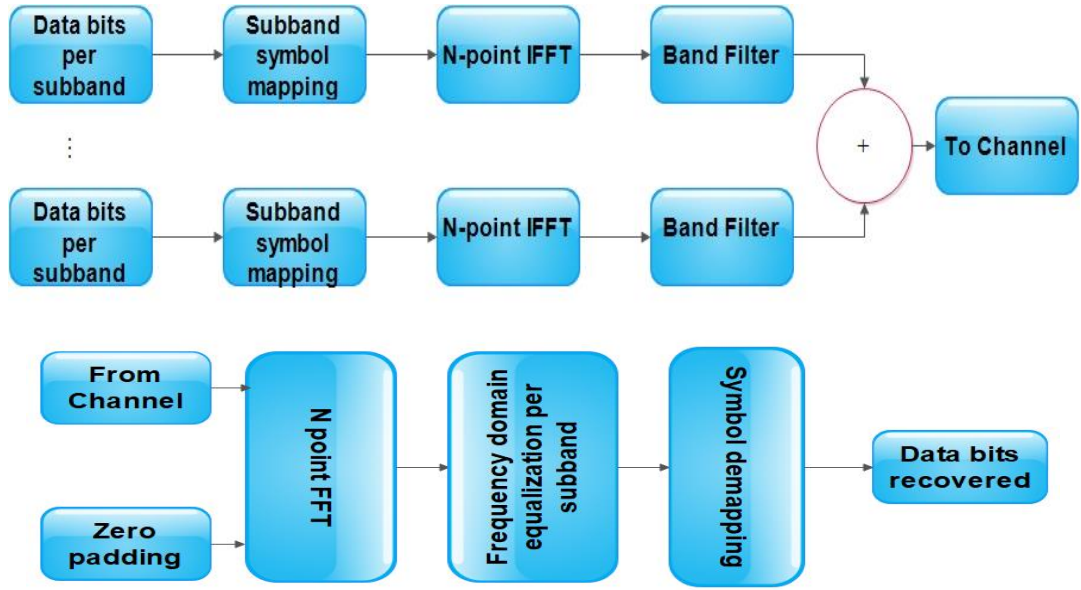


Figure 3.8: UFMC transceiver.

These MCM sub-bands are created by splitting the full band; modulation is conducted on specific sub-bands that consist of a specified number of subcarriers. The individuals are closely spaced to foster each sub-band in the time domain, and constricted sub-bands are subjected to N-point IFFT. The output IFFT of N-point is given as

$$Y_i = IFFT\{x_i\} \quad (3.10)$$

The signal's output after being filtered by length L is represented as

$$y = H \cdot \sim Q \cdot y_i \quad (3.11)$$

Here H is the matrix of Toeplitz for dimensions  $(N+L-1)*N$  and  $\sim Q$  is the IFFT matrix.

The UFMC receiver executes N point FFT on data obtained from the channel. To avoid ISI caused by the sent filter, a guard of interval 0's is attached between consecutive IFFT signals and is specified as

$$\sim Y = FFT\{|y^T, 0,0,0 \dots \dots .0\} \quad (3.12)$$

By removing even subcarrier points, the obtained signal Y contains the length of N in the frequency domain for odd points of the subcarrier. Equalization is done to identify the supplied signal, followed by symbol de-mapping to the specific data bits.

### 3.6 GFDM SYSTEM MODEL

It is a non-orthogonal resource [106-107]. The sub carrier filtered pulse used in the GDFM leads to non-orthogonality condition causing ISI and ICI in the received signals. It has emerged as one of the most MCM schemes for 5G networks. The primary benefit of GFDM is that it has a lesser latency, a lesser PAPR, a lesser OOB, and a lesser neighbouring channel leakage ratio. It has a flexible design of transceiver. It ensures a high degree of adaptability in transceiver development, making it suited for a wide range of applications, including cognitive and full-duplex radio. For spectrum management in 5G WCS, GFDM cognitive and full-duplex radio are viable options. Figure 3.9 depicts the GFDM transceiver.

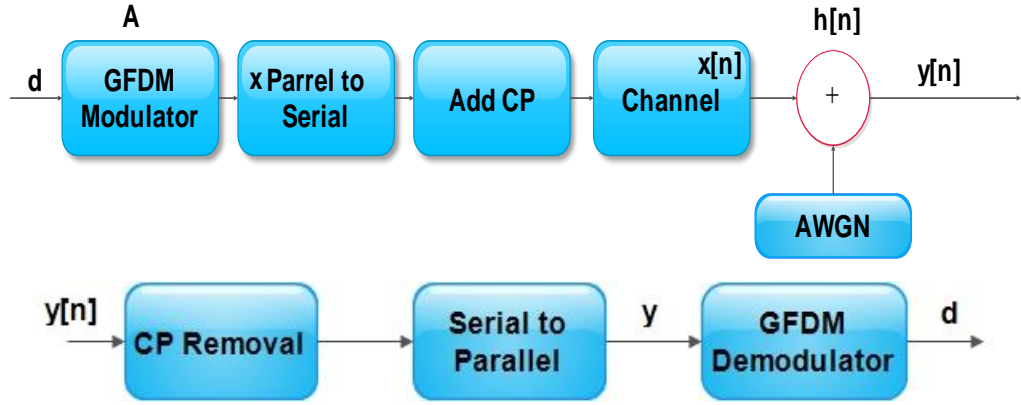


**Figure 3.9:** GFDM transceiver.

GFDM is a proposed waveform based on blocks [108]. It has subcarriers of value  $K$  for every complex value of the  $M$  sub symbol sent. The absolute number of signals sent inside the block is indicated as

$$D = KM \quad (3.13)$$

GFDM block's vector of pulse shaped is provided as

$$[g_{k,m}]_n = [g]_{(n-mK)D} e^{j2\pi kn/K} \quad (3.14)$$

The  $m^{\text{th}}$  symbol appears on the  $k^{\text{th}}$  subcarrier. The filter prototype is provided as

$$g \in \mathbb{C}^D \quad (3.15)$$

The sample vector for the transmitter is specified as

$$x = Ad \quad (3.16)$$

Here  $A$  is the sent matrix and  $d$  is the block of GFDM for  $d \in \mathcal{C}^D$ .

The vector of sample for the transmitter is specified as

$$[x]_n = \sum_{k=0}^{K-1} \sum_{m=0}^{M-1} [d]_{k+mK} [g]_{(n-mK)D} e^{j2\pi kn/K} \quad (3.17)$$

After sending  $x$ , a parallel to serial conversion is conducted, and CP with a length  $L$  is added to produce a GFDM digital baseband transmitted signal. The baseband obtained output is presented as

$$y[n] = h[n] * x[n] + w[n] \quad (3.18)$$

Here  $h$  is response of impulse of a LTI casual system with a wireless channel of  $N$ -tap,  $x$  is the sent vector, and  $w$  is AWGN noise vector.

Circular convolution with CP and linear convolution is used to represent the frequency selective multipath channel. As a result, after subtracting CP, the receiver vector is acquired, and serial to parallel conversion is conducted, and it is provided as

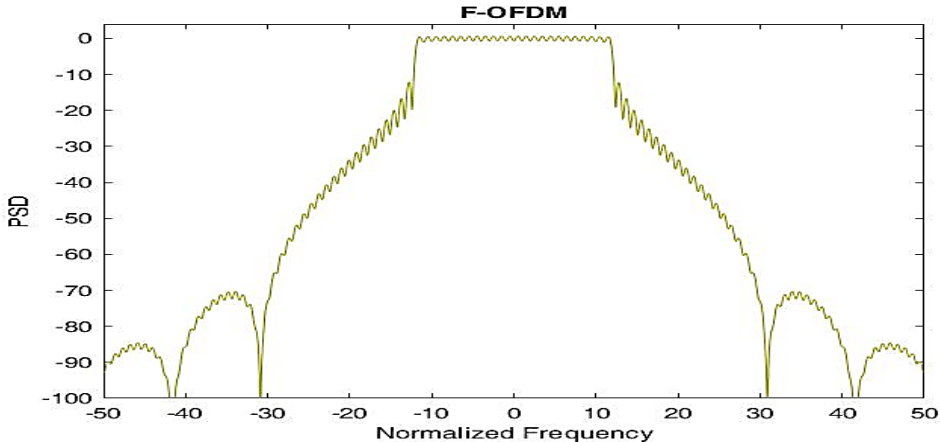
$$y = Hx + w = HAd + w = W_D^H \text{diag}(W_D A d) F_N h + w \quad (3.19)$$

$F_N = [\sqrt{D} W_D]_{:,1:N}$  and  $H \in \mathcal{C}^{D \times D}$  is the circular matrix. Following demodulation, the estimated  $d$  is obtained for the GFDM block. The demodulation is affected by the obtainer's targeted applications. The restriction of GFDM is a lesser-complexity transceiver design; an emulsion of mMIMO-GFDM results in a vast size of the block, making the demodulation a convolutional technique infeasible, and synchronization error arises. The training-based channel estimate is problematic due to these synchronization issues.

### 3.7 SIMULATION RESULTS & DISCUSSION

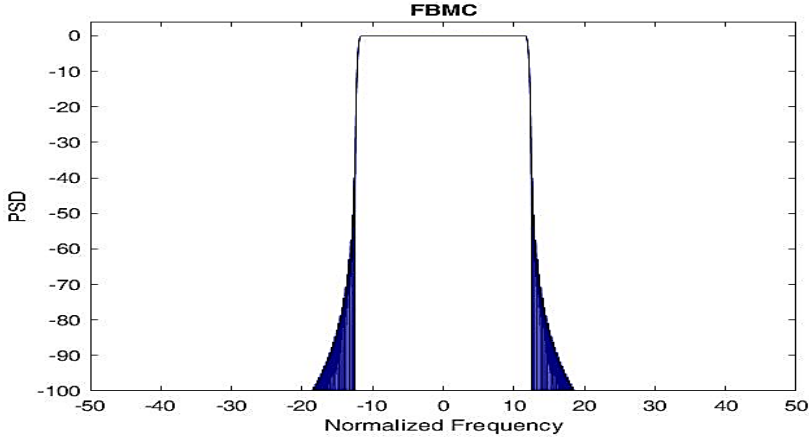
The PSD demonstrates the magnitude of the fluctuations as a function of frequency. It demonstrates which frequencies have high variations and which have mild variations. OOB is reduced when the PSD is higher over the frequency range. Using the PSD profile, we can find the frequency components with relatively lower power levels in the specified frequency range of interest. A spectrum analyzer is used to examine the control signal. The PSD profile is evaluated and compared to the PSD of the reference signal prior to transmission over the channel. We can

discover the frequency components with lower power levels due to channel noise by evaluating the PSD profile. When contrast to the other frequency components contained in the signal, they have proved substantially more susceptible to noise. Power levels need to be adjusted to fight the impacts of channel noise. The figures from 3.10 to 3.14 depicts the PSD of OFDM, F-OFDM, FBMC, UFMC, and GFDM.



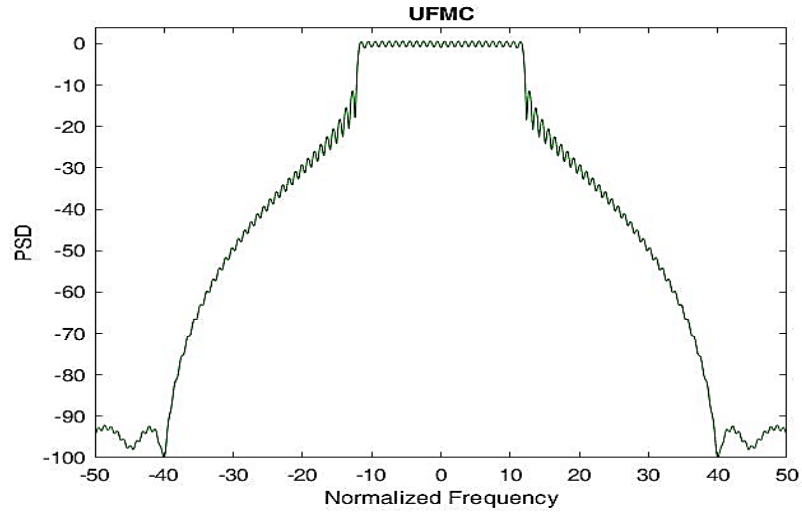
**Figure 3.10: F-OFDM PSD.**

Figure 3.10 depicts the PSD of F-OFDM at Normalized frequency with 96 subcarriers and a subcarrier spacing frequency of 30KHz.



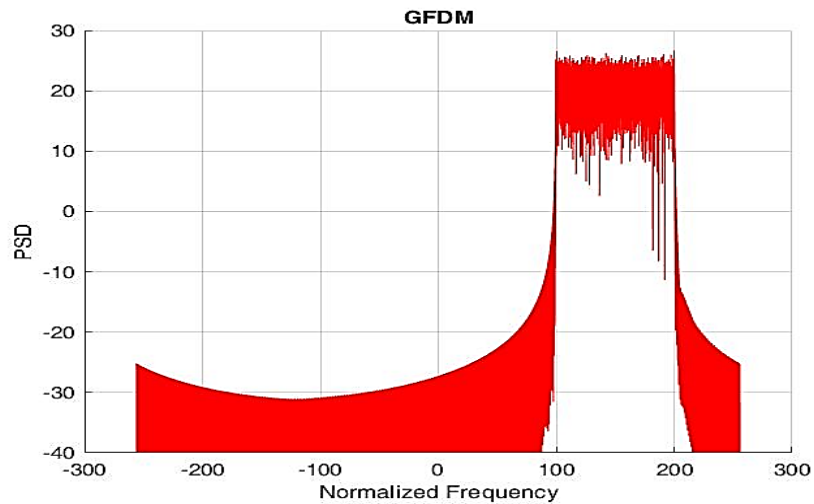
**Figure 3.11: PSD of FBMC.**

Figure 3.11 depicts the PSD of FBMC at Normalized frequency with 96 subcarriers and a subcarrier spacing frequency of 30KHz.



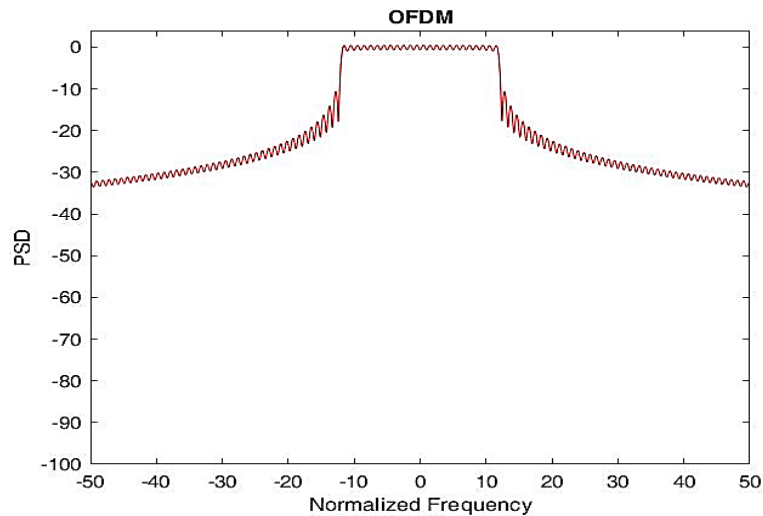
**Figure 3.12:** PSD of UPMC.

Figure 3.12 depicts the PSD of UPMC at Normalized frequency with 96 subcarriers and a subcarrier spacing frequency of 30KHz.



**Figure 3.13:** PSD of GFDM.

Figure 3.13 depicts the PSD of F-OFDM at Normalized frequency with 96 subcarriers and a subcarrier spacing frequency of 30KHz.



**Figure 3.14:** PSD of OFDM.

Figure 3.14 depicts the PSD of OFDM at Normalized frequency with 96 subcarriers and a subcarrier spacing frequency of 30KHz.

Figures 3.10 to 3.14 PSD of MCM techniques are plotted and compared. From the results, it is evident that the FBMC and UFMC have lower sidelobes compared to OFDM, F-OFDM, and GFDM. Compared to OFDM, F-OFDM has lower sidelobes, but the problem is that it can exceed the CP length. In UFMC length of the filter is constrained and is always equal to CP length. Filter design for F-OFDM causes a little loss in orthogonality, which impacts the edge subcarriers. FBMC has a longer filter delay (compared to UFMC) because of the per subcarrier filtering, and it also requires OQAM processing, which requires changes for mMIMO processing. GFDM also has higher sidelobes compared to OFDM. So based on the comparison, the UFMC outperforms better.

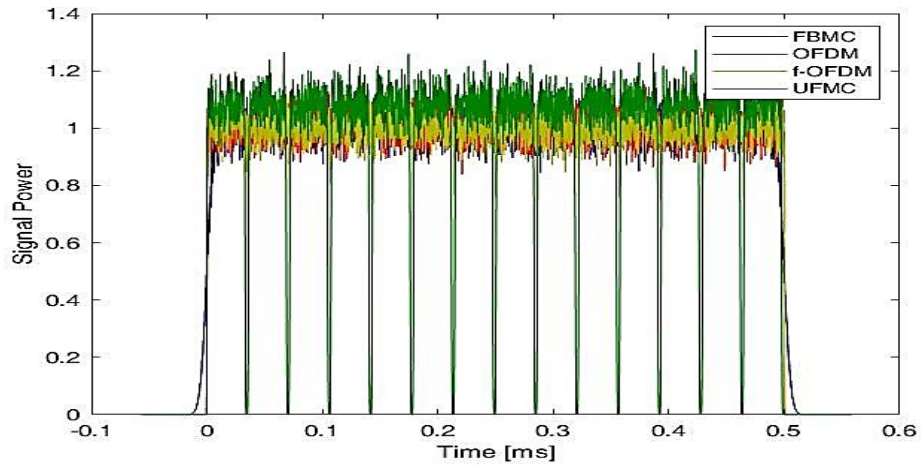


**Figure 3.15:** Signal power of the CW.

A BER is the measure with which errors occur in a transmission system. This may be easily converted into the number of errors in a sequence of a certain length. The concept of bit error rate may be simplified as follows:

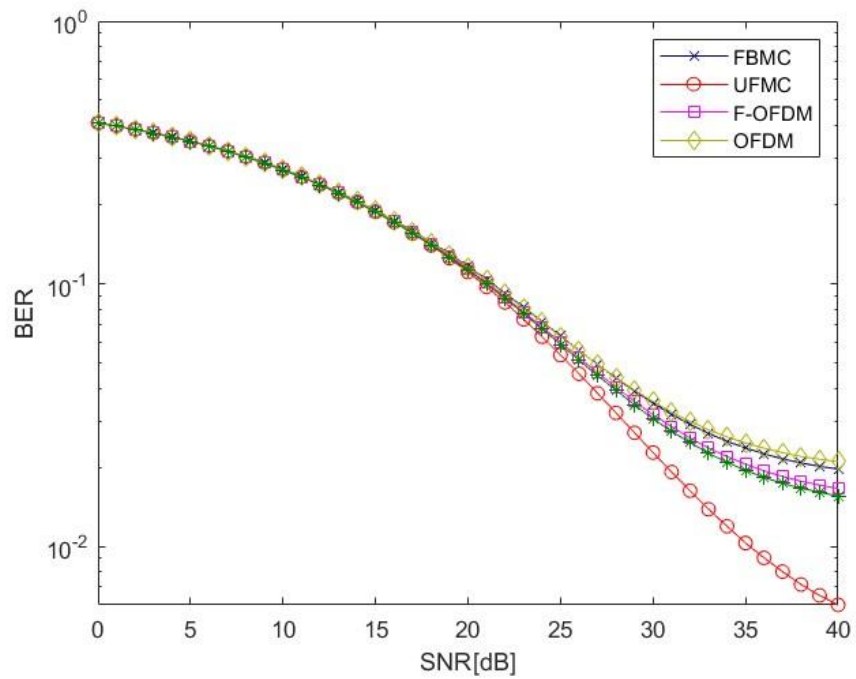


**Figure 3.16:** BER of the CW.



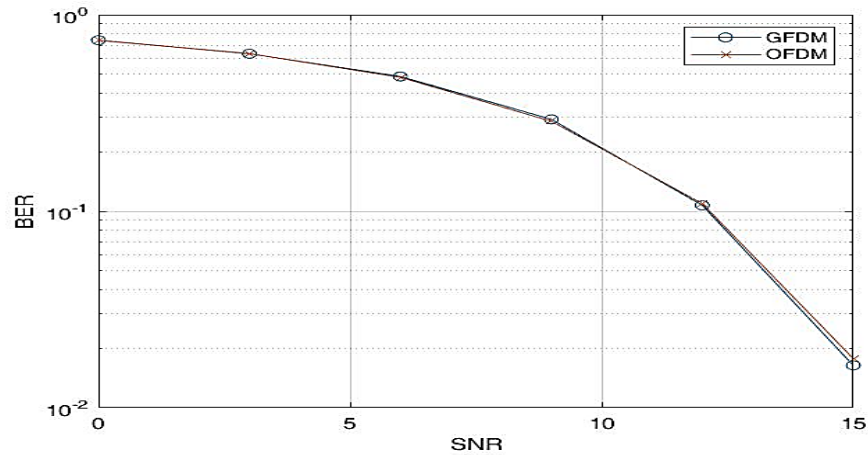


**Figure 3.17:** BER of the GFDM and OFDM.

A BER is a measure with which errors occur in a transmission system. It may be easily converted into the number of errors in a sequence of a certain length. The concept of bit error rate may be simplified as follows:

$$BER = \frac{\text{Total number of errors}}{\text{Total number of bits}} \quad (3.20)$$

Suppose the medium between the transceiver is good and the SNR ratio is high. In that case, the BER will be very low, potentially negligible, and have no discernible influence on the entire system. However, if noise is found, it is possible that the BER needs to be addressed. Figure 3.16 and 3.17 depicts the BER of all MCM techniques. From figure 3.16, it is evident that the UFMC BER value is decreased compared to other MCM techniques. In figure 3.17, GFDM BER is less compared to the OFDM system. The problem with GFDM is that as it is a non-orthogonal system, it cannot be used in mMIMO systems. The comparison of all MCM techniques is displayed in table 3.1.

**Table 3.1:** Analogy of MCM technique (High-↑, Medium-↔, Low-↓)

Specifications	CP-OFDM	F-OFDM	FBMC	UFMC	GFDM
OOB Emission	↑	↓	↓	↓	↓
Computational complexity	↓	↔	↑	↑	↑
Spectral efficiency	↓	↓	↑	↑	↑
PAPR	↑	↑	↔	↑	↔
Latency	↔	↑	↑	↑	↑
Flexibility	↑	↔	↔	↔	↑
Robustness to CFO	↓	↔	↑	↑	↑

### 3.8 SUMMARY

This chapter completely focuses on the 5G multicarrier modulation techniques. MCM techniques are discussed, such as OFDM, F-OFDM, FBMC, UFMC, and GFDM, with their transceivers. The wireless system's connection is rapidly increasing, with virtually an exponential increase in data for wireless. The next generation 5G WCS has been considered a viable technology for increasing higher information rates, QoS, and connection. The 5G WCS supports new applications such as IOV, IOT, and smart grids. Many promising MCMs are required for 5G. Other possible waveforms are more suitable for the 5G WCS than OFDM. This study uses a 16QAM modulation scheme to demonstrate the PSD and BER performance of all MCM schemes. As GFDM is a non-orthogonal MCM technique, its performance is only compared to that of OFDM because it is primarily used in cognitive radio applications.

## CHAPTER-4

### CHANNEL ESTIMATION

#### 4.1 WIRELESS CHANNEL MODELLING

The channel is a medium in communication systems that transfers data from sender to receiver. The channel is modelled to compute the physical process that affects the transmitted signal. Figure 4.1 depicts a block schematic of a simple communication system.



**Figure 4.1:** Basic block diagram of communication system.

##### 4.1.1 FADING CHANNEL

Over a specific range of transmission media, the signal suffers from fading distortion. When a fading occurs in a channel, it is described as a fading channel. Reflections in the atmosphere from sender to receiver create many routes for a transmitted signal. It generates several duplications of the transmitted signal routed through various pathways. The received signal will suffer from interference and attenuation as a result. Attenuation is the shift in signal strength from the transmitter to the receiver during transmission.

Classification of fading is done into two types.

- Fast fading
- Slow fading

When the channel varies quicker than the symbol rate, fast fading occurs, and slow fading occurs when the channel varies more slowly than the symbol rate.

LOS determines the other sort of fading channel. Classification of fading channel is done into two types based on this. They are

- Rayleigh fading
- Rician fading

Rayleigh fading occurs when there is a NLOS component in the received signal, while Rician fading occurs when there is a LOS component in the obtained signal.

The time required to obtain all of the components delayed of the transmitted signal is known as delay spread. Coherence BW is the range of frequency across which a response of flat fading is obtained. The delay spread is inversely linked to the coherence bandwidth. Therefore, the fading channel is divided into two categories based on delay spread and coherence bandwidth.

- Flat fading
- Frequency selective fading

Flat fading occurs when the channel's delay spread is less than the symbol period, while frequency selective fading occurs when the symbol period is substantially less than the delay spread. Figure 4.2 depicts the categorization of fading channels.

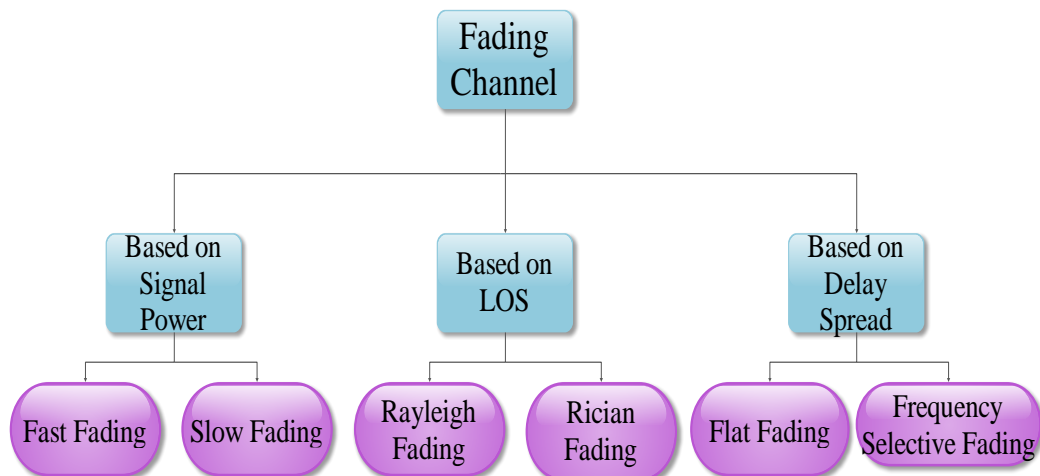


**Figure 4.2:** Tier of wireless channels.

## 4.2 CHANNEL ESTIMATION

The goal of CE is to characterise the influence of the input sequence on the physical medium. Figure 4.3 depicts the fundamental schematic diagram of CE.

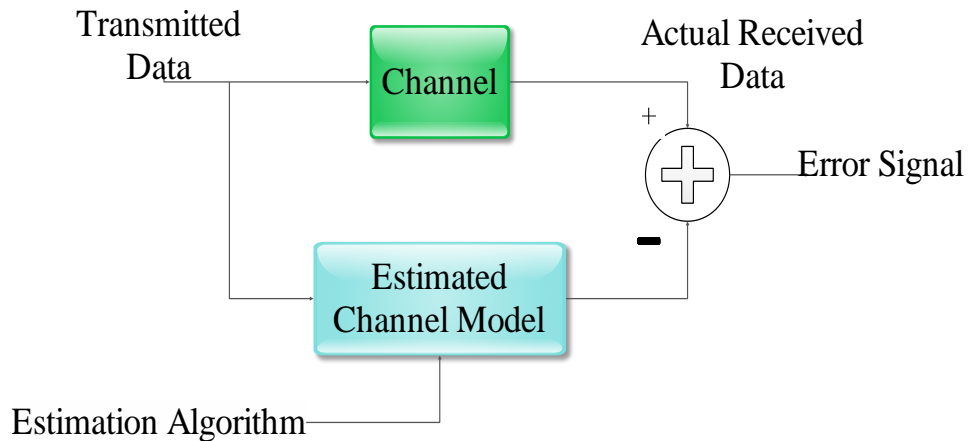


**Figure 4.3:** Basic block diagram of channel estimation.

Symbols are often transmitted in WCS channels, and they encounter a diversity of detrimental consequences as they travel across the channel. This negative effect is caused by contact with ambient entities such as mountains, buildings, and so on, which causes fading in multipath and attenuation in signal [109]. In this regard, we must guarantee that sending signals are detected accurately. As a result, CE [110] has become extremely valuable in wireless communication systems [111]. Precision CE is imperative for the reliable detection of transmitted signals. CE allows the receiver to be imprecise of the communication channel's CIR and predict the impingements of the communication channel on the broadcast symbols. It is compulsory for the accurate reconstruction of the sent symbols. Many CE algorithms for generic WCS's have been suggested in chapter 2.

Several CE approaches have been offered in the literature throughout the years to overcome the variable channel nature. The suggested solutions focus on improving system performance in terms of BER, BLER, SER, SNR and WER. Some of the CE approaches define the decrease in computational sophistication. The study examines

the methods used to give the beneficial approaches that demonstrate the improvement in the performance of CE techniques and the limits of each strategy used. This thesis, in general, narrows the use of various CE approaches for massive MIMO systems. Figure 4.4 depicts the many channel estimation approaches that control wireless communication networks. CE approaches may be divided into three groups. There are three types of estimating systems: non-blind, semi-blind, and blind CE schemes. These CE algorithms are presented to create radio channel air interface networks.

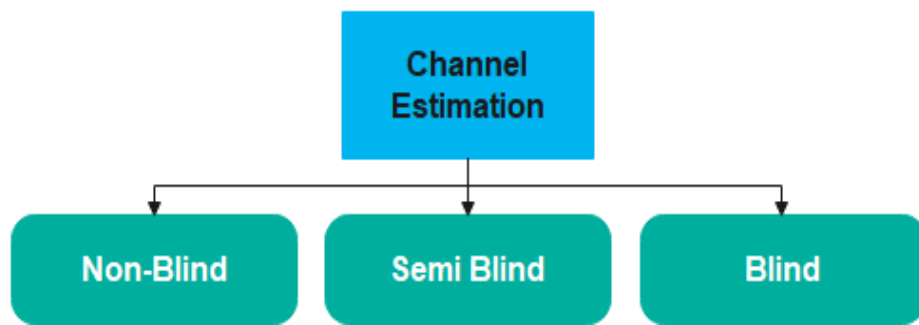


**Figure 4.4:** Tier of CE schemes.

Several CE approaches are being developed to increase CE adaptation, power usage, bandwidth use, and computational sophistication. The thesis discusses the broad categorization of each channel estimate approach.

#### **4.2.1 NON-BLIND CHANNEL ESTIMATION SCHEME**

Non-Blind CE is also known as pilot-based CE. The term "pilot-based" refers to the fact that the learning or pilot symbols are already known at the output end. There are two types of non-blind CE schemes. They include

- Decision directed CE
- Training based CE

For practical CE, pilot symbols are introduced with data symbols at the transmitted end in a training-based CE method [112]. As a result, the data symbols are precisely calculated at the receiver with no data loss. The greater the number of pilot symbols,

the greater the system exactness. The SE of this approach is limited because of increased overhead caused by the pilot symbols. The system's performance is computed in the time domain and explored for slow multipath fading channels.

Pilot symbols and re-modulated observed message symbols are used for channel estimate in decision-directed CE [113][114]. The prior symbols are used to detect the present estimates, which are utilized to detect the next estimations, and so on. The CE of decision-directed is again tiered into two types. They include

- Hard decision
- Soft decision

The soft detection approach utilizes detection in bitwise, but the hard decision method requires a particular constellation. Figure 4.5 depicts the categorization of a non-blind system.

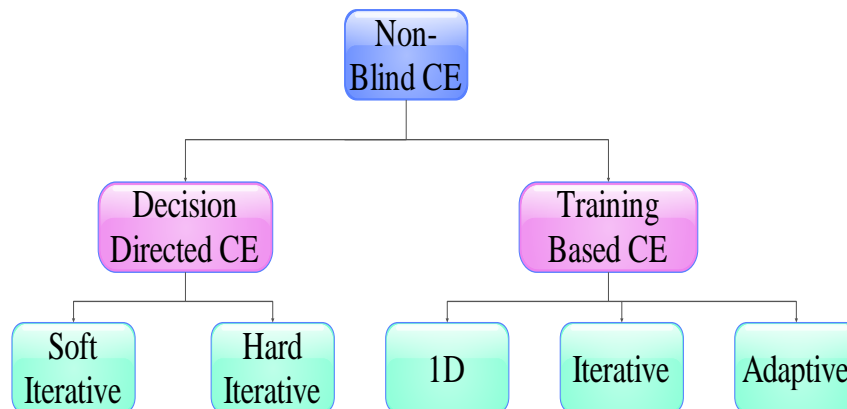


**Figure 4.5:** Classification of pilot-based CE scheme.

Based on the pilot setup, three kinds of pilot arrangements are explored [115-119]. They include

**Block Type**

Pilot symbols at all subcarriers are periodically sent in this mode for CE. Figure 4.6 depicts a pilot layout of the block type.

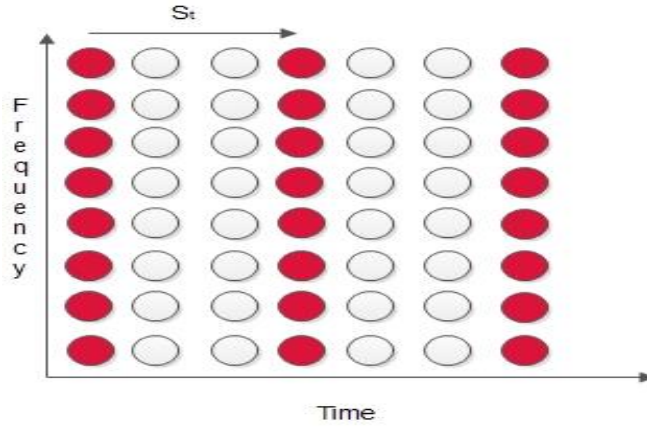


**Figure 4.6:** Pilot arrangement of block type.

Utilizing these training symbols, a time-domain interpolation is used to CE along with the time axis.  $S_t$  represents the symbols that are periodically trained. The channel properties that change over time are constantly recorded. As a result, the learning symbols are typically put as a time coherence. The training symbol must meet inequality, wherein coherence time is inversely related to doppler frequency.

$$S_t \leq \frac{1}{f_{doppler}} \quad (4.1)$$

Pilot tones are inserted into all learned symbol subcarriers over time in a block-type pilot symbol arrangement for frequency selective channels. When the pilot symbol time is decreased due to channel variation, too much pilot overhead is identified for rapidly fading channels.

### **Comb Type**

Pilot tones are present at the regularly positioned subcarriers in every comb-type symbol. Utilizing these training symbols, a frequency-domain interpolation is used for CE along the frequency axis. Figure 4.7 depicts the comb-style pilot configuration.  $S_f$  provides the frequency for the duration of pilot tones. The frequency selective characteristics are recorded continuously, and the training symbols are stored as frequently as coherent BW. In addition, the training symbol must meet the requirement that the coherence BW be inversely related to maximum delay spread.



$$S_f = \frac{1}{\sigma_{max}} \quad (4.2)$$

The comb type pilot layout is employed for rapid fading channels but not for frequency selective channels.

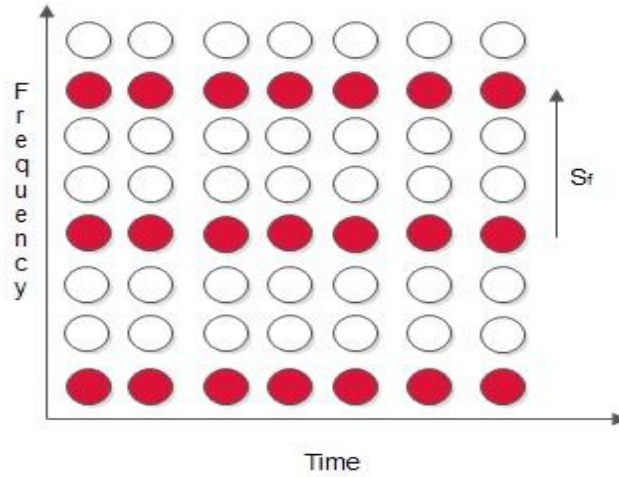


**Figure 4.7:** Pilot arrangement of comb type.

### Lattice Type

Pilot tones are injected at predetermined intervals along the frequency and time axes. Because the pilot tones are distributed in both the frequency and time domain axes, it enables time and frequency domain interpolations for CE. Figure 4.8 depicts the lattice-style pilot arrangement. The pilot configuration must meet the following equations to capture frequency-selective and time-varying channels.

$$S_t \leq \frac{1}{f_{doppler}} \text{ and } S_f = \frac{1}{\sigma_{max}} \quad (4.3)$$

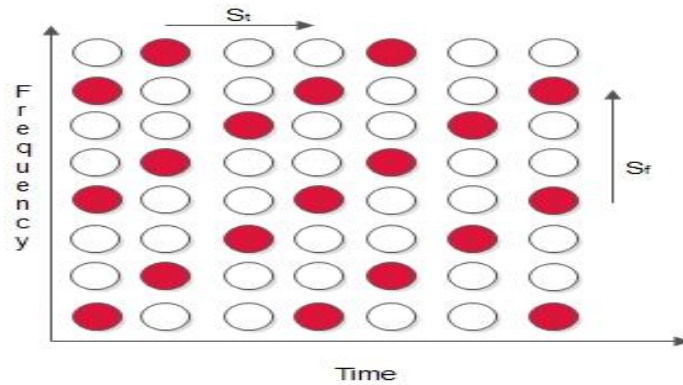


**Figure 4.8:** Pilot arrangement of lattice type.

#### 4.2.2. SEMI-BLIND CHANNEL ESTIMATION SCHEME

The semi-blind CE technique combines training sequences and signals statistical features to estimate the CIR. It is a hybrid channel estimating approach that combines blind and non-blind CE. The BS, in this manner, is aware of the large-scale fading coefficients of its own cell but is unaware of interfering cells [120]. It enhances the system's information throughput and SE by using the semi-blind CE approach [121]. In the semi-blind CE approach, the pilot overhead is decreased.

#### 4.2.3 BLIND CHANNEL ESTIMATION SCHEME

Blind CE schemes evaluate transmitted data using statistical and mathematical features of the channel [122]. There are no training sequences or pilot symbols to estimate a channel. As a result, the system's computational sophistication arises. Blind CE techniques are classified into two categories. They include

- Deterministic CE
- Statistical CE

With the restriction of high computational cost, the deterministic CE approach enhances system performance. When compared to the statistical CE approach, it also boosts the constellation order of modulated signal. A statistical CE technique

estimates a channel using statistical features. Blind CE is a BW efficient method because it does not require the usage of pilot symbols to predict channels but has high computational complexity. Figure 4.9 depicts the categorization of blind CE schemes.

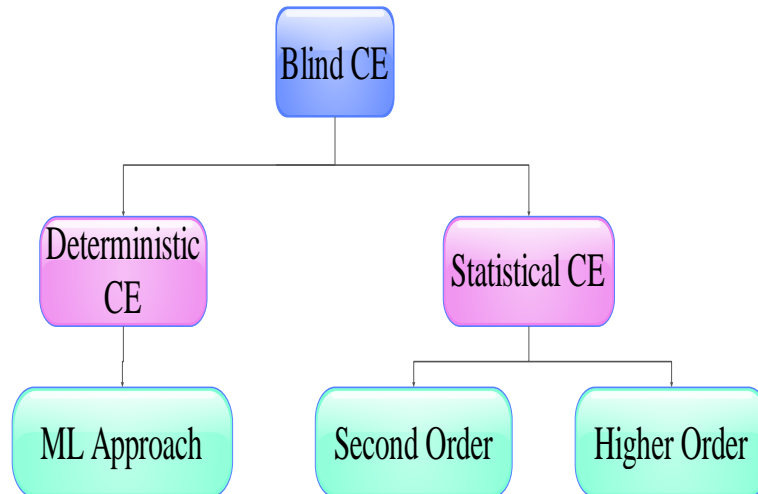


**Figure 4.9:** Classification of blind CE scheme.

Depending on the types of CE techniques as discussed to satisfy objective 1 some of the existing CE techniques are reviewed and they are discussed below.

### 4.3 CHANNEL ESTIMATION ALGORITHMS

Preamble symbols that are recognised at both the transmission and reception are typically used for CE. To measure the responsiveness of the subcarrier channel, it uses a variety of interpolation techniques between the pilot tones. When choosing a CE for any MCM technique, several implementation factors such as computation, performance, and time-variation of the channel must be taken into account. Some of the current techniques that are examined in this research are listed below.

### 4.3.1 LS CE TECHNIQUE

The CE is premised on pilots transferred at particular marks in the MCM system's time and frequency grid. The channel attenuations are estimated employing interpolations between these pilots, where we assume that CEs can use all transmitted pilots in both instances. There is only one physical channel between transceivers; therefore, channel attenuation frequency points are correlated, which can be utilized for CE. Only pilots transmitted by that user can be used to estimate the attenuations for that user. Pilots are transmitted to certain positions in the time-frequency grid using a two-dimensional generalization of pilot symbol-assisted modulation of known symbols. The number of pilots to use is a trade between the data rate and CE performance. This LS CE is one of the conventional CE methods that is developed for OFDM systems.

In mathematical statistics, the LS algorithm is used to fit curves. When only considering the pilot signal in the OFDM system CE, the LS CE transmitted signal can be written as

$$s(k) = h.p(k) + m(k) \tag{4.4}$$

Where,  $s(k)$ -Obtained Symbol

$h$ -Unknown Coefficient of channel

$p(k)$ -Sent Symbol

$m(k)$ -Additive Gaussian Noise.

The basic LS CE diagram is given in the figure 4.10.

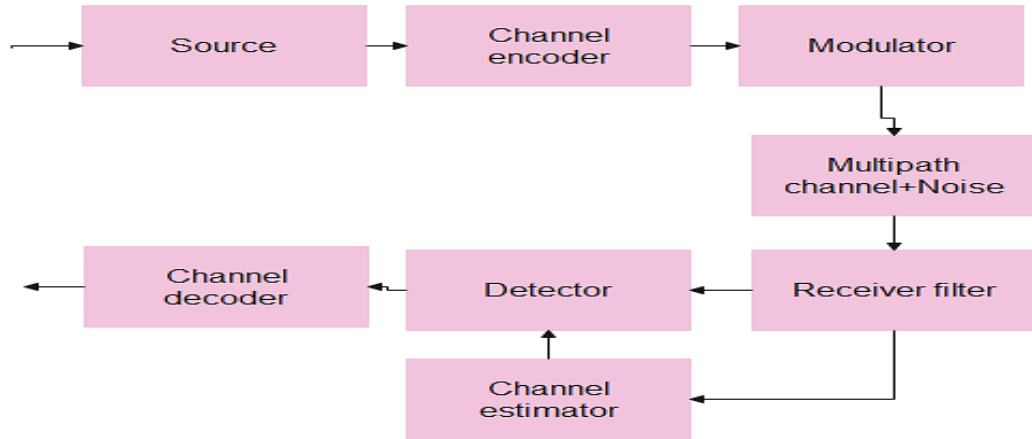


**Figure 4.10:** LS CE block diagram.

The joint probability of the obtained signal w.r.t to the transmitted signal is given as

$$F_{S(k)}(s(k)) = \frac{1}{\sqrt{2\pi\sigma^2}} e^{-\frac{1}{2\sigma^2}(s(k) - h.p(k))^2} \quad (4.5)$$

Where,  $M(1), M(2), \dots, M(N)$  are noise samples which are Independent Identically Distributed (IID),  $(s(1), s(2), \dots, s(N))$  are independent and

$$F_{S(1)S(2)\dots S(N)}(s(1), s(2), \dots, s(N)) = F_{S(1)}(s(1)) \cdot F_{S(2)}(s(2)) \dots F_{S(N)}(s(N)) \quad (4.6)$$

Where,  $F_{S(1)S(2)\dots S(N)}(s(1), s(2), \dots, s(N))$  are Joint PDF of Observations and  $F_{S(1)}(s(1)) \cdot F_{S(2)}(s(2)) \dots F_{S(N)}(s(N))$  are Product of individual PDF's of  $S(1)S(2) \dots S(N)$ .

The function

$$F_{S(1)}(s(1)) \cdot F_{S(2)}(s(2)) \dots F_{S(N)}(s(N)) = \frac{1}{\sqrt{2\pi\sigma^2}} e^{-\frac{1}{2\sigma^2}(s(1)-h.p(1))^2} \cdot \frac{1}{\sqrt{2\pi\sigma^2}} e^{-\frac{1}{2\sigma^2}(s(2)-h.p(2))^2} \dots \frac{1}{\sqrt{2\pi\sigma^2}} e^{-\frac{1}{2\sigma^2}(s(N)-h.p(N))^2} = \left(\frac{1}{\sqrt{2\pi\sigma^2}}\right)^N e^{-\frac{1}{2\sigma^2} \sum_{k=1}^N (s(k)-h.p(k))^2} \quad (4.7)$$

The equation 4.7 is obtained as the function of the unknown parameter  $h$ , which is a likelihood function of  $P(\bar{s}; h)$ , where  $h$  is a wireless coefficient of channel. The vector of observation is given as

$$\bar{s} = \begin{bmatrix} s(1) \\ \vdots \\ s(N) \end{bmatrix} \quad (4.8)$$

The log likelihood of  $h$  is given as

$$\mathcal{L}(\bar{s}; h) = \ln p(\bar{s}; h) \quad (4.9)$$

Where

$$\mathcal{L}(\bar{s}; h) = -\frac{N}{2} \ln 2\pi\sigma^2 - \frac{1}{2\sigma^2} \sum_{k=1}^N (s(k) - h.p(k))^2 \quad (4.10)$$

To find maximum likelihood (ML) estimate, maximize  $\mathcal{L}(\bar{s}; h)$  then differentiate w.r.t 'h' and set equal to 0.

$$\frac{d\mathcal{L}(\bar{s}; h)}{dh} = -\frac{1}{2\sigma^2} \sum_{k=1}^N 2(s(k) - h.p(k)) \cdot (-p(k)) = 0 \quad (4.11)$$

$$\Rightarrow \sum_{k=1}^N p(k)(s(k) - h.p(k)) = 0$$

$$\Rightarrow \sum_{k=1}^N p(k)s(k) = h \sum_{k=1}^N p^2(k)$$

$$\hat{h} = \frac{\sum_{k=1}^N p(k)s(k)}{\sum_{k=1}^N p^2(k)} \quad (4.12)$$

After simplifying equation 4.12 the LS CE is given as

$$\hat{h} = P^{-1}S \quad (4.13)$$

### 4.3.2 MMSE CE TECHNIQUE

All pilots in this pilot-aided MMSE CE method are multiplexed with a wide range of data symbols in distinct subcarriers. The input symbols are linked directly to the output symbols. The computational difficulty of the MMSE approach is also low, whereas the computational sophistication of the LS CE method is high. The fundamental principle of the MMSE CE is to minimize the channel's MSE or BER. The MMSE block diagram is depicted in figure 4.11.

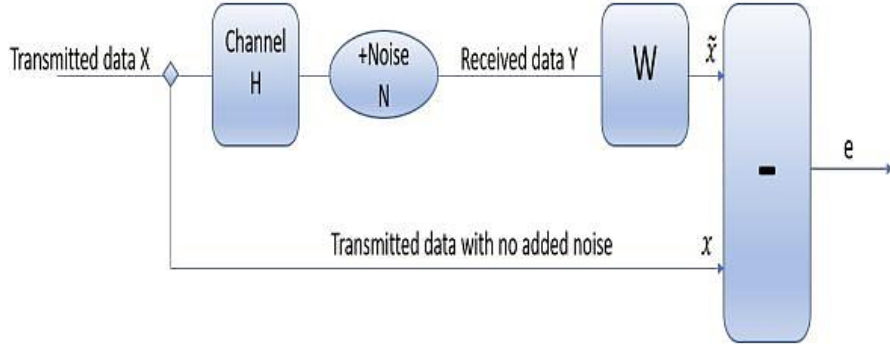


**Figure 4.11:** MMSE CE block diagram.

The MMSE Weight matrix is planned in such a manner that it produces a low MSE. The correlation between the approximated error and the signal received must fulfill the following condition in order to determine the weight matrix.

$$W.E\{e . Y^H\} = 0 \quad (4.14)$$

Where  $E\{.\}$  is the mathematical expression value and  $(.)^H$  is the Hermitian transpose, which transposes the matrix that contains a combination of real and imaginary elements. From the above equation

$$E\{e . Y^H\} = 0 \quad (4.15)$$

$$E\{(WY - X). Y^H\} = 0 \quad (4.16)$$

$$E\{WYY^H - XY^H\} = 0 \quad (4.17)$$

$$E\{WYY^H\} - E\{XY^H\} = 0 \quad (4.18)$$

$$WE\{YY^H\} - E\{XY^H\} = 0 \quad (4.19)$$

By solving above equations, we get

$$W = E\{XY^H\} . E\{YY^H\}^{-1} \quad (4.20)$$

Where  $E\{XY^H\} = R_{XY}$  is cross correlation of matrix X and Y,  $E\{YY^H\}$  is auto correlation of the matrix Y.

Assume, there is no correlation between transmitted data and noise, then

$$E\{X . n^H\} = 0 \ \& \ E\{n . X^H\} = 0 \quad (4.21)$$

To solve weight matrix W from equation,

$$\begin{aligned}
R_{YY} &= E\{YY^H\} & (4.22) \\
&= E\{(HX + n)(HX + n)^H\} \\
&= E\{(HX + n)(X^H H^H + n^H)\} \\
&= E\{HXX^H H^H + HXn^H + nX^H H^H + nn^H\} \\
&= E\{HXX^H H^H + nn^H\} \\
&= HE\{XX^H\}H^H + E\{nn^H\} \\
&= H(P \cdot I)H^H + \sigma^2 \cdot I & (4.23)
\end{aligned}$$

Where P is the power of the transmitted signal,  $\sigma$  is the Gaussian additive channel noise with variance and I is the identity matrix. H is the channel coefficient.

$$\begin{aligned}
R_{XY} &= E\{XY^H\} & (4.24) \\
&= E\{X(HX + n)^H\} \\
&= E\{X(X^H H^H + n^H)\} \\
&= E\{XX^H H^H + Xn^H\} \\
&= E\{XX^H\}H^H \\
&= (P \cdot I)H^H & (4.25)
\end{aligned}$$

The weight matrix for MMSE estimators is derived from equations

$$\begin{aligned}
W &= E\{XY^H\}E\{YY^H\}^{-1} & (4.26) \\
&= (P \cdot I)H^H(H(P \cdot I)H^H + \sigma^2 \cdot I)^{-1} \\
&= P \cdot H^H(PHH^H + \sigma^2 \cdot I)^{-1} \\
&= H^H(HH^H + \frac{\sigma^2}{P} \cdot I)^{-1} & (4.27)
\end{aligned}$$

By using equation, the baseline algorithms can be written as:

$$H_{MMSE} = H^H(HH^H + \frac{\sigma^2}{P} \cdot I)^{-1}H_{LS} \quad (4.28)$$



### 4.3.3 DFT CE TECHNIQUE

The DFT-based CE technique is developed to remove the noise effect outside the optimum delay in channel and to boost effectiveness of MMSE or LS. Figure 4.12 depicts the DFT-based CE block diagram. It improves CE performance.

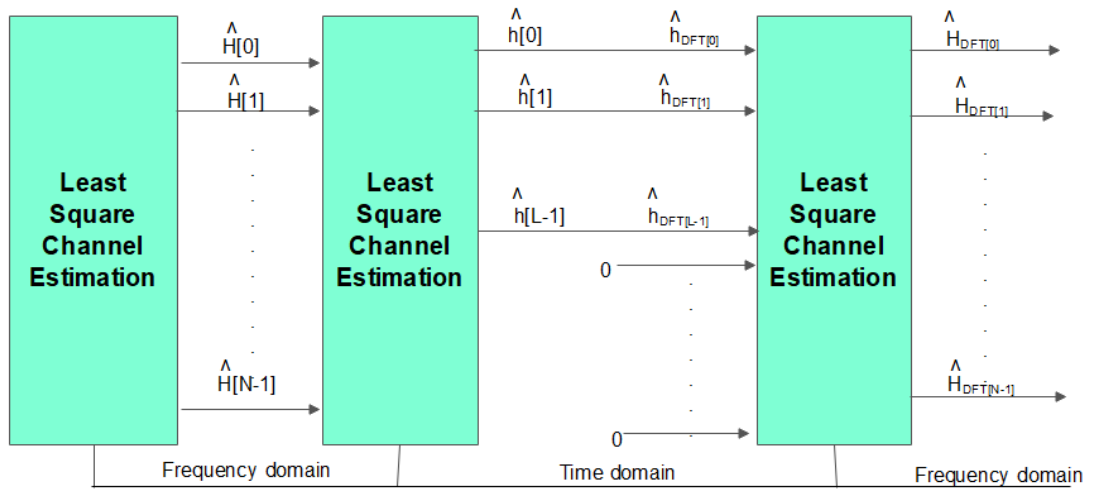


**Figure 4.12:** The DFT based CE block diagram.

The IDFT of the CE is performed after receiving channel gain of the  $k$ th subcarrier utilizing any MMSE or LS.

$$IDFT\{\hat{H}[k]\} = h[n] + z[n] \triangleq \hat{h}[n] \quad n = 0, 1, \dots, N - 1 \quad (4.29)$$

Where  $\hat{H}[k] = k^{\text{th}}$  subcarrier estimation of channel gain

$Z[n]$  = Time domain component of noise

Coefficients for optimum  $L$  channel delay are described by neglecting the coefficients that comprise noise and are given as

$$\widehat{h}_{DFT}[n] = \begin{cases} h[n] + z[n], & n = 0, 1, 2, \dots, L - 1 \\ 0, & \text{otherwise} \end{cases} \quad (4.30)$$

The leftover L elements are transformed once more to frequency domain and are given as

$$\widehat{H}_{DFT}[k] = DFT\{\widehat{h}_{DFT}[n]\} \quad (4.31)$$

#### 4.3.4 SPARSE CE TECHNIQUE

Channels with a higher delay spread but a lesser number of non-zero taps are encountered in underwater acoustics, HDTV, and mobile communications. To decrease ISI just at the obtained end, efficient CE with improved equalization is required for such types of applications. To address this issue, a MP CE algorithm is being employed. MP algorithms are classified into several types, with only minor differences in their performance. When contrasted to other MP, BMP has low complexity. The sparse CE implemented in this concept uses the OMP algorithm. Sequentially, the column that closely fits the residual is chosen until the finalization of the requirements is obtained. Iterations are repeated until the necessary amount of taps P is selected, or the residual becomes less. The residual vector is denoted by

$$b_p = b_{p-1} - \frac{(a_{k_p}^H b_{p-1}) a_{k_p}}{\|a_{k_p}\|^2} \quad (4.32)$$

Where  $b_{p-1}$  is the  $(p-1)^{\text{th}}$  residual vector iteration,

$a_{k_p}$  is A column matrix element at  $p^{\text{th}}$  iteration.

$k_p$  position by the value of tap is denoted by

$$\widehat{c}_{k_p} = \frac{(a_{k_p}^H b_{p-1})}{\|a_{k_p}\|^2} \quad (4.33)$$

### 4.3.5 ALAMOUTI CE TECHNIQUE

The alamouti CE is one of the blind CE algorithms. The 2x2 transceiver of alamouti CE with OFDM system is displayed in the figure 4.13.

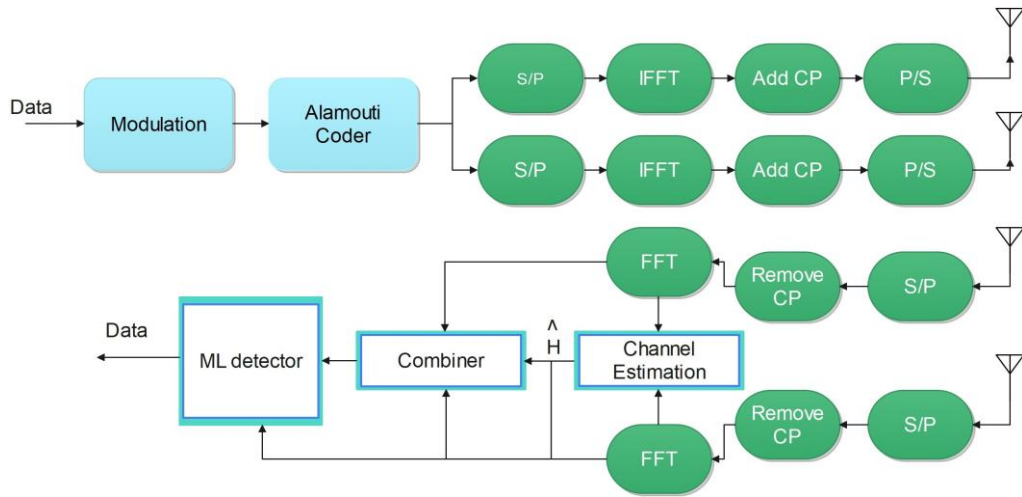


**Figure 4.13:** Alamouti CE block diagram.

In this method, the transmitter of the signals of pilot tones is added into a data symbol for CE. Then the data and tones are encoded, and encoded data is modulated using the QAM modulation technique. In this transmission in time and space domains, the blocks of data are orthogonal. The data streams are then divided into sub-streams and sent through the OFDM system. Therefore, the transmitted block at the transmitter end is given as

$$S^{tx} = [S_p^{tx}(0) \dots \dots \dots S_p^{tx}(N - 1)] \quad (4.34)$$

These transmitted symbols are performed IFFT after the transmission of Alamouti coding. The assumption of the channel is constant for two intervals in time. The signal of modulation on the transmitter antenna is given as

$$S_p^{tx}(n) = IFFT\{S_p^{tx}\} \quad (4.35)$$

Later on, to avoid ISI in the OFDM system, CP is added. Finally, the data is sent over a channel. At the destination end, the channel coefficients are for  $k^{\text{th}}$  subcarrier is for  $p^{\text{th}}$  interval is given as

$$y_p^{rx}(n) = \sum_{tx \in 1,2} s_p^{tx}(n) \otimes h_{tx,rx}(n) + w_p^{rx}(n) \quad (4.36)$$

Where  $h$  is the CIR between the transceiver, after removing the CP, the complex symbols are retrieved by FFT. The CE is done after FFT using alamouti detector at every subcarrier. After the detection, the space diversity is used to extract every subcarrier by maximum ratio combining. Then apply, a ML detector to detect each subcarrier.

#### 4.3.6 DOUBLE SELECTIVE CE TECHNIQUE

To estimate double selective channels, scattered pilots are used based on the time-frequency domain. Interference is reduced at the information and positions of pilot by using the iterative interference cancellation method [123-125]. The benefits of CE is that it downgrades interference, and it does not necessitate clustered pilots or BEM. The confinement of this approach is the presumption of delay taps that are restricted over a period of time and computational sophistication.

The transmitted signal's input-output connection across the doubly selective channel is represented as

$$y = Dx + n \quad (4.37)$$

Where 'X' represents vectorized transmitted data, vectorized received data, and vectorized noise  $n$ .  $D$  is a sender matrix, and it is denoted as

$$D = Q^H HG \quad (4.38)$$

The channel estimate for one tap channel is done utilizing the LS method, and its CE is provided as

$$\hat{h}_p^{LS} = \text{diag}\{x_p\}^{-1} y_p \quad (4.39)$$

### 4.3.7 DNN CE TECHNIQUE

The LSTM-based neural network is trained for a single subcarrier [126], and the BER is computed and compared to the LS and MMSE estimates. The wireless channel is considered fixed during the offline training and online deployment stages. Each transmitted OFDM packet performs a random phase shift to evaluate the neural network's stability. The effects of many pilot symbols and the length of the CP are taken into account. The DNN model was used to train the simulated data offline, and then the dual-CE was done online.

Meanwhile, a pre-training strategy for DNN was developed to increase the algorithm's performance. The DNN approaches described above essentially use the deep version of ANNs to complete CE and detection of signal. However, alternative neural network models are more favourable to mining sequence data characteristics and increasing the system's performance. The obtained signal in the time domain is written as

$$y = h \otimes d + e \quad (4.40)$$

Where  $h$ = matrix of channel.

$\otimes$ =cyclic convolution

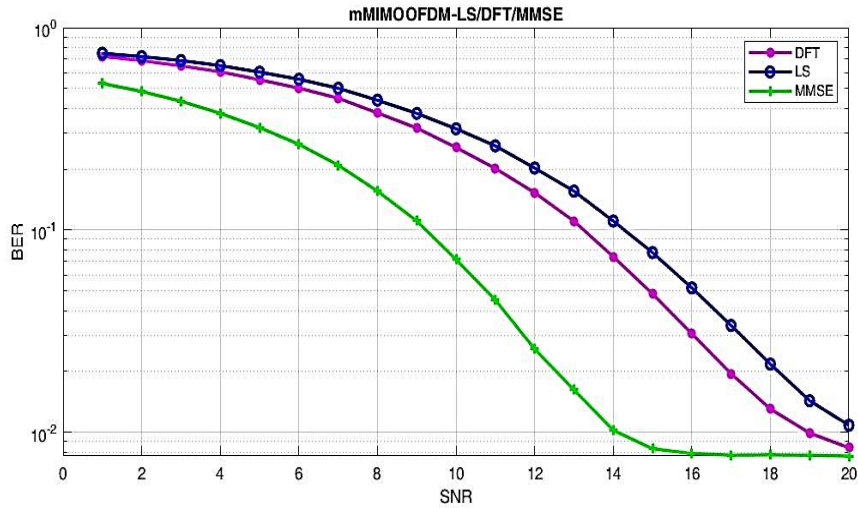
$y$ = received signal

$e$ = AWGN noise.

The sender signal reaches the equalizer after FFT and then carries out MLD is expressed as

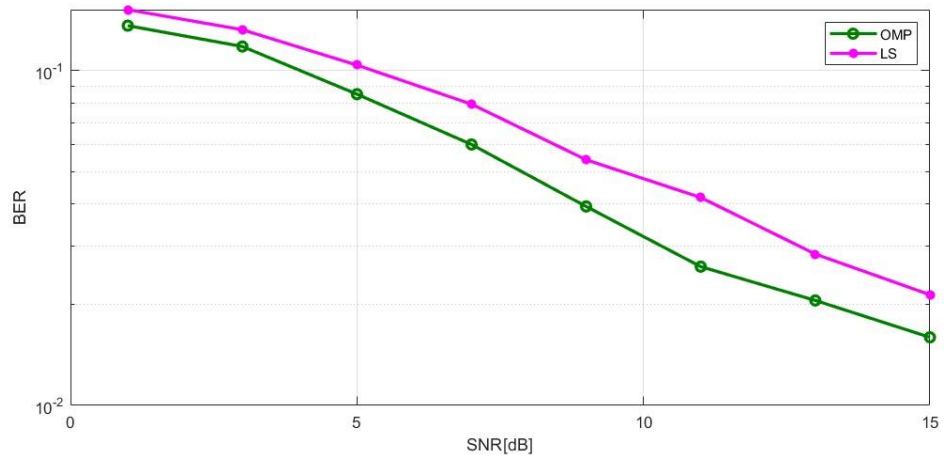
$$\hat{D} = \underset{\sim}{D} \| Y - H \underset{\sim}{D} \|^2 \quad (4.41)$$

## 4.4 SIMULATION RESULTS & DISCUSSION



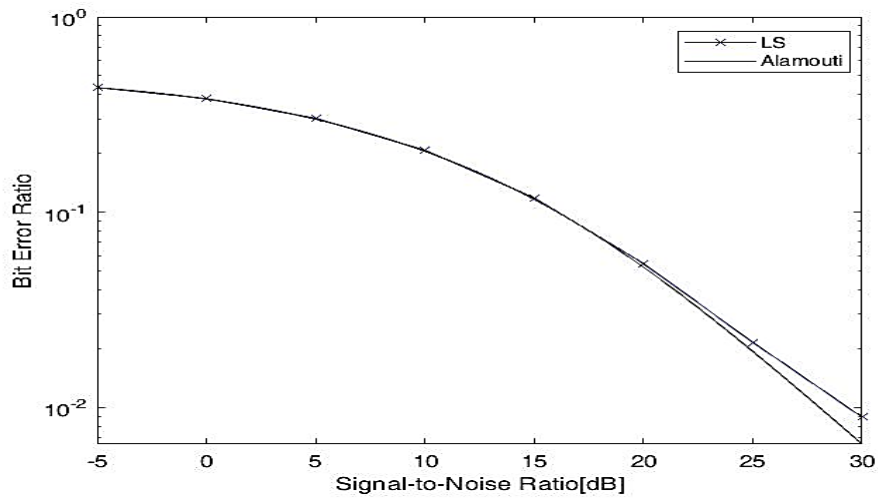
**Figure 4.14:** BER vs SNR [dB] analogy of LS, MMSE and DFT CE.

Figure 4.14 compares LS, DFT, and MMSE OFDM CE approaches, and the results display that the MMSE CE approach outperforms DFT and LS. The problem with this approach is contamination because of the pilot, which occurs because of the huge proportion of pilots utilized to estimate the channel.



**Figure 4.15:** BER vs SNR [dB] analogy of LS and OMP CE.

The sparse CE using OMP algorithms is shown in Figure 4.15. The results show that sparse CE outperforms the LS CE algorithm. The iterations utilizing time-varying channels are the algorithm's limitation. Even as many iterations increases, so does the system's complexity.



**Figure 4.16:** BER vs SNR analogy of alamouti and LS CE.

From figure 4.16, it is observed that the alamouti CE performance is better as the BER of this CE is less compared to the conventional LS method.

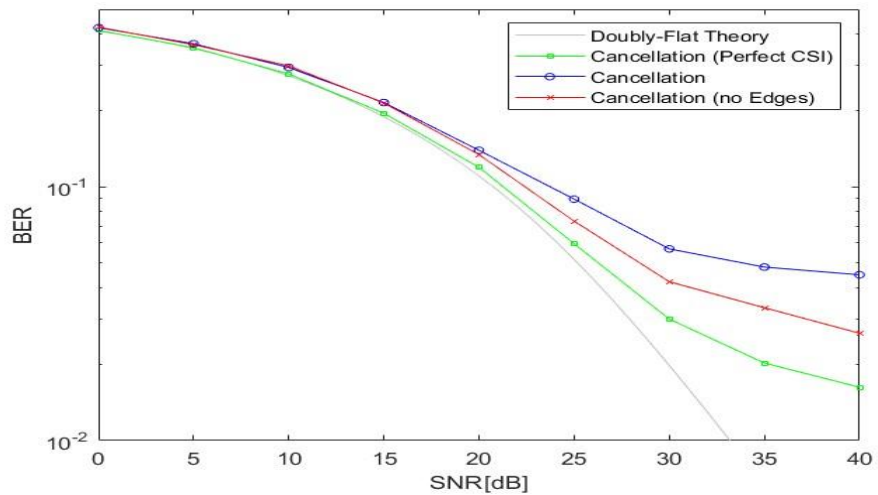


**Figure 4.17:** BER vs SNR [dB] analogy of doubly selective CE with and without cancellation.

Figure 4.17 displays the doubly-selective CE in OFDM systems. The benefits of CE are that it downgrades interference and does not necessitate clustered pilots or BEM. However, the confinement of this approach is the presumption of delay taps that are restricted over the time and computational sophistication.

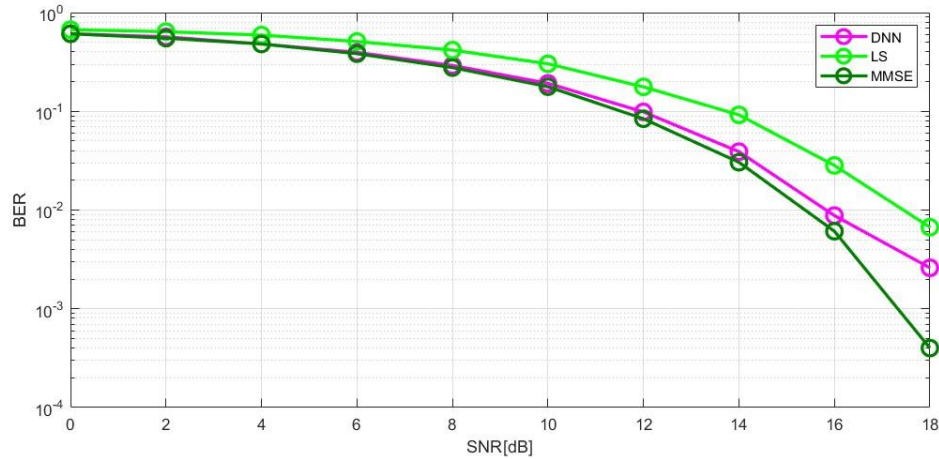


**Figure 4.18:** BER vs SNR [dB] analogy of DNN, LS and MMSE CE.

Figure 4.18 shows the CE technique using DNN's. The analogy results show that the deep learning CE technique performs well in analogy to LS CE technique and almost shows a comparable performance concerning MMSE CE technique. The main benefits of this approach are the improvement in the performance of the system. The limitation of this channel estimation technique is the use of test vectors and training data sets by which the system's complexity rises. The other disadvantage of the system is, again, the same as it uses the OFDM MCM technique. The simulation parameters of the executed CE's are displayed in the table 4.1.



**Table 4.1:** Simulation parameters utilized for executing the specified CE's.

<b>Parameters/ Algorithms</b>	<b>LS, MMSE, DFT</b>	<b>Sparse, LS</b>	<b>Alamouti, LS</b>	<b>Double Selective CE</b>	<b>DNN, LS, MMSE</b>
<b>Number of subcarriers</b>	128	128	24	128	64
<b>Type of modulation</b>	QAM	QAM	QAM	QAM	QPSK
<b>Number of transmitters antennas</b>	10	10	10	15	10
<b>Number of receivers antennas</b>	10	10	5	10	10
<b>Order of modulation</b>	8	4	256	256	8
<b>Multi carrier modulation</b>	OFDM	OFDM	OFDM	FBMC and OFDM	OFDM
<b>Length of guard interval</b>	8	8	4	4	16
<b>SNR</b>	20	15	40	40	40
<b>Number of iterations</b>	10	2	25	10	2
<b>Number of symbols</b>	114	26	14	14	2
<b>Channel taps</b>	2	2	2	2	2

#### 4.5 SUMMARY

This chapter mainly discusses CE techniques for wireless systems. It mainly focuses on types of CE methods and pilot arrangements. Some of the existing CE methods are also discussed depending on the type of CE methods, which were implemented

for OFDM systems only. The CE techniques are executed using MATLAB software. The effectiveness of the current methods is demonstrated using BER concerning SNR. These existing methods have various limits depending on system performance, pilot contamination, and system complexity. To address this, numerous CE techniques were developed. However, the primary disadvantage of all known methods is that they are only implemented for OFDM multi-carrier systems. A practical multicarrier-based CE must be created as a need for a physical layer in order to meet the critical necessities of the 5G mMIMO WCS.

## **CHAPTER-5**

### **MODIFIED ENTROPY BASED LEAST SQUARE CHANNEL ESTIMATION TECHNIQUE**

As mMIMO systems have become popular because of their enhanced data transmission rates, robustness against multipath fading, enhanced SE, and ability to communicate with several users with extensive coverage. The important challenge of the mMIMO systems is the replenishment of the CSI precisely, along with the synchronization between the receiver and transmitter. The CSI is recovered with the help of various estimation of channel techniques. This thesis presents a MELs CE technique for 5G mMIMO-UFMC systems. From chapter 3, it is evident that the UFMC system outperforms better than the other MCM approaches. So, the proposed CE is designed for the UFMC system.

#### **5.1 UFMC SYSTEM MODEL**

UFMC is a high-speed transmission technology for 5G [127] mobile and wireless communication. UFMC addresses the need for high bandwidth efficacy and increased implementation through the use of FFT and IFFT, as well as the reduction of ISI with the use of the Dolph Chebyshev filter, ruggedness to multi-path fading, and delay. The Dolph Chebyshev filter eliminates the insertion of CP, a significant shortcoming of the OFDM system, and increases symbol length. A Dolph Chebyshev filter is employed in signal processing to attain precise frequency response attributes, all the while minimizing transition bandwidth and minimizing passband and stopband ripples. A Dolph-Chebyshev filter is effective in reducing interference by employing its distinctive frequency response characteristics to suppress out-of-band emissions and attenuate unwanted signals. This filter's design minimizes passband and stopband ripples while maintaining a steep roll-off in the transition region between them. As a result, the filter can significantly diminish the energy of signals that fall outside the desired frequency range, thereby reducing the potential for interference with neighbouring channels or systems. This precise control over the filter's frequency response aids in mitigating interference and

improving the overall performance and reliability of the system. A typical pilot-aided UFMC for a 5G system is displayed in figure 5.1. At the transmitter, the data symbols are combined and mapped into multi amplitude-phase signals using QAM modulation. By using IFFT, the complex signals are modulated by N subcarriers.

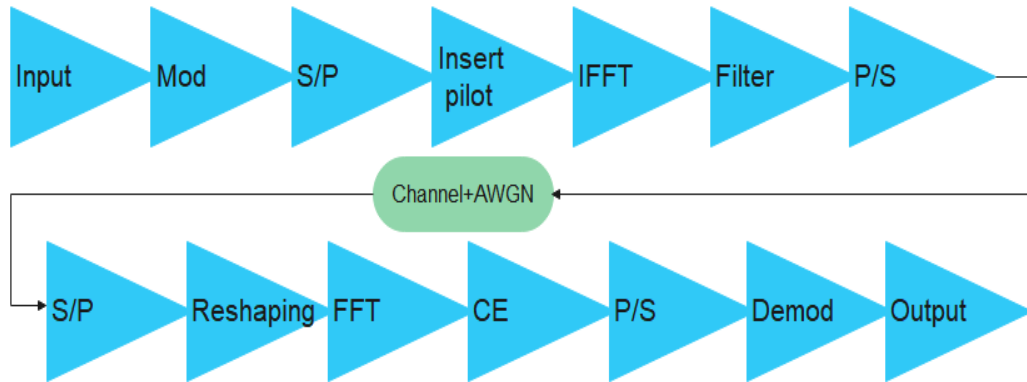


**Figure 5.1:** Pilot-aided UFMC system.

Assuming N sub-carriers within the UFMC system, all subcarriers are divided into A subbands, with each subband comprising many subcarriers successively. Each sub-band is comprised of  $K=N/A$  subcarriers. There are numerous other techniques for splitting the subcarriers, such as random or average distribution. The  $S_a$  ( $a=1, 2, \dots, A$ ) is the modulated OQAM symbols in the  $a^{\text{th}}$  sub bands. It also includes  $Q_a$  subcarriers and is given as

$$\sum_{a=1}^A Q_a = N \quad (5.1)$$

The modulated symbols in each subband are sent to an N-point FFT and then to the Dolph Chebyshev filter. In order to reject the effect of ISI in the UFMC system, the Dolph Chebyshev filter [128] is used. The function of Dolph Chebyshev is constructed based on the well-known polynomials of Chebyshev, designed to simplify the issue of designing a radio antenna with optimal directional characteristics. The equation of Chebyshev polynomials is given as

$$T_p(y) = \begin{cases} \cos(p \cos^{-1}y) & \text{for } |y| \leq 1 \\ \cosh(p \cosh^{-1}y) & \text{for } |y| > 1 \end{cases} \quad (5.2)$$

The recurrence relation of the defined polynomials is given as

$$\begin{aligned}
T_0(y) &= 1, \quad T_1(y) = y, \\
T_p(y) &= 2yT_{p-1}(y) - T_{p-2}(y) \quad \text{for } p \geq 2
\end{aligned} \tag{5.3}$$

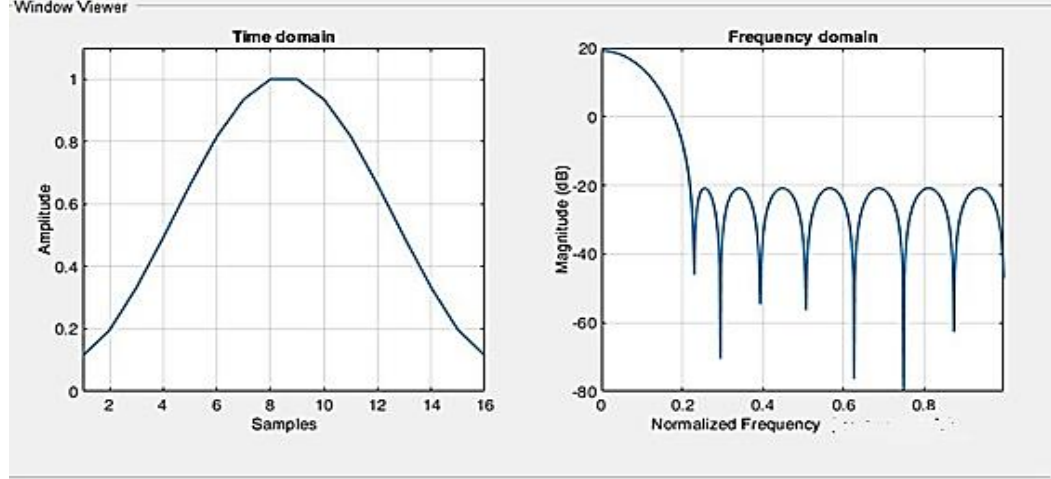


**Figure 5.2:** Dolph Chebyshev filter window in time-frequency domain.

Figure 5.2 displays the window of Dolph Chebyshev filter in time and frequency domain with the filter of 16 and side lobe attenuation of 40 dB.

These properties are derived from  $p^{\text{th}}$  order polynomial in  $y$ .  $T_p(y)$  in the open interval of  $(-1, +1)$  has  $p$  zeros and in the closed interval of  $[-1, +1]$  has  $p+1$  extrema.  $T_p(y)$  will oscillates between  $-1$  and  $+1$  for  $p$  in  $[-1, +1]$ .  $T_p(y) > 1$  if  $y > 1$  for large  $y$ ,  $T_p(y) \approx 2^{p-1}y^p$ . The filtered messages out of each sub band are added together to form  $X$ . As a consequence, the UPMC's transmitted signal is provided as

$$X = \sum_{a=1}^A \text{IFFT}(S_a) * f_a \tag{5.4}$$

Where  $f_a$ =filter coefficient for sub band  $a$ . By using pilot-based CE technique with UPMC system improves the overall efficacy [129] of the 5G wireless communication system.

## 5.2 LSCE FOR UPMC SYSTEM

The mathematical statistics of the LS algorithm [130-131] are developed from the curve fitting. The LS CE for the mMIMO-UPMC system is displayed in figure 5.3.

For the mMIMO-UFMC system, the CE is considered using the known signal, and its estimate is written as

$$Y_k = X_k(l)H_k(l) + N_k(l) \quad (5.5)$$

Where  $Y_k$ = Received pilot signal

$X_k$ = Pilot signal of transmitted

$H_k$  = Frequency domain response of a channel and

$N_k$ = AWGN of channel.

The LS estimate has less computational sophistication and the estimate is given as

$$\hat{h}_{ls}(l) = X(l)^{-1}Y(l) \quad (5.6)$$

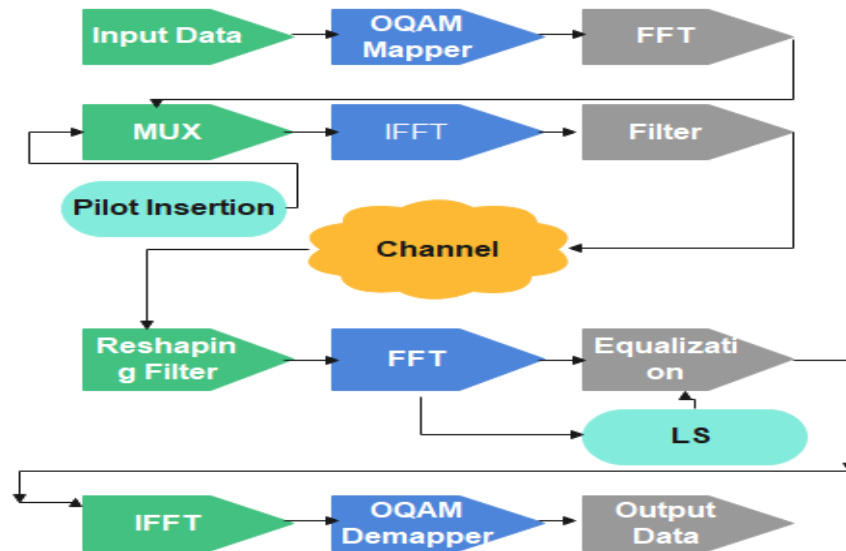


**Figure 5.3:** MIMO-UFMC system with LS.

### 5.3 MMSE CE FOR UFMC SYSTEM

In this pilot-aided MMSE CE method, all the pilots are multiplexed with several data symbols in different subcarriers [132-133]. The input symbols are directly linked with the output symbols. The computational complexity is also less in the MMSE method, but in contrast to the LS CE method, the computational sophistication is high. The main rule of the MMSE CE is to degrade the MSE or BER of the channel. The MMSE CE is shown in figure 5.4

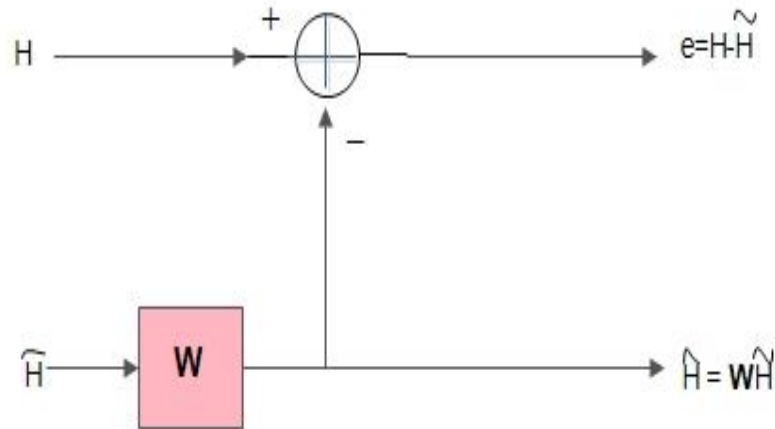


**Figure 5.4:** Multiplying weight vector with LS estimate to obtain MMSE CE.

The MMSE estimation is given as

$$h_{MMSE} = W e_{mmse} \quad (5.7)$$

Where  $W$  = weight vector

$e_{mmse}$  = energy estimator. It is given as

$$e_{mmse} = R_{ey} R_{yy}^{-1} y \quad (5.8)$$

Where  $R_{ey}$  = Auto covariance of  $e$  matrix that is channel energy

$R_{yy}$  = Auto covariance of  $y$  matrix that is received signal.

The auto variance of the  $e$  matrix and  $y$  matrix is given as

$$R_{ey} = E\{e y^H\} = R_{ee} W^H x^H \quad (5.9)$$

$$R_{yy} = E\{y y^H\} = x W R_{ee} F^H x^H + n^2 I_n \quad (5.10)$$

Where  $x$  = transmitted signal

$n^2$  = Noise variance and

$I$  = Identity matrix.

## 5.4 MELS CE FOR UFMC SYSTEM

The entropy-based method evaluates antennas through their transmitted information to and from other antennas. So, the LS CE algorithm under modified entropy is proposed for MIMO-UFMC. Let P be the transmitter node, and T be the receiver node consisting of N transmitter antennas and M receiver antennas. As there are N antennas at node P, the received signal is given as

$$Y_p = S_p h_1 + S_t h_2 + F \tilde{n}_p \quad (5.11)$$

Where  $S_p$  and  $S_t$  = pilot matrix that are known at the receiver end.

$h_1, h_2$  = channel matrices estimate.

Therefore, the received signal equation is rewritten and is given as

$$Y_p = Sh + F \tilde{n}_p \quad (5.12)$$

The MELS procedure is shown in figure 5.5.

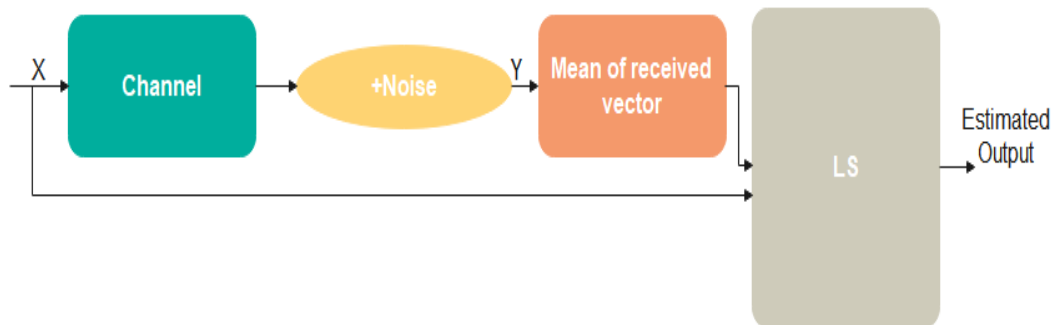


**Figure 5.5:** MELS block diagram.

The mMIMO-UFMC system with MELS is displayed in the figure 5.6.



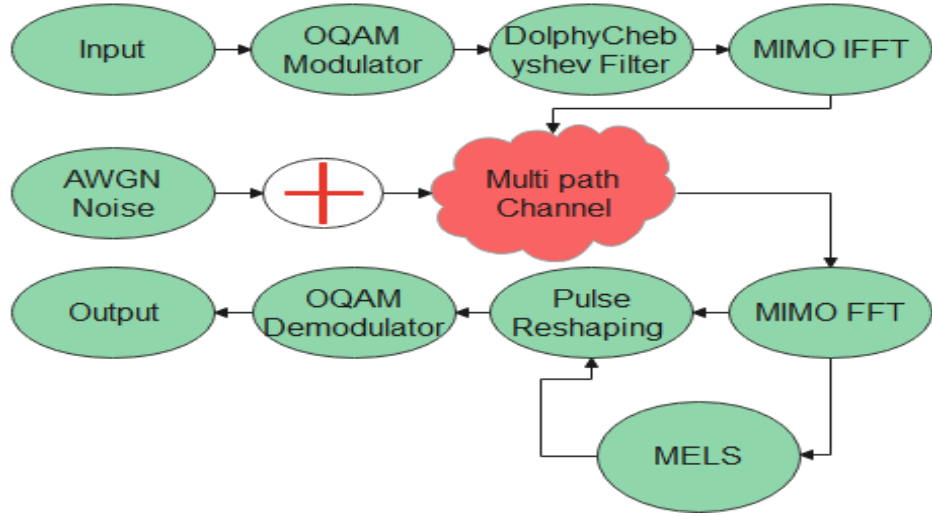


**Figure 5.6:** mMIMO-UFMC system with MELS.

In modified entropy, first, the summation of all the received inputs must be calculated. Later on, the mean is calculated based on the modulation order of the signal. The modified entropy is given as

$$S^\theta = \frac{X_1 + X_2 + \dots + X_p}{M} \quad (5.13)$$

Where M= Modulation order

$X_1 + X_2 + \dots + X_p$  = Summation of the received inputs at the receiver.

Finally, the LS estimate after the modified entropy  $S^\theta$  of the received signal is given as

$$\hat{h} = S^\theta (X^{-1} Y_p) \quad (5.14)$$

Where  $S^\theta$  = modified entropy of the S.

BER and the MSE are mainly considered for every wireless communication system design. The BER analysis of MIMO-UFMC in AWGN is obtained at the receiver end. In UFMC, first, each subcarrier is filtered using the Dolphy Chebyshev filter, and each subband needs to perform the inverse process of the filter. The noise variance of  $i^{\text{th}}$  subcarrier of the UFMC system in the  $i^{\text{th}}$  sub-band is given as

$$\sigma_a^2 = \frac{\sigma_n^2}{|r_k^2|} \quad (5.15)$$

Where  $r_k$  = Equivalent response of the filter related to  $k^{\text{th}}$  subcarrier

$\sigma_n$ = Variance of AWGN.

Finally, BER of UFMC with M-QAM under AWGN channel for the proposed CE is given as

$$P_e = \frac{1}{AI} \sum_{a=1}^A \sum_{i=1}^I \frac{2(\sqrt{M}-1)}{\sqrt{M} \log_2 \sqrt{M}} Q * \sqrt{\frac{6E_b}{N_0}} |r_k|^2 \cdot \frac{\log_2 \sqrt{M}}{M-1} \quad (5.16)$$

Where A=Total subcarriers

I=Total sub bands.

As the UFMC is entirely not an orthogonal waveform complete, the band's subbands and subcarriers are orthogonal. Therefore, the overall average BER of the proposed CE with UFMC is reduced.

The MSE of MELS CE for mMIMO-UFMC is given as

$$P_{MSE} = \left\{ \|S^\theta F \tilde{n}_p\|^2 \right\} \quad (5.17)$$

The analytical analysis of the mMIMO-UFMC system with MELS CE to calculate BER & MSE a step-by-step procedure is represented. The procedure is as follows

i. Signal generation and transmission

The transmitted signal consists of multiple subbands, each containing QAM-modulated symbols. The time-domain signals from each subband are filtered using a prototype filter and then combined to form the transmitted signal. For each subband i (1 to numSubbands)

Generate random bits:

$$bitsIn_i(bitspersubcarrier * subbandsizebits) \quad (5.18)$$

QAM-modulate bits:

$$symbolsIn_i = qammod(bitsIn_i, 2^{bitspersubcarrier}) \quad (5.19)$$

Create subband UFMC symbol:

$$symbolsufmc_i = [zeros(offset_i, 1); symbolsIn_i; zeros(numFFT - offset_i - subbandsize, 1)] \quad (5.20)$$

Compute IFFT:

$$ifftout_i = ifft(ifftshift(symbolsInufmc_i)) \quad (5.21)$$

Apply subband filter:

$$filterout_i = conv(bandfilter_i, ifftout_i) \quad (5.22)$$

Aggregate filtered subband responses:

$$txsig = txsig + filterout_i \quad (5.23)$$

ii. Channel and reception

The transmitted signal is received, passed through an AWGN channel, and then down sampled. The received symbols are equalized using a zero-forcing equalizer, and the data symbols are demodulated.

Receive signal in time domain:

$$rxsig = awgn(txsig, SNR_{dB}, measured) \quad (5.24)$$

Pad receive vector:

$$yrxpadded = [rxsig; zeros(2 * numFFT - numel(txsig), 1)] \quad (5.25)$$

Perform FFT and down sample:

$$rxsymbols = fftshift(fft(yrxpadded)) \quad (5.26)$$

Select data subcarriers:

$$datarxsymbols = rxsymbols[subbandoffset + (1: numsubbands * subbandsize)] \quad (5.27)$$

Equalize per subband:

$$equalizedrxsymbols = bsxfun(@times, datarxsymbolsmat, prototypefilterInv) \quad (5.28)$$

Demodulate received symbols:

$$rxbits = qamdemod(equalizedrxsymbols, 2^{bitspersubcarrier}) \quad (5.29)$$

iii. Channel estimation

The channel is estimated using pilot symbols, and modified entropy is applied to the estimated channel coefficients. For each block nb and receive antenna (1 to Nb and 1 to Nr)

Construct matrix A with QAM-modulated symbols for pilots:

$$A = [diag(dmod(PPos, nb, 1)).F(PPos, :); ...] \quad (5.30)$$

Compute channel estimates:

$$chanestim = pinv(A).fft(PPos, nb, nr) \quad (5.31)$$

Apply modified entropy:

$$chanest = mentropy(chanestim(:, 1)) \quad (5.32)$$

Store channel estimates:

$$coeffest(nt, nr, :, nb) = chanest((1:L) + (nt - 1).L) \quad (5.33)$$

iv. BER and MSE calculation

The BER and MSE are computed based on the received and demodulated symbols.

Initialize BER calculator:

$$BER = comm.errorrate \quad (5.34)$$

Demodulate received data symbols:

$$rxbits = qamdemod(equalizedrxsymbols, 2^{bitpersubcarrier}) \quad (5.35)$$

Compute BER:

$$ber = BER(inpdata(:), rxbits) \quad (5.36)$$

Compute MSE:

$$MSE = var(inpdata(:), rxbits) \quad (5.37)$$

$$if SNR_{dB} > 1 \text{ cn: } op.BER = ber, \text{cn: } op.MSE = MSE.cn \quad (5.38)$$

$$Else: op.BER = ber(1), op.MSE = MSE(1) \quad (5.39)$$

The code involves multiple matrix operations, function calls, and modulation/demodulation steps, making it a complex simulation of a mMIMO - UFMC system with MELS CE method. The equations provided here give an overview of the mathematical operations performed in each section.

## 5.5 SIMULATION RESULTS & DISCUSSION

The CSI performance is estimated and the its simulation parameters are enumerated in table 5.1.

**Table 5.1:** Simulation parameters of MELS CE.

S. No	Simulation Parameters	Numbers
1	Subcarriers	1024
2	Number of transmitter antennas	10
3	Number of receiver antennas	10

4	Bits per subcarrier	8
5	Modulation	OQAM
6	Modulation Order	256
7	Number of Taps	3
8	SNR (dB)	15
7	Number of iterations	25

The two parameters estimated for the system's performance are BER and MSE. The MSE measures the average square of the error. The MSE is estimated between the estimated CSI and the original channel CSI. CSI is computed at all pilot sub-channels. Therefore, MSE is used to measure the uncertainty in estimating a channel. BER [134] is another important parameter that characterizes channel performance. It is defined as many bits that are changed to the transmission medium per second using a digitally modulated signal. If the probability of error is reduced while estimating a channel, the BER is reduced, which enhances the system's performance.

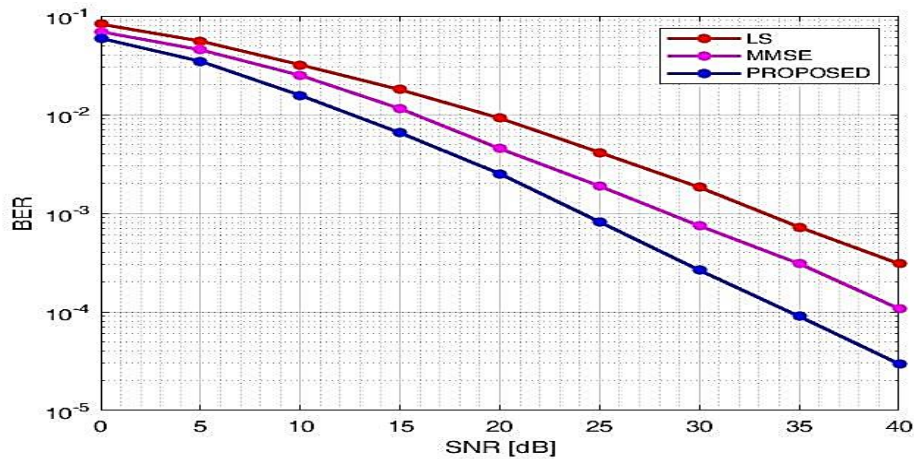


**Figure 5.7:** BER vs SNR analogy of MELs, LS and MMSE.

**Table 5.2:** BER vs SNR analogy of MELS, LS and MMSE.

SNR (dB)	Proposed CE (MELS)	MMSE	LS
0	0.05928	0.06917	0.08248
5	0.03466	0.04533	0.05555
10	0.01566	0.02497	0.03196
15	0.006525	0.01148	0.01788
20	0.00251	0.004513	0.009192
25	0.0008155	0.001881	0.004129
30	0.0002641	0.0007452	0.001831
35	$8.99 \times 10^{-5}$	0.0003081	0.0007227
40	$2.97 \times 10^{-5}$	0.0001077	0.0003077

Figure 5.7 displays that the proposed MELS approach has a lower BER than conventional LS and MMSE techniques for MIMO-UFMC systems. If the BER is reduced, the system performance is increased. Hence, the proposed CE method works better compared to the previous existing CE methods.

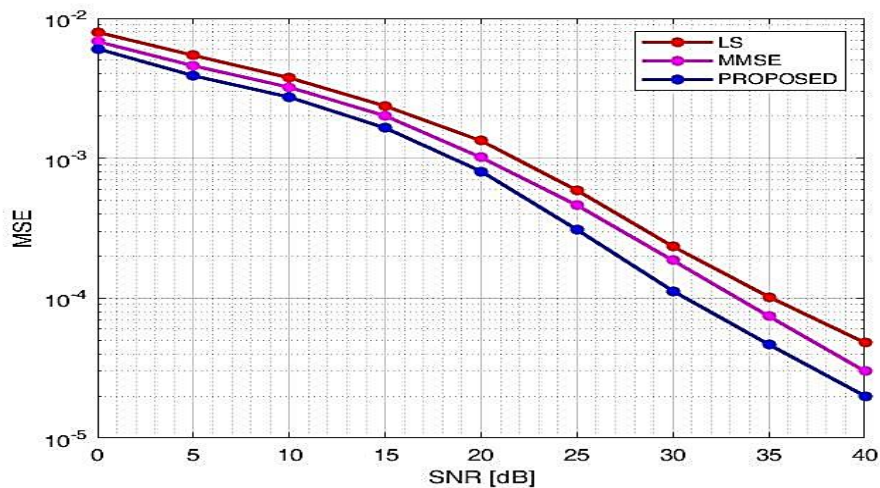


**Figure 5.8:** MSE vs SNR analogy of MELS, LS and MMSE.

**Table 5.3:** MSE vs SNR analogy of MELS, LS and MMSE.

SNR (dB)	Proposed CE (MELS)	MMSE	LS
0	0.006047	0.006811	0.007947
5	0.003881	0.004569	0.005424
10	0.002729	0.003211	0.00375
15	0.001644	0.002006	0.002357
20	0.0008051	0.001011	0.001331
25	0.000308	0.0004606	0.0005884
30	0.0001124	0.0001857	0.0002338
35	$4.66 \times 10^{-5}$	$7.42 \times 10^{-5}$	0.0001021
40	$2 \times 10^{-5}$	$3.01 \times 10^{-5}$	$4.81 \times 10^{-5}$

Figure 5.8 shows that the proposed MELS approach reduces the MSE analogy to conventional LS and MMSE techniques for MIMO-UFMC systems. MSE is a linear estimation method and an essential parameter in statistical learning. Optimizing the MSE values gives an enhanced system performance. The proposed CE method and UFMC technique provide a low MSE value compared to the previous methods. The above-explained conventional CE methods are implemented along with the UFMC MCM technique.

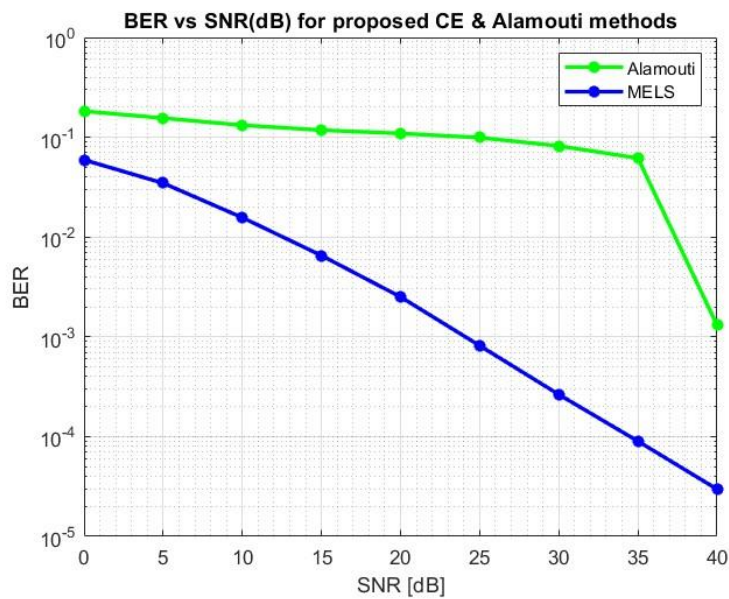
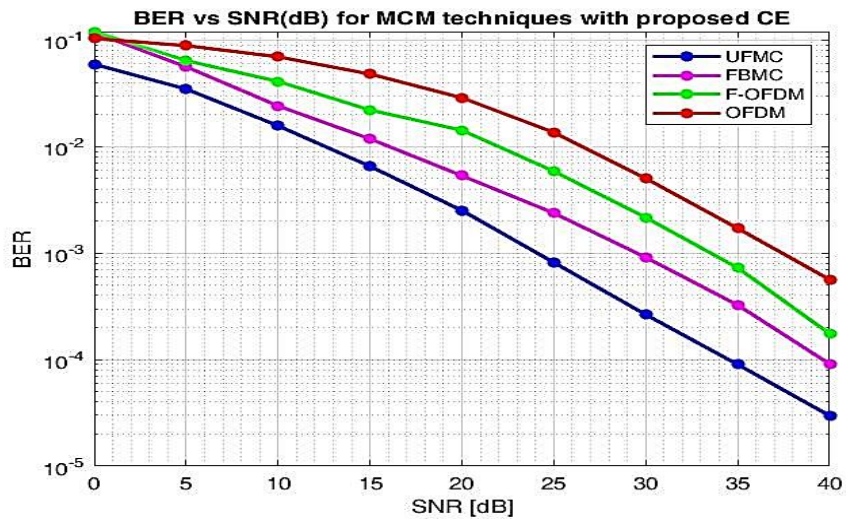


**Figure 5.9:** BER vs SNR analogy of MELS and Alamouti.

**Table 5.4:** BER vs SNR analogy of MELS and Alamouti.

SNR (dB)	Proposed CE (MELS)	Alamouti
0	0.05928	0.182477
5	0.03466	0.155549
10	0.01566	0.131962
15	0.006525	0.117885
20	0.00251	0.109192
25	0.0008155	0.0991288
30	0.0002641	0.0818308
35	$8.99 \times 10^{-5}$	0.0617227
40	$2.97 \times 10^{-5}$	0.00130769

Figure 5.9 displays that the proposed MELS approach has a lower BER than Alamouti method for MIMO-UFMC systems. If the BER is reduced, the system performance is increased. Hence, the proposed CE method works better compared to the previous existing Alamouti CE method.



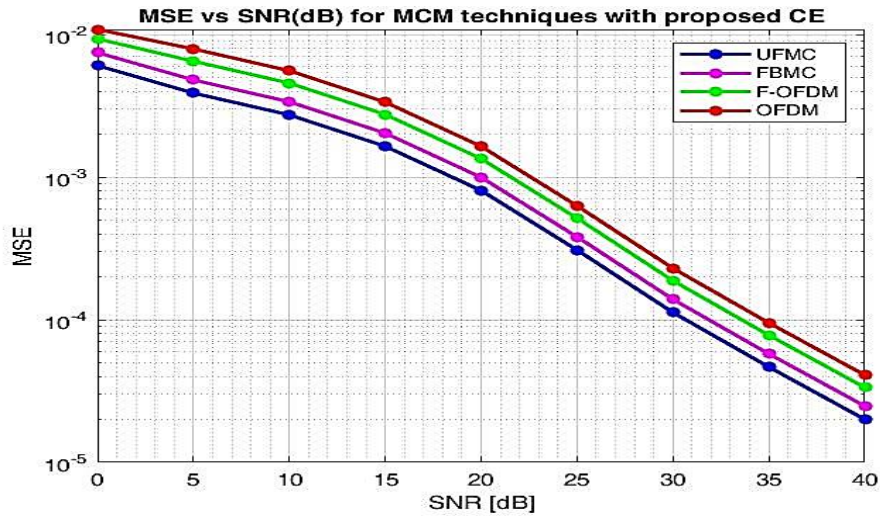
**Figure 5.10:** BER vs SNR analogy of MCM's utilizing MELS.



Figure 5.10 shows that the proposed CE technique works better with the UFMC system compared to OFDM, FBMC, and F-OFDM MCM techniques. The obtained BER is lower than that of the mMIMO-UFMC system. Table 5.5 shows the comparative result as well.

**Table 5.5:** BER vs SNR for MCM techniques using MELS.

SNR (dB)	UFMC	FBMC	F-OFDM	OFDM
0	0.05928	0.1201	0.1201	0.1031
5	0.03466	0.05614	0.06411	0.08859
10	0.01566	0.02408	0.04089	0.06962
15	0.006525	0.0118	0.02203	0.04498
20	0.00251	0.005327	0.01422	0.02869
25	0.0008155	0.002373	0.005865	0.01358
30	0.0002641	0.0009103	0.002156	0.005018
35	8.99x10 <sup>-5</sup>	0.000325	0.000727	0.001708
40	2.97x10 <sup>-5</sup>	9.1x10 <sup>-5</sup>	0.000175	0.0005635



**Figure 5.11:** MSE vs SNR analogy of MCM's utilizing MELS.

Figure 5.11 shows that the proposed CE technique works better with the UFMC system analogy to OFDM, FBMC, and F-OFDM MCM techniques. The MSE obtained is less for the mMIMO-UFMC system.

**Table 5.6:** MSE vs SNR for MCM techniques using MELS.

SNR (dB)	UFMC	FBMC	F-OFDM	OFDM
0	0.006047	0.007461	0.009323	0.01085
5	0.003881	0.004799	0.00649	0.007918
10	0.002729	0.003374	0.004563	0.005567
15	0.001644	0.002032	0.002748	0.003353
20	0.0008051	0.0009954	0.001346	0.001642
25	0.000308	0.0003809	0.0005151	0.0006284
30	0.0001124	0.0001389	0.0001879	0.0002292
35	4.66x10 <sup>-5</sup>	5.76x10 <sup>-5</sup>	7.79x10 <sup>-5</sup>	9.5x10 <sup>-5</sup>
40	2x10 <sup>-5</sup>	2.48x10 <sup>-5</sup>	3.35x10 <sup>-5</sup>	4.09x10 <sup>-5</sup>

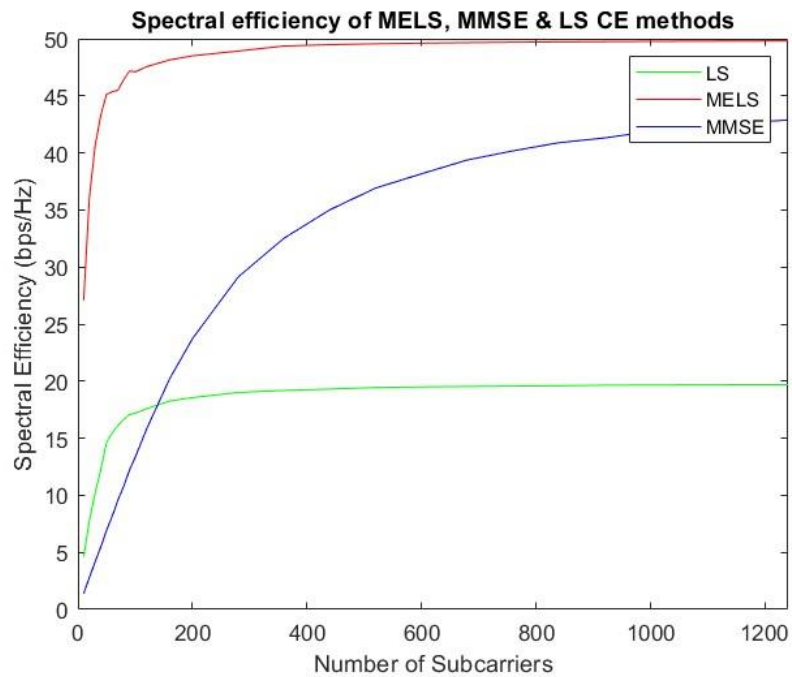


**Figure 5.12:** Spectral efficiency of proposed CE, MMSE & LS CE methods.

Figure 5.12 shows the SE of MELS, MMSE and LS CE methods. From the graph it is evident that the SE of proposed CE method is increasing with the increase in number of subcarriers compared to MMSE and LS CE methods.

## 5.6 SUMMARY

This chapter mainly discusses the proposed channel estimation technique for UFMC based 5G system. It also explains the mathematical analysis of the MELS channel estimation technique. It also explains the Dolph Chebyshev filter used in the UFMC system to reduce interference. The other conventional methods, such as LS and MMSE CE, are implemented in the UFMC system for comparison with the proposed CE technique. All the results are executed using MATLAB software. The number of transmit and receiver antennas used are 10 stating it mMIMO system. The results are executed based on the Montecarlo analysis. So, the number of iterations to apply for execution is considered 25 in the results. The results show that the proposed CE works well for the MIMO-UFMC system where it limits the problem of using cyclic prefix as used in OFDM is reduced by using the Dolph Chebyshev filter. The executed results prove that the proposed CE technique performs better than conventional LS, MMSE and Alamouti CE techniques. The reduction of BER and MSE of the proposed CE shows an enhancement in the overall MIMO-UFMC wireless system. The proposed CE also works well for the MIMO-UFMC system compared to other MCM methods such as OFDM, F-OFDM, and FBMC techniques. SE is another important performance metric to check the overall performance of the system that is also considered in the results. From the results it is evident that the proposed CE method has high SE compared to other conventional LS and MMSE CE methods. In this chapter the analytical analysis of BER and MSE are also explained for mMIMO-UFMC system with MELS CE method.

## **CHAPTER-6**

### **CONCLUSION AND FUTURESCOPE**

#### **6.1 CONCLUSION**

With the tremendous growth in devices and the users that need to be connected, 5G technology has to provide a high data rate, LL, QoS, reliability, better SE, EE, and low OOB. It presents the overview of 5G wireless communication systems to utilize it for achieving higher data rates and to connect several numbers of users. This thesis review some of the key points of 5G architecture, its open challenges and issues. It also reviews some of the applications that are related to 5G. In this 5G, WCS mMIMO is one of the promising technologies to achieve high data rates and connect several numbers of users. To enhance the accuracy and data rate of the mMIMO system, the estimation of the channel with the efficient MCM technique is required.

Chapter1 commences with an exploration of wireless communication technology, encompassing the diverse range of wireless technologies in use. It commences by delving into the 5G vision, including its architectures such as HetNet and C-RAN. Subsequently, the focus shifts to an in-depth discussion of mMIMO systems, a cornerstone of 5G wireless communication. mMIMO systems play a pivotal role in achieving elevated data rates and facilitating the connection of numerous users. The chapter also assesses the strengths and limitations inherent in mMIMO systems, shedding light on their advantages and constraints. Leveraging the architectural framework and capabilities of mMIMO systems, the text also explores the array of applications within the realm of 5G. Furthermore, drawing from the advantageous attributes of 5G for emerging applications, the chapter expounds upon the motivation, research objectives, and the chosen research methodology underpinning the subsequent research endeavour.

Chapter 2 commences with an overview of existing CE techniques. It extensively examines the mMIMO-OFDM system, incorporating an analysis of prevailing CE methods. The study also delves into the optimization of pilot design and placement,

as well as the exploration of diverse CE strategies. Furthermore, the chapter draws upon a comprehensive literature review to pinpoint the research imperatives. It elucidates the principal findings derived from the ongoing study. Additionally, the chapter distinctly outlines the research goals that steer the thesis, accompanied by a delineation of the methodology meticulously crafted to fulfil these objectives.

Chapter 3 exclusively delves into the realm of 5G multicarrier modulation techniques. It provides a comprehensive examination of various MCM techniques, including but not limited to OFDM, F-OFDM, FBMC, UFMC, and GFDM, accompanied by a detailed analysis of their corresponding transceiver architectures. As the demand for wireless connectivity experiences exponential growth, particularly with an unprecedented surge in wireless data consumption, the significance of the next-generation 5G WCS becomes paramount. This technology is poised to elevate data rates, bolster QoS, and enhance overall connectivity. Notably, the 5G WCS stands poised to facilitate novel applications such as the IOV, IoT, and smart grids. To address the multifaceted requirements of 5G, an array of promising MCM techniques comes to the forefront. It's worth noting that alternative waveforms might be better suited for the 5G WCS, surpassing the traditional OFDM approach. This study employs a QAM modulation scheme to provide a vivid demonstration of PSD and BER performance across all the considered MCM schemes. Of particular interest, the chapter 3 focuses on comparing the performance of GFDM a non-orthogonal MCM technique with that of OFDM, primarily in the context of its utility within cognitive radio applications.

Chapter 4 provides an in-depth exploration of Channel Estimation (CE) techniques within wireless systems. The primary focus centers on different categories of CE methods and the strategic placement of pilot signals. A notable portion of the discussion revolves around established CE methods, particularly those tailored for OFDM systems. Notably, the implementation and evaluation of these CE techniques are carried out using the MATLAB software platform. The chapter effectively illustrates the potency of the current methods through the lens of BER under varying SNR conditions. These existing methods exhibit certain limitations tied to system performance, the phenomenon of pilot contamination, and overall system complexity. Addressing these concerns, a range of alternative CE techniques have

been developed. However, a noteworthy drawback is that these methodologies have exclusively been applied to OFDM-based multi-carrier systems. Recognizing the essential demand for a practical multicarrier-oriented CE methodology, there arises a compelling necessity to create solutions at the physical layer to fulfill the critical requisites of the 5G mMIMO WCS.

Chapter 5 provides an extensive exploration of a novel CE technique tailored for UFMC-based 5G systems. It elucidates the intricate mathematical underpinnings of the MELS CE method. Furthermore, the incorporation of the Dolph-Chebyshev filter within the UFMC framework is expounded upon, highlighting its pivotal role in mitigating interference. To establish a comprehensive benchmark, the chapter implements conventional CE methods namely LS and MMSE within the UFMC system for comparative analysis against the proposed CE technique. The entire analysis is conducted through the MATLAB software platform. In line with a mMIMO setup consisting of 10 transmit and receiver antennas, the study employs a Montecarlo analysis with 25 iterations for result assessment. The outcomes underscore the efficacy of the proposed CE method in the context of the MIMO-UFMC system. This approach effectively addresses the challenges associated with cyclic prefix utilization, commonly encountered in OFDM, through the integration of the Dolph-Chebyshev filter. The executed results corroborate the superiority of the proposed CE technique over conventional LS, MMSE, and Alamouti CE methods. This is evidenced by the diminished BER and MSE, indicating a notable enhancement in the overall performance of the MIMO-UFMC wireless system. Additionally, the proposed CE technique is found to outperform other MCM methods, such as OFDM, F-OFDM, and FBMC, within the MIMO-UFMC system. The assessment of SE, another critical performance metric, further solidifies the proposed method's prowess. The results convincingly demonstrate that the proposed CE method yields higher SE when contrasted with traditional LS and MMSE CE methods.

To prove the efficiency of the system BER and MSE, w.r.t SNR is shown. The proposed CE works well for the MIMO-UFMC system where it reduces the problem of using cyclic prefixes as used in OFDM by the Dolph Chebyshev filter. The executed results prove that the proposed CE technique gives better performance

results compared to conventional LS and MMSE CE techniques. The reduction of BER and MSE of the proposed CE shows an enhancement in the overall MIMO-UFMC wireless system. The proposed CE also works well for the MIMO-UFMC system compared to other MCM methods such as OFDM, F-OFDM, and FBMC techniques. If the BER of the system is decreased, the efficiency and accuracy of the system increases. The SE of the system is also simulated over number of subcarriers. As the number of subcarriers increases the SE of the systems increases. If the SE of the system is high the efficiency of the system is increased and performance of the system is also increased. So, the proposed MELS channel estimation algorithm is best suitable and an efficient channel estimation algorithm for 5G wireless communication system.

## 6.2 FUTURE SCOPE

MELS CE with UFMC is developed for 5G mMIMO systems to attain high data rates and accuracy. The proposed system shows an efficient result compared to the conventional CE methods and other MCM techniques. In this thesis, the main work is focused on the design of an efficient CE method for the best suitable MCM technique for 5G systems. Considering the advantages of the proposed MELS CE with the UFMC system to achieve efficiency of the 5G systems, this research work can be extended. This part explains the work that can be extended for future research work is given as follows

The focus of this thesis revolves around mMIMO (systems, employing a configuration of ten transmitters and ten receiver antennas. It's worth noting that the mMIMO technology, integral to 5G, facilitates the connection of numerous users. Furthermore, the mMIMO setup's versatility allows for scalability, accommodating anywhere from 3 to 100 transmitter and receiver antennas. Hence, this research lays the groundwork for potential future extensions by exploring the implications of expanding the number of transmitter and receiver antennas.

The MELS CE method introduced in this context employs specific parameter settings, including 8 bits for each subcarrier, a total of 1024 subcarriers, 256 subcarriers spacing, 256 modulation orders, 10 transceiver antennas, and 25 Monte Carlo simulation parameters. It's important to acknowledge that further increases in these parameter values will lead to heightened computational complexity. Consequently, an avenue for future research lies in the potential to enhance this work by devising techniques that mitigate or minimize the associated computational intricacies while maintaining the method's effectiveness.

The efficacy of the proposed MELS-UFMC system is substantiated through the evaluation of critical parameters, namely BER and MSE in relation to SNR. Additionally, SE concerning the number of subcarriers is incorporated to calculate the system's performance. However, there remains a potential for expanding the scope of this study by incorporating supplementary parameters like throughput, robustness, complexity, etc. This broader assessment could provide a more comprehensive understanding of the MELS-UFMC system's capabilities and



advantages, enriching the overall findings and contributing to a more thorough analysis of its efficiency and potential for diverse applications.

## RESEARCH PUBLICATIONS

### Published Papers

1. Shaik, N., & Malik, P. K. (2021). A comprehensive survey 5G wireless communication systems: open issues, research challenges, channel estimation, multi carrier modulation and 5G applications. *Multimedia Tools and Applications*, 80(19), 28789-28827.
2. Shaik, N., & Malik, P. K. (2023). Modified entropy based least square channel estimation technique for 5G massive multiple input multiple output universal filtered multicarrier systems. *Engineering Research Express*, 5(1), 015050.
3. Shaik, N., & Malik, P. K. (2022). Modified Entropy based Least Square Channel Estimation for OFDM and UFMC 5G Systems. *Turkish Journal of Computer and Mathematics Education (TURCOMAT)*, 13(03), 1006-1016.
4. Nilofer, S. (2020). A review of massive multiple input multiple output for 5G communication: benefits and challenges. *Int. J. Intelligent Communication, Computing and Networks*, 1, 22-026.
5. Shaik, N., & Malik, P. K. (2020). A retrospection of channel estimation techniques for 5G wireless communications: Opportunities and challenges. *International Journal of Advanced Science and Technology*, 29(05), 8469-8479.

### Papers Communicated

1. Nilofer Shaik and Praveen Kumar Malik, "5G Multi-Carrier Modulation Techniques: Prototype Filters, Power Spectral Density, and Bit Error Rate", *Journal of Wireless personal communication*.

## Patents

1. Performance of multi carrier modulation techniques with and without proposed MELS channel estimation method with patent ID:202211040825 is published.
2. Modified entropy-based LS channel estimation for 5G multi-carrier modulation techniques with patent ID: 202211034501 is published.

## Copyright

1. A graphical abstract titled “Modified entropy LS channel estimation for UFMC based 5G wireless communication system”, with registration L-127123/2023 received a copyright.

## Book Chapter

1. Shaik N., Malik P.K. (2022) 5G Massive MIMO-OFDM System Model: Existing Channel Estimation Algorithms and Its Review. In: Malik P.K., Lu J., Madhav B.T.P., Kalkhambkar G., Amit S. (eds) Smart Antennas. EAI/Springer Innovations in Communication and Computing. Springer, Cham. [https://doi.org/10.1007/978-3-030-76636-8\\_15](https://doi.org/10.1007/978-3-030-76636-8_15).

## Conferences

1. “Analytical Analysis on LS, MMSE and Modified Entropy based LS Channel Estimation Techniques for 5G Massive MIMO Systems” is

- presented in 6<sup>th</sup> international conference on micro-electronics and telecommunication engineering on 23<sup>rd</sup> & 24<sup>th</sup> September, 2022, springer.
2. “Filter Bank Multi-Carrier Modulation with OQAM based Sparse Channel Estimation”, presented in 7<sup>th</sup> series of international conference on information system design and intelligent application INDIA-2022 Springer conference on 25<sup>th</sup> & 26<sup>th</sup> February, 2022.
  3. “Bit error rate performance in modified entropy-based LS channel estimation for UFMC-5G systems”, presented paper in 6<sup>th</sup> international conference on signal processing, communications & system design on 23<sup>rd</sup> & 24<sup>th</sup> January, 2021 with ISBN: 978-81-947249-9-5.

## Bibliography

1. Rappaport, T. S., Roh, W., & Cheun, K. (2014). Wireless engineers long considered high frequencies worthless for cellular systems. they couldn't be more wrong. *IEEE SPECTRUM*, 51(9), 34-+.
2. Shaik, N., & Malik, P. K. (2021). A comprehensive survey 5G wireless communication systems: open issues, research challenges, channel estimation, multi carrier modulation and 5G applications. *Multimedia Tools and Applications*, 80(19), 28789-28827.
3. Andrews, J. G., Buzzi, S., Choi, W., Hanly, S. V., Lozano, A., Soong, A. C., & Zhang, J. C. (2014). What will 5G be?. *IEEE Journal on selected areas in communications*, 32(6), 1065-1082.
4. Wang, Q., Mu, N., Wang, L., Safavi-Naeini, S., & Liu, J. (2017). 5G MIMO conformal microstrip antenna design. *Wireless Communications and Mobile Computing*, 2017.
5. Rashmitha, R., Niran, N., Jugale, A. A., & Ahmed, M. R. (2020). Microstrip patch antenna design for fixed mobile and satellite 5G communications. *Procedia Computer Science*, 171, 2073-2079.
6. Khan, F., Pi, Z., & Rajagopal, S. (2012, October). Millimeter-wave mobile broadband with large scale spatial processing for 5G mobile communication. In 2012 50th annual allerton conference on communication, control, and computing (Allerton) (pp. 1517-1523). IEEE.
7. Adhikari, P. (2008). Understanding millimeter wave wireless communication. Loea Corporation, 1-6.
8. Intelligence, G. S. M. A. (2014). Understanding 5G: Perspectives on future technological advancements in mobile. White paper, 1-26.
9. Chen, S., & Zhao, J. (2014). The requirements, challenges, and technologies for 5G of terrestrial mobile telecommunication. *IEEE communications magazine*, 52(5), 36-43.
10. Osseiran, A., Boccardi, F., Braun, V., Kusume, K., Marsch, P., Maternia, M., ... & Fallgren, M. (2014). Scenarios for 5G mobile and wireless communications:

- the vision of the METIS project. *IEEE communications magazine*, 52(5), 26-35.
11. 5G Forum. (2015). Make it happen: Creating New values Together [Online]. Available: <http://www.5gforum.org/>.
  12. Qualcomm Technologies, (2014) Inc., “Qualcomm’s 5G vision,” White paper.
  13. Huawei (2013), “5G a technology vision,” White paper.
  14. Nokia Networks (2014), “Looking ahead to 5G: Building a virtual zero latency gigabit experience,” White paper.
  15. Samsung Electronics Co. (2015), “5G vision, white paper”.
  16. NTT Docomo (2015), “5G radio access: Requirements, concepts technologies,” White paper.
  17. Boccardi, F., Heath, R. W., Lozano, A., Marzetta, T. L., & Popovski, P. (2014). Five disruptive technology directions for 5G. *IEEE communications magazine*, 52(2), 74-80.
  18. Feng, Z., & Zhang, Z. (1999). Dynamic spatial channel assignment for smart antenna. *Wireless Personal Communications*, 11(1), 79-87.
  19. Pi, Z., & Khan, F. (2011). An introduction to millimeter-wave mobile broadband systems. *IEEE communications magazine*, 49(6), 101-107.
  20. Bae, J., Choi, Y. S., Kim, J. S., & Chung, M. Y. (2014, October). Architecture and performance evaluation of MmWave based 5G mobile communication system. In 2014 International Conference on Information and Communication Technology Convergence (ICTC) (pp. 847-851). IEEE.
  21. Checko, A., Christiansen, H. L., Yan, Y., Scolari, L., Kardaras, G., Berger, M. S., & Dittmann, L. (2014). Cloud RAN for mobile networks—A technology overview. *IEEE Communications surveys & tutorials*, 17(1), 405-426.
  22. Cvijetic, N. (2014, September). Optical network evolution for 5G mobile applications and SDN-based control. In 2014 16th International Telecommunications Network Strategy and Planning Symposium (Networks) (pp. 1-5). IEEE.
  23. Agyapong, P. K., Iwamura, M., Staehle, D., Kiess, W., & Benjebbour, A. (2014). Design considerations for a 5G network architecture. *IEEE Communications Magazine*, 52(11), 65-75.

24. Abd El-atty, S. M., & Gharsseldien, Z. M. (2013, April). On performance of HetNet with coexisting small cell technology. In 6th Joint IFIP Wireless and Mobile Networking Conference (WMNC) (pp. 1-8). IEEE.
25. Makhanbet, M., Zhang, X., Gao, H., & Suraweera, H. A. (2017). An overview of cloud RAN: Architecture, issues and future directions. In *Emerging Trends in Electrical, Electronic and Communications Engineering: Proceedings of the First International Conference on Electrical, Electronic and Communications Engineering (ELECOM 2016)*, Bagatelle, Mauritius, November 25-27, 2016 (pp. 44-60). Springer International Publishing.
26. Zhang, N., Cheng, N., Gamage, A. T., Zhang, K., Mark, J. W., & Shen, X. (2015). Cloud assisted HetNets toward 5G wireless networks. *IEEE communications magazine*, 53(6), 59-65.
27. Lai, C. F., Hwang, R. H., Chao, H. C., Hassan, M. M., & Alamri, A. (2015). A buffer-aware HTTP live streaming approach for SDN-enabled 5G wireless networks. *IEEE network*, 29(1), 49-55.
28. Wu, H., Zhang, N., Tao, X., Wei, Z., & Shen, X. (2017). Capacity-and trust-aware BS cooperation in nonuniform hetnets: Spectral efficiency and optimal BS density. *IEEE Transactions on Vehicular Technology*, 66(12), 11317-11329.
29. Cho, H. H., Lai, C. F., Shih, T. K., & Chao, H. C. (2014). Integration of SDR and SDN for 5G. *Ieee Access*, 2, 1196-1204.
30. Arslan, M. Y., Sundaresan, K., & Rangarajan, S. (2015). Software-defined networking in cellular radio access networks: potential and challenges. *IEEE Communications Magazine*, 53(1), 150-156.
31. Lu, L., Li, G. Y., Swindlehurst, A. L., Ashikhmin, A., & Zhang, R. (2014). An overview of massive MIMO: Benefits and challenges. *IEEE journal of selected topics in signal processing*, 8(5), 742-758.
32. Mehmood, Y., Afzal, W., Ahmad, F., Younas, U., Rashid, I., & Mehmood, I. (2013, September). Large scaled multi-user MIMO system so called massive MIMO systems for future wireless communication networks. In *2013 19th International Conference on Automation and Computing* (pp. 1-4). IEEE.

33. Gesbert, D., Kountouris, M., Heath, R. W., Chae, C. B., & Salzer, T. (2007). Shifting the MIMO paradigm. *IEEE signal processing magazine*, 24(5), 36-46.
34. WANG, W., CUI, G., LU, S., & ZHANG, Y. (2011). Requirements for Further Advancements for Evolved Universal Terrestrial Radio Access (E-UTRA) Requirements for Further Advancements for Evolved Universal Terrestrial Radio Access (E-UTRA), 2009. *IEICE transactions on communications*, 94(12), 3391-3394.
35. Larsson, E. G., Edfors, O., Tufvesson, F., & Marzetta, T. L. (2014). Massive MIMO for next generation wireless systems. *IEEE communications magazine*, 52(2), 186-195.
36. Liu, W., Han, S., Yang, C., & Sun, C. (2013, April). Massive MIMO or small cell network: Who is more energy efficient?. In *2013 IEEE Wireless Communications and Networking Conference Workshops (WCNCW)* (pp. 24-29). IEEE.
37. Nguyen, M. (2018). Massive mimo: A survey of benefits and challenges. *ICSES Trans. Comput. Hardw. Electr. Eng*, 4, 1-4.
38. Hoydis, J., Hosseini, K., Ten Brink, S., & Debbah, M. (2013). Making smart use of excess antennas: Massive MIMO, small cells, and TDD. *Bell Labs Technical Journal*, 18(2), 5-21.
39. Jungnickel, V., Manolakis, K., Zirwas, W., Panzner, B., Braun, V., Lossow, M., ... & Svensson, T. (2014). The role of small cells, coordinated multipoint, and massive MIMO in 5G. *IEEE communications magazine*, 52(5), 44-51.
40. Marzetta, T. L. (2010). Noncooperative cellular wireless with unlimited numbers of base station antennas. *IEEE transactions on wireless communications*, 9(11), 3590-3600.
41. Popovski, P., Stefanović, Č., Nielsen, J. J., De Carvalho, E., Angelichinoski, M., Trillingsgaard, K. F., & Bana, A. S. (2019). Wireless access in ultra-reliable low-latency communication (URLLC). *IEEE Transactions on Communications*, 67(8), 5783-5801.
42. Hoydis, J., Ten Brink, S., & Debbah, M. (2013). Massive MIMO in the UL/DL of cellular networks: How many antennas do we need?. *IEEE Journal on selected Areas in Communications*, 31(2), 160-171.



43. Rappaport, T. S., Sun, S., Mayzus, R., Zhao, H., Azar, Y., Wang, K., ... & Gutierrez, F. (2013). Millimeter wave mobile communications for 5G cellular: It will work!. *IEEE access*, 1, 335-349.
44. Rajagopal, S., Abu-Surra, S., Pi, Z., & Khan, F. (2011, December). Antenna array design for multi-gbps mmwave mobile broadband communication. In *2011 IEEE Global Telecommunications Conference-GLOBECOM 2011* (pp. 1-6). IEEE.
45. Tiwari, P., & Malik, P. K. (2020, January). Design of UWB antenna for the 5G mobile communication applications: a review. In *2020 International Conference on Computation, Automation and Knowledge Management (ICCAKM)* (pp. 24-30). IEEE.
46. Roh, W., Seol, J. Y., Park, J., Lee, B., Lee, J., Kim, Y., ... & Aryanfar, F. (2014). Millimeter-wave beamforming as an enabling technology for 5G cellular communications: Theoretical feasibility and prototype results. *IEEE communications magazine*, 52(2), 106-113.
47. Mohr, W. (2015, July). The 5G infrastructure public-private partnership. In *Proc. Presentation ITU GSC Meeting* (p. 35).
48. Perera, C., Zaslavsky, A., Christen, P., & Georgakopoulos, D. (2013). Context aware computing for the internet of things: A survey. *IEEE communications surveys & tutorials*, 16(1), 414-454.
49. Alcaraz-Calero, J., Belikaidis, I. P., Cano, C. J. B., Bisson, P., Bourse, D., Bredel, M., ... & Wang, Q. (2017, October). Leading innovations towards 5G: Europe's perspective in 5G infrastructure public-private partnership (5G-PPP). In *2017 IEEE 28th Annual International Symposium on Personal, Indoor, and Mobile Radio Communications (PIMRC)* (pp. 1-5). IEEE.
50. Asadi, A., Wang, Q., & Mancuso, V. (2014). A survey on device-to-device communication in cellular networks. *IEEE Communications Surveys & Tutorials*, 16(4), 1801-1819.
51. Zhang, Y., Yu, R., Nekovee, M., Liu, Y., Xie, S., & Gjessing, S. (2012). Cognitive machine-to-machine communications: Visions and potentials for the smart grid. *IEEE network*, 26(3), 6-13.

52. Xu, B., Da Xu, L., Cai, H., Xie, C., Hu, J., & Bu, F. (2014). Ubiquitous data accessing method in IoT-based information system for emergency medical services. *IEEE Transactions on Industrial informatics*, 10(2), 1578-1586.
53. Kumar, N., Misra, S., Rodrigues, J. J., & Obaidat, M. S. (2015). Coalition games for spatio-temporal big data in internet of vehicles environment: A comparative analysis. *IEEE Internet of Things Journal*, 2(4), 310-320.
54. Wu, X., Subramanian, S., Guha, R., White, R. G., Li, J., Lu, K. W., ... & Zhang, T. (2013). Vehicular communications using DSRC: challenges, enhancements, and evolution. *IEEE Journal on Selected Areas in Communications*, 31(9), 399-408.
55. Rutherford, J. J. (2010). Wearable technology. *IEEE Engineering in Medicine and Biology Magazine*, 29(3), 19-24.
56. Gao, Y., Li, H., & Luo, Y. (2015). An empirical study of wearable technology acceptance in healthcare. *Industrial Management & Data Systems*.
57. Zhiying, Z., Lingzhen, Q., & Yu, J. (2009, May). Study on application of grid computing technology in financial industry. In *2009 International Forum on Information Technology and Applications* (Vol. 2, pp. 344-346). IEEE.
58. Accenture (2014), "Rise of fintech," White Paper.
59. Erol-Kantarci, M., & Mouftah, H. T. (2014). Energy-efficient information and communication infrastructures in the smart grid: A survey on interactions and open issues. *IEEE Communications Surveys & Tutorials*, 17(1), 179-197.
60. Li, Y. (2000). Pilot-symbol-aided channel estimation for OFDM in wireless systems. *IEEE transactions on vehicular technology*, 49(4), 1207-1215.
61. Sathananthan, K., & Tellambura, C. (2001, October). Performance analysis of an OFDM system with carrier frequency offset and phase noise. In *IEEE 54th Vehicular Technology Conference. VTC Fall 2001. Proceedings* (Cat. No. 01CH37211) (Vol. 4, pp. 2329-2332). IEEE.
62. Jalloh, M., Al-Gharabally, M., & Das, P. (2006, October). Performance of OFDM systems in Rayleigh fading channels with phase noise and channel estimation errors. In *MILCOM 2006-2006 IEEE Military Communications conference* (pp. 1-7). IEEE.

63. Wu, S., & Bar-Ness, Y. (2004). OFDM systems in the presence of phase noise: consequences and solutions. *IEEE Transactions on Communications*, 52(11), 1988-1996.
64. Mallick, S., & Majumder, S. P. (2008, December). Performance analysis of an OFDM system in the presence of carrier frequency offset, phase noise and timing jitter over Rayleigh fading channels. In 2008 International Conference on Electrical and Computer Engineering (pp. 205-210). IEEE.
65. Daryasafar, N., Lashkari, A., & Ehyae, B. (2012). Channel estimation in MIMO-OFDM systems based on comparative methods by LMS algorithm. *International Journal Of Computer Science Issues (IJCSI)*, 9(3), 188.
66. Bengan, M., Kirar, V. P. S., & Burse, K. (2012, November). Phase noise reduction and tracking in OFDM using extended Kalman Filter. In 2012 Fourth International Conference on Computational Intelligence and Communication Networks (pp. 402-406). IEEE.
67. Xu, P., Wang, J., Wang, J., & Qi, F. (2014). Analysis and design of channel estimation in multicell multiuser MIMO OFDM systems. *IEEE transactions on vehicular technology*, 64(2), 610-620.
68. Lee, D. (2016). MIMO OFDM channel estimation via block stagewise orthogonal matching pursuit. *IEEE Communications letters*, 20(10), 2115-2118.
69. Qin, Q., Gui, L., Gong, B., & Luo, S. (2018). Sparse channel estimation for massive MIMO-OFDM systems over time-varying channels. *IEEE Access*, 6, 33740-33751.
70. Chen, C. Y., & Wu, W. R. (2018). Joint AoD, AoA, and channel estimation for MIMO-OFDM systems. *IEEE Transactions on Vehicular Technology*, 67(7), 5806-5820.
71. Khan, I., Zafar, M. H., Ashraf, M., & Kim, S. (2018). Computationally efficient channel estimation in 5G massive multiple-input multiple-output systems. *Electronics*, 7(12), 382.
72. Nayebi, E., & Rao, B. D. (2018, April). Semi-blind channel estimation in massive MIMO systems with different priors on data symbols. In 2018 IEEE

- International Conference on Acoustics, Speech and Signal Processing (ICASSP) (pp. 3879-3883). IEEE.
73. Al-Salihi, H., Nakhai, M. R., & Le, T. A. (2018, June). DFT-based channel estimation techniques for massive MIMO systems. In 2018 25th International Conference on Telecommunications (ICT) (pp. 383-387). IEEE.
  74. Kuai, X., Chen, L., Yuan, X., & Liu, A. (2019). Structured turbo compressed sensing for downlink massive MIMO-OFDM channel estimation. *IEEE Transactions on Wireless Communications*, 18(8), 3813-3826.
  75. Araújo, D. C., De Almeida, A. L., Da Costa, J. P., & de Sousa, R. T. (2019). Tensor-based channel estimation for massive MIMO-OFDM systems. *IEEE Access*, 7, 42133-42147.
  76. Uwaechia, A. N., & Mahyuddin, N. M. (2019). Spectrum-efficient distributed compressed sensing based channel estimation for OFDM systems over doubly selective channels. *IEEE Access*, 7, 35072-35088.
  77. Mirzaei, J., Adve, R. S., & Shahbazpanahi, S. (2018). Semi-blind time-domain channel estimation for frequency-selective multiuser massive MIMO systems. *IEEE Transactions on Communications*, 67(2), 1045-1058.
  78. Akbarpour-Kasgari, A., & Ardebilipour, M. (2018). Massive mimo-ofdm channel estimation via distributed compressed sensing. *IEEE Wireless Communications Letters*, 8(2), 376-379.
  79. Huang, Y., He, Y., Luo, Q., Shi, L., & Wu, Y. (2018). Channel estimation in MIMO-OFDM systems based on a new adaptive greedy algorithm. *IEEE Wireless Communications Letters*, 8(1), 29-32.
  80. Khan, I., Rodrigues, J. J., Al-Muhtadi, J., Khattak, M. I., Khan, Y., Altaf, F., ... & Choi, B. J. (2019). A robust channel estimation scheme for 5G massive MIMO systems. *Wireless Communications and Mobile Computing*, 2019.
  81. Singh, P., & Vasudevan, K. (2019). Time domain channel estimation for MIMO-FBMC/OQAM systems. *Wireless Personal Communications*, 108(4), 2159-2178.
  82. Riadi, A., Boulouird, M., & Hassani, M. M. R. (2018, December). Least squares channel estimation of an OFDM massive MIMO system for 5G wireless communications. In International conference on the Sciences of Electronics,

- Technologies of Information and Telecommunications (pp. 440-450). Springer, Cham.
83. Chen, J., Zhang, X., & Zhang, P. (2020, June). Bayesian learning for BPSO-based pilot pattern design over sparse OFDM channels. In ICC 2020-2020 IEEE International Conference on Communications (ICC) (pp. 1-6). IEEE.
  84. Mawatwal, K., Sen, D., & Roy, R. (2020). Performance analysis of a SAGE-based semi-blind channel estimator for pilot contaminated MU massive MIMO systems. *IEEE Access*, 8, 46682-46700.
  85. Liao, Y., Sun, G., Cai, Z., Shen, X., & Huang, Z. (2020). Nonlinear Kalman filter-based robust channel estimation for high mobility OFDM systems. *IEEE Transactions on Intelligent Transportation Systems*, 22(11), 7219-7231.
  86. Balevi, E., Doshi, A., & Andrews, J. G. (2020). Massive MIMO channel estimation with an untrained deep neural network. *IEEE Transactions on Wireless Communications*, 19(3), 2079-2090.
  87. Wang, H., Du, W., Wang, X., Yu, G., & Xu, L. (2020). Channel estimation performance analysis of FBMC/OQAM systems with bayesian approach for 5G-enabled IoT applications. *Wireless Communications and Mobile Computing*, 2020.
  88. Le Ha, A., Van Chien, T., Nguyen, T. H., & Choi, W. (2021, January). Deep learning-aided 5G channel estimation. In 2021 15th international conference on ubiquitous information management and communication (IMCOM) (pp. 1-7). IEEE.
  89. Zhang, Z., Xiong, L., Yao, D., & Wang, Y. (2022). The AI-Based Channel Prediction Scheme for the 5G Wireless System in High-Speed V2I Scenarios. *Wireless Communications and Mobile Computing*, 2022.
  90. Jain, A., & Nagaria, D. (2015, November). Filter bank spectrum sensing for Cognitive Radio oriented wireless network. In 2015 Communication, Control and Intelligent Systems (CCIS) (pp. 133-136). IEEE.
  91. Farhang-Boroujeny, B. (2008). Filter bank spectrum sensing for cognitive radios. *IEEE Transactions on signal processing*, 56(5), 1801-1811.
  92. Matz, G., Schafhuber, D., Grochenig, K., Hartmann, M., & Hlawatsch, F. (2007). Analysis, optimization, and implementation of low-interference

- wireless multicarrier systems. *IEEE Transactions on Wireless Communications*, 6(5), 1921-1931.
93. Kaur, A., & Malik, P. K. (2020, January). Tri state, T shaped circular cut ground antenna for higher 'X'band frequencies. In 2020 International Conference on Computation, Automation and Knowledge Management (ICCAKM) (pp. 90-94). IEEE.
  94. Malik, P. K., & Tripathi, M. P. (2017). OFDM: a mathematical review. *Journal on Today's Ideas-Tomorrow's Technologies*, 5(2), 97-111.
  95. Sahin, A., Guvenc, I., & Arslan, H. (2013). A survey on multicarrier communications: Prototype filters, lattice structures, and implementation aspects. *IEEE communications surveys & tutorials*, 16(3), 1312-1338.
  96. Zhang, X., Jia, M., Chen, L., Ma, J., & Qiu, J. (2015, December). Filtered-OFDM-enabler for flexible waveform in the 5th generation cellular networks. In 2015 IEEE global communications conference (GLOBECOM) (pp. 1-6). IEEE.
  97. Zhang, L., Ijaz, A., Xiao, P., Molu, M. M., & Tafazolli, R. (2017). Filtered OFDM systems, algorithms, and performance analysis for 5G and beyond. *IEEE Transactions on Communications*, 66(3), 1205-1218.
  98. Zhang, X. (2009). Design of FIR halfband filters for orthonormal wavelets using Remez exchange algorithm. *IEEE Signal Processing Letters*, 16(9), 814-817.
  99. Zhang, L., Ijaz, A., Xiao, P., Quddus, A., & Tafazolli, R. (2016, September). Single-rate and multi-rate multi-service systems for next generation and beyond communications. In 2016 IEEE 27th Annual International Symposium on Personal, Indoor, and Mobile Radio Communications (PIMRC) (pp. 1-6). IEEE.
  100. Haas, R., & Belfiore, J. C. (1997). A time-frequency well-localized pulse for multiple carrier transmission. *Wireless personal communications*, 5(1), 1-18.
  101. Nissel, R., & Rupp, M. (2016, March). On pilot-symbol aided channel estimation in FBMC-OQAM. In 2016 IEEE international conference on acoustics, speech and signal processing (ICASSP) (pp. 3681-3685). IEEE.
  102. Bellanger, M. G. (2001, May). Specification and design of a prototype filter for filter bank based multicarrier transmission. In 2001 IEEE International

- Conference on Acoustics, Speech, and Signal Processing. Proceedings (Cat. No. 01CH37221) (Vol. 4, pp. 2417-2420). IEEE.
103. Mirabbasi, S., & Martin, K. (2002, May). Design of prototype filter for near-perfect-reconstruction overlapped complex-modulated transmultiplexers. In 2002 IEEE International Symposium on Circuits and Systems. Proceedings (Cat. No. 02CH37353) (Vol. 1, pp. I-I). IEEE.
104. Geng, S., Xiong, X., Cheng, L., Zhao, X., & Huang, B. (2015, October). UFMC system performance analysis for discrete narrow-band private networks. In 2015 IEEE 6th International Symposium on Microwave, Antenna, Propagation, and EMC Technologies (MAPE) (pp. 303-307). IEEE.
105. Fettweis, G., & Alamouti, S. (2014). 5G: Personal mobile internet beyond what cellular did to telephony. *IEEE Communications Magazine*, 52(2), 140-145.
106. Michailow, N., Matthé, M., Gaspar, I. S., Caldevilla, A. N., Mendes, L. L., Festag, A., & Fettweis, G. (2014). Generalized frequency division multiplexing for 5th generation cellular networks. *IEEE Transactions on Communications*, 62(9), 3045-3061.
107. Bhimsing, D. V., & Bhagali, A. C. (2017, September). Performance of channel estimation and equalization in OFDM system. In 2017 IEEE International Conference on Power, Control, Signals and Instrumentation Engineering (ICPCSI) (pp. 1003-1005). IEEE.
108. Pu, L., Liu, J., Fang, Y., Li, W., & Wang, Z. (2010, April). Channel estimation in mobile wireless communication. In 2010 International Conference on Communications and Mobile Computing (Vol. 2, pp. 77-80). IEEE.
109. Desta, Y. T., Tao, J., & Zhang, W. (2011). Review on selected channel estimation algorithms for orthogonal frequency division multiplexing System. *Information Technology Journal*, 10(5), 914-926.
110. Ogundile, O. O., Oyerinde, O. O., & Versfeld, D. J. (2015). Decision directed iterative channel estimation and Reed–Solomon decoding over flat fading channels. *IET Communications*, 9(17), 2077-2084.
111. Ogundile, O. O., & Versfeld, D. J. (2016). A low complexity iterative channel estimation and decoding receiver based on reed-solomon PTA. *IEEE Access*, 4, 8805-8813.

112. Park, S., Shim, B., & Choi, J. W. (2015). Iterative channel estimation using virtual pilot signals for MIMO-OFDM systems. *IEEE Transactions on Signal Processing*, 63(12), 3032-3045.
113. Jones, V. K., & Raleigh, G. C. (1998, November). Channel estimation for wireless OFDM systems. In *IEEE GLOBECOM 1998* (Cat. NO. 98CH36250) (Vol. 2, pp. 980-985). IEEE.
114. Coleri, S., Ergen, M., Puri, A., & Bahai, A. (2002). Channel estimation techniques based on pilot arrangement in OFDM systems. *IEEE Transactions on broadcasting*, 48(3), 223-229.
115. Terry, J., & Heiskala, J. (2002). *OFDM wireless LANs: A theoretical and practical guide*. Sams publishing.
116. Hsieh, M. H., & Wei, C. H. (1998). Channel estimation for OFDM systems based on comb-type pilot arrangement in frequency selective fading channels. *IEEE Transactions on Consumer Electronics*, 44(1), 217-225.
117. Nee, R. V., & Prasad, R. (2000). *OFDM for wireless multimedia communications*. Artech House, Inc..
118. Hsieh, M. H., & Wei, C. H. (1998). Channel estimation for OFDM systems based on comb-type pilot arrangement in frequency selective fading channels. *IEEE Transactions on Consumer Electronics*, 44(1), 217-225.
119. Mawatwal, K., Sen, D., & Roy, R. (2016). A semi-blind channel estimation algorithm for massive MIMO systems. *IEEE Wireless Communications Letters*, 6(1), 70-73.
120. Ban, Y., Hu, Q., Mao, Z., & Zhao, Z. (2016). Semi-blind pilot-aided channel estimation in uplink cloud radio access networks. *China Communications*, 13(9), 72-79.
121. Qi, C., & Wu, L. (2011, May). A hybrid compressed sensing algorithm for sparse channel estimation in MIMO OFDM systems. In *2011 IEEE International Conference on Acoustics, Speech and Signal Processing (ICASSP)* (pp. 3488-3491). IEEE.
122. Alaghbari, K. A., Siong, L. H., & Tan, W. C. (2015). Correntropy-Based Blind Channel Estimation for MIMO-OFDM Systems. *Journal of Applied Sciences*, 15(3), 602-605.



123. Nissel, R., Schwarz, S., & Rupp, M. (2017). Filter bank multicarrier modulation schemes for future mobile communications. *IEEE Journal on Selected Areas in Communications*, 35(8), 1768-1782.
124. Nissel, R., Ademaj, F., & Rupp, M. (2018, August). Doubly-selective channel estimation in FBMC-OQAM and OFDM systems. In *2018 IEEE 88th Vehicular Technology Conference (VTC-Fall)* (pp. 1-5). IEEE.
125. Nissel, R., Zochmann, E., & Rupp, M. (2017, June). On the influence of doubly-selectivity in pilot-aided channel estimation for FBMC-OQAM. In *2017 IEEE 85th Vehicular Technology Conference (VTC Spring)* (pp. 1-5). IEEE.
126. Balevi, E., Doshi, A., & Andrews, J. G. (2020). Massive MIMO channel estimation with an untrained deep neural network. *IEEE Transactions on Wireless Communications*, 19(3), 2079-2090.
127. Rani, P. N., & Rani, C. S. (2016, December). UFMC: The 5G modulation technique. In *2016 IEEE international conference on computational intelligence and computing research (ICCIC)* (pp. 1-3). IEEE.
128. Lynch, P. (1997). The Dolph–Chebyshev window: A simple optimal filter. *Monthly weather review*, 125(4), 655-660.
129. Singh, B., Tripathy, M. R., & Asthana, R. (2021, October). BER Reduction of UFMC for 1024-QAM. In *2021 IEEE International Conference on RFID Technology and Applications (RFID-TA)* (pp. 293-296). IEEE.
130. Kewen, L. (2010, December). Research of MMSE and LS channel estimation in OFDM systems. In *The 2nd international conference on information science and engineering* (pp. 2308-2311). IEEE.
131. Khlifi, A., & Bouallegue, R. (2011). Performance analysis of LS and LMMSE channel estimation techniques for LTE downlink systems. *arXiv preprint arXiv:1111.1666*.
132. Ma, J., Yu, H., & Liu, S. (2009, September). The MMSE channel estimation based on DFT for OFDM system. In *2009 5th International Conference on Wireless Communications, Networking and Mobile Computing* (pp. 1-4). IEEE.
133. Srivastava, V., Ho, C. K., Fung, P. H. W., & Sun, S. (2004, March). Robust MMSE channel estimation in OFDM systems with practical timing

synchronization. In 2004 IEEE Wireless Communications and Networking Conference (IEEE Cat. No. 04TH8733) (Vol. 2, pp. 711-716). IEEE.

134. Comisso, M., Vatta, F., Buttazzoni, G., & Babich, F. (2019, September). Estimation of the bit error rate (BER) for uplink millimeter-wave line-of-sight communications. In 2019 International Conference on Software, Telecommunications and Computer Networks (SoftCOM) (pp. 1-6). IEEE.